Report T-26

A STUDY OF THE DYNAMICS ASSOCIATED WITH A NON-LINEAR CLOSED LOOP SYSTEM

Benedict O. Olson June - 1952

PUBLISHED BY
INSTRUMENTATION LABORATORY

MASSACHUSETTS INSTITUTE OF TECHNOLOGY

Cambridge 39, Mass.

A STUDY OF THE DYNAMICS ASSOCIATED WITH A NON-LINEAR CLOSED LOOP SYSTEM

by

BENEDICT O. OLSON

A.B., Clark University, 1950

SUBMITTED IN PARTIAL FULFILLMENT OF THE

REQUIREMENTS FOR THE DEGREE OF

MASTER OF SCIENCE

at

MASSACHUSETTS INSTITUTE OF TECHNOLOGY

1952

Signature of Author

Supervisor

Chairman, Departmental [illegible] dents

Report No. T-26

May 16, 1952

Prof. L. R. Hamilton
Assistant Secretary of the Faculty
Massachusetts Institute of Technology
Cambridge 39, Massachusetts

Dear Professor Hamilton:

In accordance with the regulations of the faculty, I hereby submit a thesis entitled, "A Study of the Dynamics Associated with a Non-linear Closed Loop System," in partial fulfillment of the requirements for the degree of Master of Science.

Respectfully yours,

ACKNOWLEDGMENT

The author wishes to express sincere appreciation to Professor C. S. Draper and members of the Instrumentation Laboratory for their help in the preparation of this thesis.

In particular, the author is especially grateful to the following:

Prof. Walter Wrigley for his assistance and supervision of the thesis.

Ralph R. Ragan for allowing GFCS X-1 appropriations and facilities to be used in the completion of the thesis.

Dr. Y. J. Liu for the original suggestion on this application of microsyn units, and for his helpful advice during the preparation of the thesis.

David G. Hoag for his helpful advice throughout the preparation of this thesis.

Prof. Robert Mueller for his advice on the use and theory of microsyn units.

Dr. Halcombe Laning and the Instrumentation Laboratory mathematics section for their assistance and suggestions.

Mary Lee Meagher, GFCS X-1 secretary, for the difficult task of typing the thesis.

Dorothy Ladd and the Jackson and Moreland group for the excellent job on the illustrations.

This paper was prepared under D.I.C. Project 6756, sponsored by Section Re4c, BuOrd, U. S. Navy, through contract NOrd 10796.

ABSTRACT

of thesis entitled

"A Study of the Dynamics Associated with a Non-linear Closed Loop System"

by

Benedict O. Olson

SUBMITTED IN PARTIAL FULFILLMENT OF THE REQUIREMENTS FOR THE DEGREE OF MASTER OF SCIENCE IN THE DEPARTMENT OF PHYSICS ON MAY 16, 1952

In the development of computers used in fire control systems, there arises the requirement that two vector quantities (represented as scaler signals) be added vectorally at right angles. A method that was suggested to the author by Dr. Y. J. Liu was to use a closed loop system involving the squaring property of electro-magnetic microsyn units operating on a shaft. Although the instrumentation of such a system is fairly straight forward, the dynamic analysis of the system is made complex because of the non-linearities involved. This thesis will be in the main a study of the dynamics of the proposed system.

After a brief discussion of the theory and operation of the microsyn units to be incorporated in this system, the performance equations along with stability conditions for an ideal system are developed in Chapter II. Chapter III then develops a generalized approach to the design of a practical system. To keep the dynamic qualities of the system constant a square root generator has to be incorporated in the feedback loop. What was done in Chapter III was

to develop a method specifying how close to an ideal square root characteristic we have to be in order to stay within pre-assigned tolerances of the natural undamped frequency and the damping ratio associated with the system. Chapters IV and V present transient and steady state analyses similar to the types used in linear second order systems. The final chapter shows the complete design and results of a laboratory test system using the general design criteria of the previous chapters.

Thesis supervisor: Dr. Walter Wrigley

Associate Professor of Aeronautical Engineering

TABLE OF CONTENTS

CHAPTER I

Introduction to the Problem

In the instrumentation of systems related to a wide variety of problems, there often arises the need to add vectorally two quantities at right angles. In general, the two vector quantities are represented as scalar signals, and it is the requirement of some instrument or system to treat these signals as vectors and perform the right angle addition. In this thesis, we shall represent the two signals as voltage quantities E_x and E_y. The desired result will then be $E_o = \sqrt{E_x^2 + E_y^2}$ where again E_o is a scalar quantity. It is to be noted here that we are not interested in the actual position with respect to inertial space of the two vectors, but merely in restoring their right angle relationship with respect to each other.

The quantities E_x and E_y will fluctuate either periodically or haphazardly, but they will never change direction. The reason why E_x and E_y can only be fluctuating direct voltages of the same sign will be shown later in the chapter. A major portion of this thesis will be devoted to a study and analysis of the dynamics associated with the proposed system. In short, we shall attempt to answer the two questions, "how does the system respond to fluctuating inputs?"- and given certain tolerances on how well the system should perform, "how can we design a practical system?"

One method in use at present to obtain the result $E_o = \sqrt{E_x^2 + E_y^2}$ is to use a resolver nulling servo combination. The system is shown schematically in Fig. 1-2.

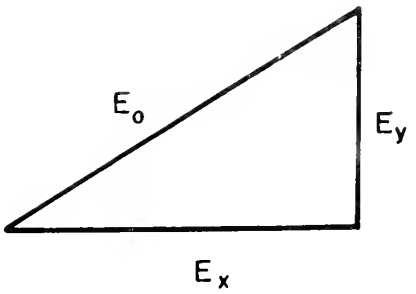

DESIRED RESULT :

$$E_o = \sqrt{E_x^2 + E_y^2}$$

FIGURE 1-1

RIGHT ANGLE RELATIONSHIPS OF QUANTITIES TO BE COMPUTED

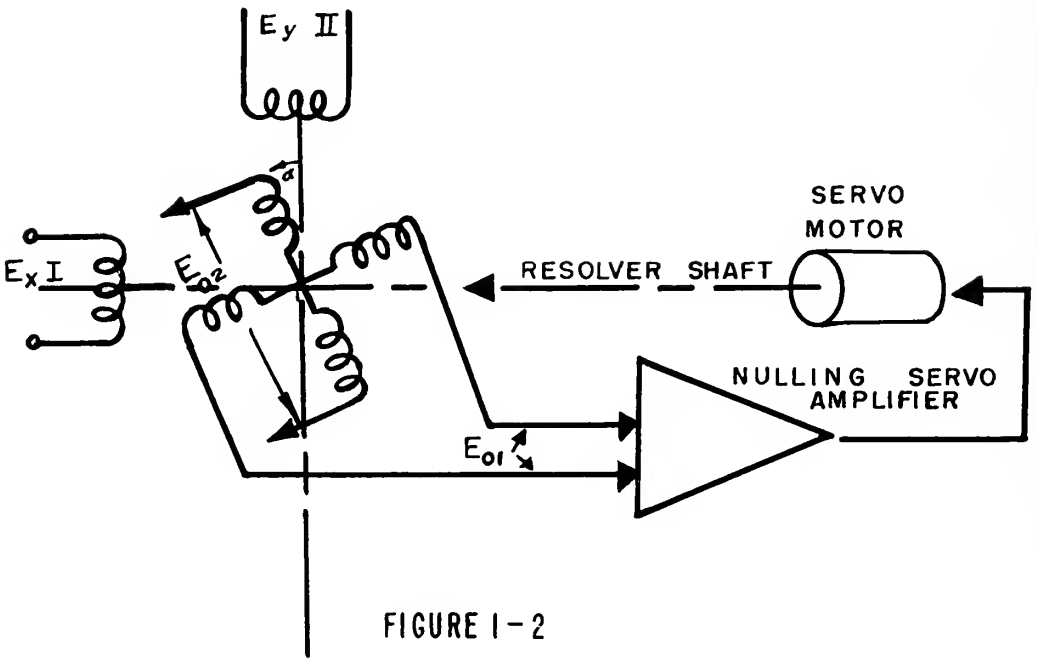

FIGURE 1-2

USUAL METHOD OF SOLVING PROBLEM

E_x and E_y are root mean square values of alternating sinusoidal voltages appearing across the stator windings I and II. E_{o1} and E_{o2} are voltages appearing across the rotor windings as shown. The axes of the two stator windings are located 90 mechanical degrees apart as are the axes of the two rotor windings. Because of the sinusoidal relationship of flux density in the air gap as a function of angular position of the stator periphery, the following relations hold for open circuit rotor windings.

$$E_{o1} = -E_x \sin \alpha + E_y \cos \alpha \qquad 1\text{-}1$$

$$E_{o2} = E_x \cos \alpha + E_y \sin \alpha \qquad 1\text{-}2$$

In the case of the resolver nulling servo combination as shown in Fig. 1-2, the shaft of the resolver is driven in a direction by the servo motor so as to null E_{o1}. If the nulling servo amplifier has a large enough gain, E_{o1} can, to a first approximation, be considered zero but it is understood that $E_{o1} = 0$ only if the gain of the nulling servo amplifier is infinite. Thus equations 1-1 and 1-2 become

$$E_{o2} = E_x \cos \alpha + E_y \sin \alpha \qquad 1\text{-}2$$

$$0 = -E_x \sin \alpha + E_y \cos \alpha \qquad 1\text{-}3$$

Squaring equation 1-2 and 1-3 and adding, we obtain

$$E_{o2}^2 = E_o^2 = E_x^2 + E_y^2$$

and thus we have our desired result

$$E_{o2} = E_o = \sqrt{E_x^2 + E_y^2} \qquad 1\text{-}4$$

This system as shown in Fig. 1-2 is a true servomechanism and its characteristics will be used later as a comparison showing the differences between this true servomechanism and the closed loop system

to be described in this thesis.

We shall hereby name the proposed system the orthogonal vector component summing system. A simplified diagram is shown in Fig. 1-3.

At this point, we shall neglect the damping and inertia terms and merely show how the steady state result is obtained. In Fig. 1-3 the two inputs E_x and E_y are acted upon by an operating component (oc) such that an output torque is produced on a shaft (torque summing member) which is proportional to the square of the input signals. The shaft rotates through an angle $A_{(rot)}$ to which is attached an operating component such that an output voltage is produced proportional to the angle of rotation. The square root of this voltage is taken and fed to the shaft through a third torque producing device which depends on the square of its actuating input quantity.

In the steady state, that is, assuming all transients have died out, we have the three torques M_1, M_2, and M_3 acting on the shaft.

$$M_1 + M_2 = M_3 \qquad 1\text{-}5$$

or

$$S_{(oc)1}\left[e^2;M\right] E_x^2 + S_{(oc)2}\left[e^2;M\right] E_z^2 = S_{(oc)3}\left[e^2;M\right] E_o^2 \ * \qquad 1\text{-}6$$

Assuming the sensitivities giving torque out for voltage square in are equal, we arrive at the desired result, namely,

$$E_o^2 = E_x^2 + E_y^2$$

$$E_o = \sqrt{E_x^2 + E_y^2} \qquad 1\text{-}7$$

The square root function in the feedback loop cascades with the squaring device to produce a linear device in the feedback

---

* Refer to the Appendix for explanation of terminology used.

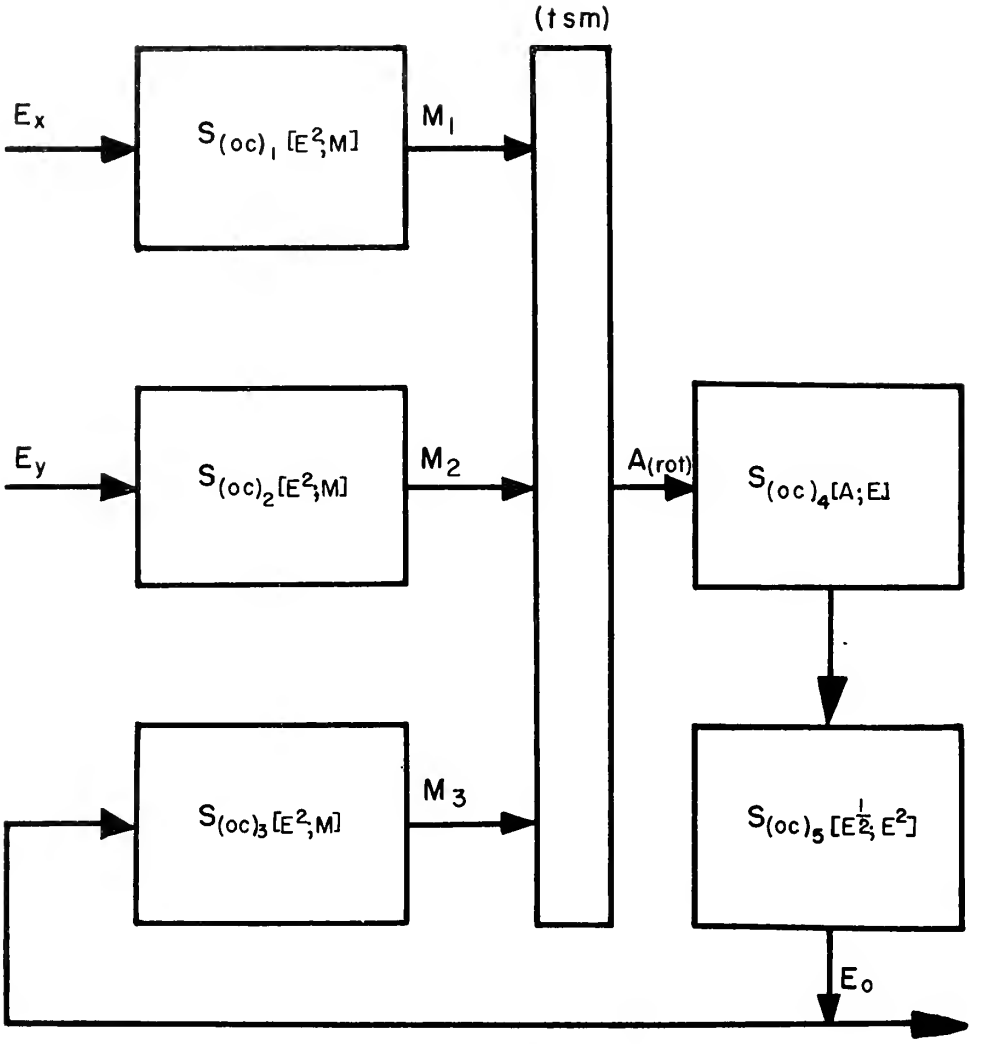

FIGURE 1-3

PROPOSED SYSTEM IN SIMPLIFIED FORM

loop. Equation 1-6 shows the very important result that in the steady state, the correct answer to the problem will be given regardless of the nature of the device used in the feedback loop. However, in the next chapter where the complete performance equations of the system will be developed, we shall show that a perfect square root function is required in the feedback loop if the dynamic qualities of the system are to remain constant. The remainder of this chapter will be devoted to a description and theory of the torque producing generator and the angle input voltage output component commonly called the signal generator.

Both the torque generator and signal generator belong to a family of devices known as microsyn electromagnetic units.[1] These units consist of a laminated ferromagnetic rotor of 180° symmetry with two poles and a laminated ferromagnetic stator of 90° symmetry having four poles about which are wound various arrangements of electrical coils depending upon the application of the unit. For the types of microsyns used in connection with this thesis, the rotor is allowed to rotate $\pm$ 10° from a zero rotor position, which is geometrically defined when a rotor pole is half way between two adjacent stator poles. Fig. 2-4 shows the general construction of a microsyn. torque generator.

The torque generator produces a torque which, in the ideal case, is proportional to the square of the current through one axis and is independent of rotor angular position over the useful range.

$$M_{(tg)} = S_{(tg)}\left[i^2;M\right] i^2 \qquad 1\text{-}8$$

We shall attempt to clarify this relationship from energy considerations in a magnetic field.

As a starting point, we note the fact that the total

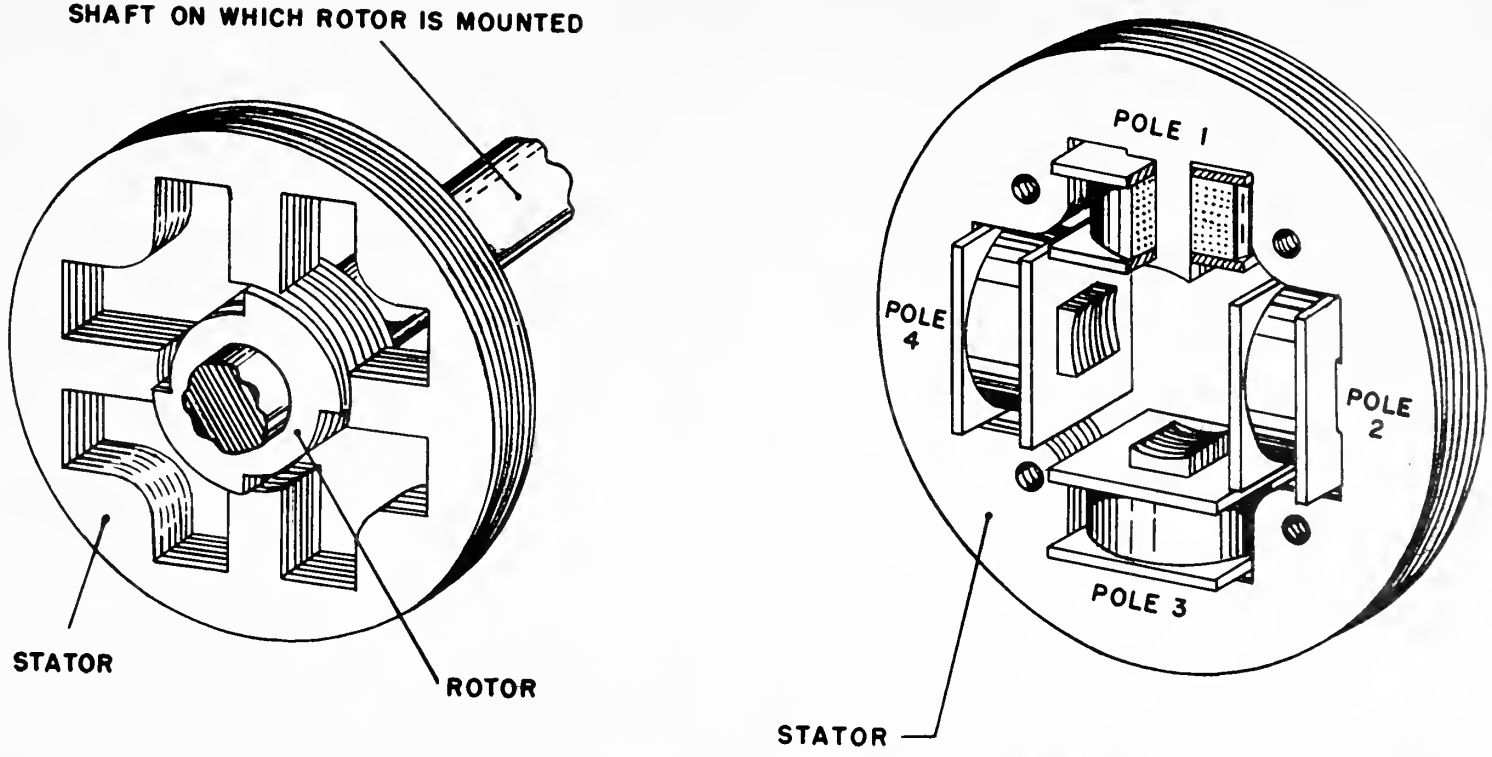

PICTORIAL VIEW OF STRUCTURE OF MICROSYN UNITS

POLE WINDINGS ON MICROSYN UNIT STATOR

FIGURE 1-4

GENERAL FEATURES OF A MICROSYN UNIT

electrical energy into the system equals the magnetically stored energy plus the work done by the system, neglecting heating losses. That is,

$$(E_n)_{(elec)} = (E_n)_{(mag)} + W \qquad 1\text{-}9$$

The instantaneous electric power delivered to the torque producing coil is ei. Thus, after a time t, the electric energy into the system, is

$$(E_n)_{(elec)} = \int_0^t ei\, dt$$

According to Faraday's law

$$e_{(ind)} = - N \frac{d\phi}{dt} \qquad 1\text{-}10$$

where

$e_{(ind)}$ = voltage induced by motion

N = the number of conductors

ϕ = magnetic flux cut by the conductors

Hence

$$(E_n)_{(elec)} = -\int_0^{t_1} N \frac{d\phi}{dt}\, idt = \int_{\phi_1}^{\phi_2} Ni\, d\phi \qquad 1\text{-}11$$

Where

ϕ_1 is flux at t = 0

ϕ_2 is flux at $t = t_1$

We shall go from ϕ_1 to ϕ_2 by two paths as shown in Fig. 1-5. First, following path 1, the current is maintained constant and hence

$$(E_n)_{(elec)} = Ni_1 (\phi_2 - \phi_1) \qquad 1\text{-}12$$

This will correspond to a certain rotation of the rotor to a point corresponding to the flux ϕ_2. Next, following path 2, we let the current drop to zero, and if we neglect any hysteréses

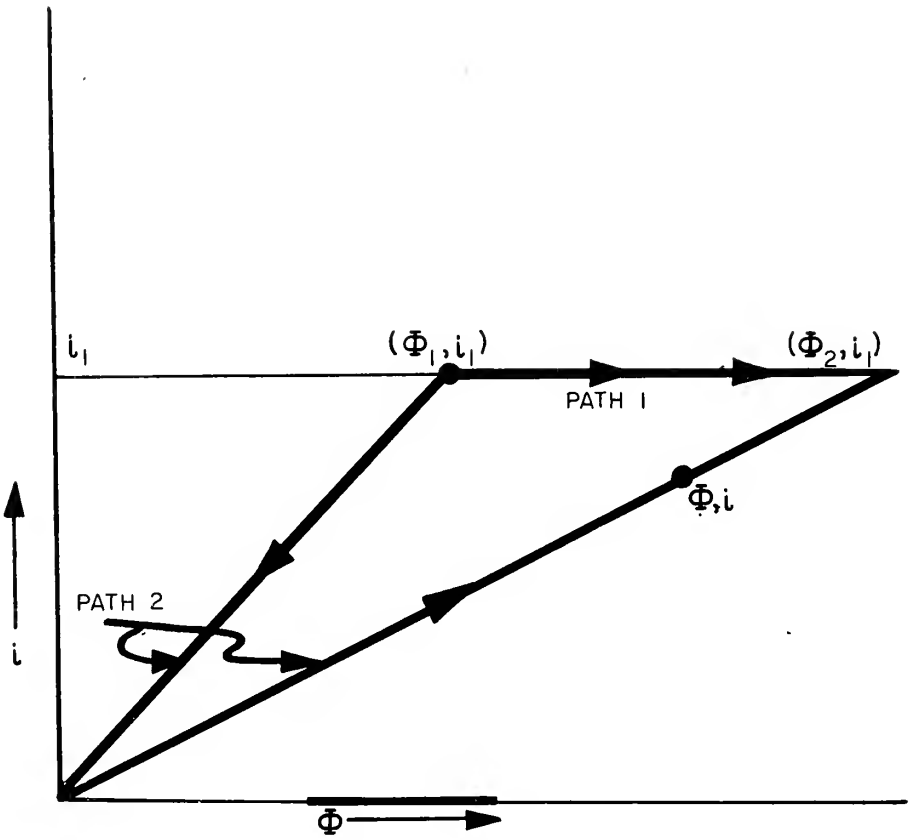

FIGURE 1-5

AMPERES VS. FLUX IN A MAGNETIC MEDIUM

effects, the flux too will drop to zero. At this point the rotor is rotated through the same angle as in the first case. However, no work is done because there is no force. Then the current is increased until the point (ϕ_2, i_1) is reached. In the second case, the magnetic energy can be written in the following form.

$$(En)_{(elec)} = -\int_{\phi_1} Nid\phi + \left[-\int_0^{\phi_2} Nid\phi\right]$$

$$= + N\int_0^{\phi_1} id\phi - N\int^{\phi_2} id\phi \qquad 1\text{-}13$$

Going from ϕ_1 to zero, denote $K_1 = \frac{i}{\phi}$ where K_1 is the slope of this line. Similarly, going from 0 to ϕ_2, denote $K_2 = \frac{i}{\phi}$ the slope of this straight path. Then 1-13 becomes

$$(En)_{(elec)} = NK_1\int_0^{\phi} \phi\, d\phi - NK_2\int_0^{\phi} \phi d\phi \qquad 1\text{-}14$$

But

$$K_1 = \frac{i_1}{\phi_1}, \quad K_2 = \frac{i_1}{\phi_2}$$

Therefore

$$(En)_{(elec)} = N\frac{i_1}{\phi_1}\int_0^{\phi_1}\phi\, d\phi - N\frac{i_1}{\phi_2}\int_0^{\phi_2}\phi d\phi$$

$$\frac{N\, i_1}{2\phi_1}\left[\phi_1^2\right] - \frac{N\, i_1}{2\phi_2}\left[\phi_2^2\right]$$

$$(En)_{(elec)} = \frac{N}{2}\, i_1\ (\phi_1 - \phi_2)$$

or finally

$$(En)_{(elec)} = -\frac{N}{2}\, i_1\ (\phi_2 - \phi_1) \qquad 1\text{-}15$$

Equation 1-12 represents the area under path 1 while 1-15 represents the difference between the areas under the two sections of path 2.

Since 1-15 is exactly half that found in 1-12, we conclude that the mechanical work done and the magnetic energy change are equal in magnitude for a given amount of input electric energy.

The fact that the magnetic energy stored in the magnetic field equals the work done under the conditions previously described enables us to calculate the work done by finding its equivalent in terms of the magnetic energy storage. Then, the torque can be found by taking the derivative of this amount of energy with respect to the rotor angle.

Before proceeding further, we shall make the following assumptions:

1. The reluctance of the magnetic circuit is concentrated almost entirely (over 90%) in the air gaps. As a consequence of this assumption, we shall assume that the entire magnetic drop around the magnetic loop produced by the sources of magnetomotive forces at opposite poles occur essentially across the air gap. Thus, we can assume to a good approximation that all the magnetic energy is stored in the air gap.
2. Leakage flux will be neglected.

From reference (2), the magnetic energy stored in a given volume is given by

$$(E_n)_{(mag)} = \frac{V}{4\pi} \int_{B_1}^{B_2} HdB \qquad 1\text{-}16$$

where V is the volume, B is the flux density. As mentioned above, this energy will be assumed to be stored in the air gap.

Hence:

$$(En)_{(mag)} = \frac{V}{4\pi\mu_o}\int_{B_1}^{B_2} BdB = \frac{V}{8\pi\mu_o}(B_2^2 - B_1^2) \qquad 1\text{-}17$$

where is the permitivity of air in MKS units.

$$(En)_{(mag)} = \frac{LA}{8\pi\mu_o}\frac{1}{A^2}(\phi_2^2 - \phi_1^2) = \frac{L}{8\pi\mu_o A}(\phi_2^2 - \phi_1^2) \qquad 1\text{-}18$$

where L is the distance between the rotor and stator.

A is total area between the rotor and the two opposite stators. Since

$$\phi = \frac{\text{mmf}}{\text{reluctance}} = \frac{\text{mmf}}{R_{(mag)}}$$

$$(En)_{(mag)} = \frac{L}{8\pi\mu_o A}\frac{1}{R^2_{(mag)}} \quad (\text{change in mmf})^2$$

$$= \frac{\mu_o A\, U_{(mag)}^2}{8\pi L} \qquad 1\text{-}19$$

where $U_{(mag)}$ is the magnetic drop across the air gaps. This drop equals to a good approximation the impressed magnetomotive forces.

Since mmf = $4\pi Ni$, we have finally

$$(En)_{(mag)} = \frac{2\pi\mu AN^2 i^2}{L} = W \quad N=\text{no. turns} \qquad 1\text{-}20$$

The torque M then is $\frac{\partial W}{\partial A_{(rot)}}$ where $A_{(rot)}$ is the rotor angle.

Thus it is shown that the torque is proportional to the current squared. An important consequence of 1-20 is the torque is independent of the direction of the current. Thus alternating current can be used as well as direct current to provide torques. This also shows why only absolute values of E_x and E_y can be considered in the orthogonal vector summing system.

The change of area A has a linear relationship to a change in rotor angle $A_{(rot)}$. Thus 1-20 becomes

$$(En)_{(mag)} = W = \frac{2\pi \mu_o KAN^2 i^2}{L} = \frac{2\pi \mu_o N^2 i^2 K A(rot)}{L}$$

where K can be calculated from the dimensions of the particular microsyn.

Finally,

$$M_{(tg)} = \frac{\partial W}{\partial A(rot)} = \frac{2\pi \mu_o KN^2 i^2}{L} = S_{(tg)}\left[i^2;M\right] i^2 \qquad 1\text{-}21$$

where we shall define

$$S_{(tg)}\left[i^2;M\right] = \frac{2\pi \mu_o KN^2}{L}$$

The signal generator provides an open circuit voltage which is proportional to the amount of angular rotation of the rotor from its null position. Thus

$$e(sg) = S_{(sg)}\left[A;e\right] A(rot) \qquad 1\text{-}22$$

Fig. 1-6 shows the details of the signal generator. There are two windings per stator pole and these windings are connected in two series circuits, each circuit using a similar set of windings. The primary circuit is excited by an alternating current which sets up flux patterns as shown. If the previously mentioned torque generator has equal excitation currents on both axes, the flux pattern will be the same as that set up by the primary excitation current of the signal generator and thus the resultant torque on the signal generator is zero since the torques on the two axes are equal and opposite. There will be no torque contribution from the secondary winding since this winding will carry no current. The series windings of the secondary

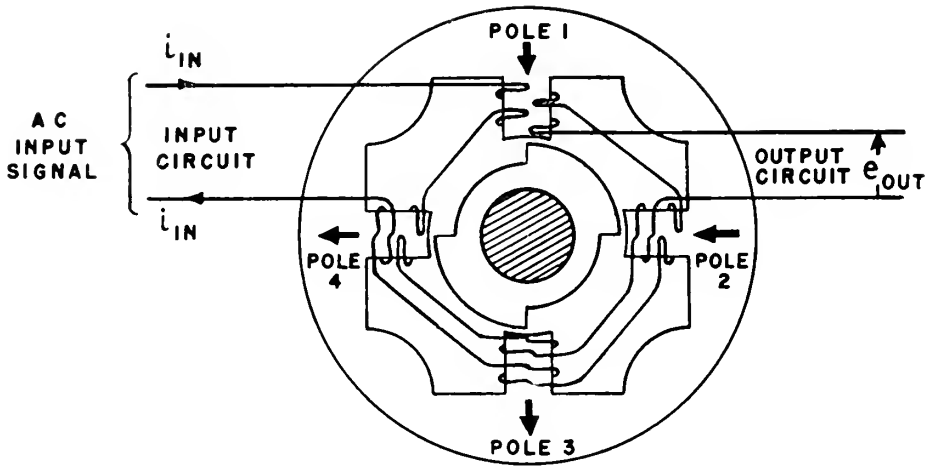

NOTE:

1. HEAVY ARROW ON EACH POLE INDICATES DIRECTION OF POLE FLUX WHEN INSTANTANEOUS DIRECTION OF i_{IN} IS THAT SHOWN.
2. ALL INPUT COIL WINDINGS HAVE THE SAME NUMBER OF TURNS AND ALL OUTPUT COIL WINDINGS HAVE THE SAME NUMBER OF TURNS.

FIGURE 1-6

MICROSYN SIGNAL GENERATOR

coils are so arranged that the instantaneous induced voltages in these secondaries are added in opposite phase for adjacent poles.

Thus,

$$e_{(out)_{(sg)}} = (E_1 + E_3) - (E_2 + E_4) \qquad 1\text{-}23$$

where E_n is the rms induced voltage in coil n. n = 1, 2, 3, or 4

When the rotor is in its null position (i.e. midway between two adjacent stator poles), we see from 1-23 that the signal generator output voltage is zero because all the induced secondary voltages are zero due to the symmetry of the system.

A positive rotation of the rotor will be defined as a rotation tending to increase the overlap area between the rotor and stator poles 2 and 4 and correspondingly, to decrease the overall overlap between the rotor and poles 1 and 3, as shown on Fig. 1-6. Thus, for a positive rotation, the reluctance of the magnetic circuit including poles 1 and 3 increases while that of 2 and 4 decreases. Hence, since the magnetomotive force at all the poles is constant, the flux in poles 1 and 3 decreases while that of 2 and 4 increases. It is to be noted that the change in reluctance and therefore the change in flux is a linear function of rotor angle. The induced root mean square voltages are proportional to the flux for constant excitation frequency. Thus for a positive rotation, the induced voltages in poles 2 and 4 are the larger and the output voltage has a phase similar to the phase of the voltages in poles 2 and 4. For negative rotations, $e_{(out)}$ is of opposite phase and of magnitude given by 1-23.

The flux in the poles of the signal generator have very nearly the same phase as that of the alternating excitation current, the only difference in phase being that attributable to the core losses.

This flux is directly proportional to the number of primary coil turns, and the magnitude of the excitation current and inversely proportional to the circuit reluctance. The secondary induced voltage has a 90° phase shift with respect to the flux and its value is proportional to the magnitude of the flux, number of secondary turns, and excitation frequency. We can thus define the output voltage as

$$e_{(out)} = S_{(sg)}\left[A;i,n;e\right] i_{(ex)}\, n_{(ex)}\, A_{(rot)} \qquad 1\text{-}24$$

$$\doteq S_{(sg)}\left[A;e\right] A_{(rot)}$$

where

$$S_{(sg)}\left[A;i,n;e\right] i_{(ex)}\, n_{(ex)} = S_{(sg)}\left[A;e\right]$$

when the excitation current and frequency are fixed, and $A_{(rot)}$ is the angle of the rotor measured from the null position with a positive rotation having been already defined as a rotation which increases the area under poles 2 and 4.

CHAPTER II

Proposed Ideal System

The orthogonal vector summing system to be described in this chapter will be considered ideal for the following reasons: First, the square root generator will be considered as producing an exact square root over the entire operating range. Second, all uncertainty torques such as those attributable to friction, hysteresis, leakage flux, plus interfering torques such as the acceleration of the case with respect to inertial space will be neglected.

Fig. 2-1 shows a line schematic diagram of the proposed assembly and Fig. 2-2 shows a functional diagram of the orthogonal vector summing system. Since this thesis is intended to be primarily a study of the dynamics associated with the proposed system, the description of the actual assembly will be mainly to establish a clear picture of what physical processes are actually taking place. The analysis to follow will be largely mathematical, but nevertheless the physical interpretation of the derived performance equations will be continually stressed.

The assembly shown in line schematic form in Fig. 2-1 is mounted inside a sealed cyclindrical container and designed to operate in an upright position. The torque summing shaft contains the rotors of the microsyn units as well as the rotor of the viscous damper. The fluid in addition to providing a damping torque, also serves to reduce friction torques at the pivots by buoying up the shaft by a sufficient amount to remove the weight of the shaft from the pivots. A float is

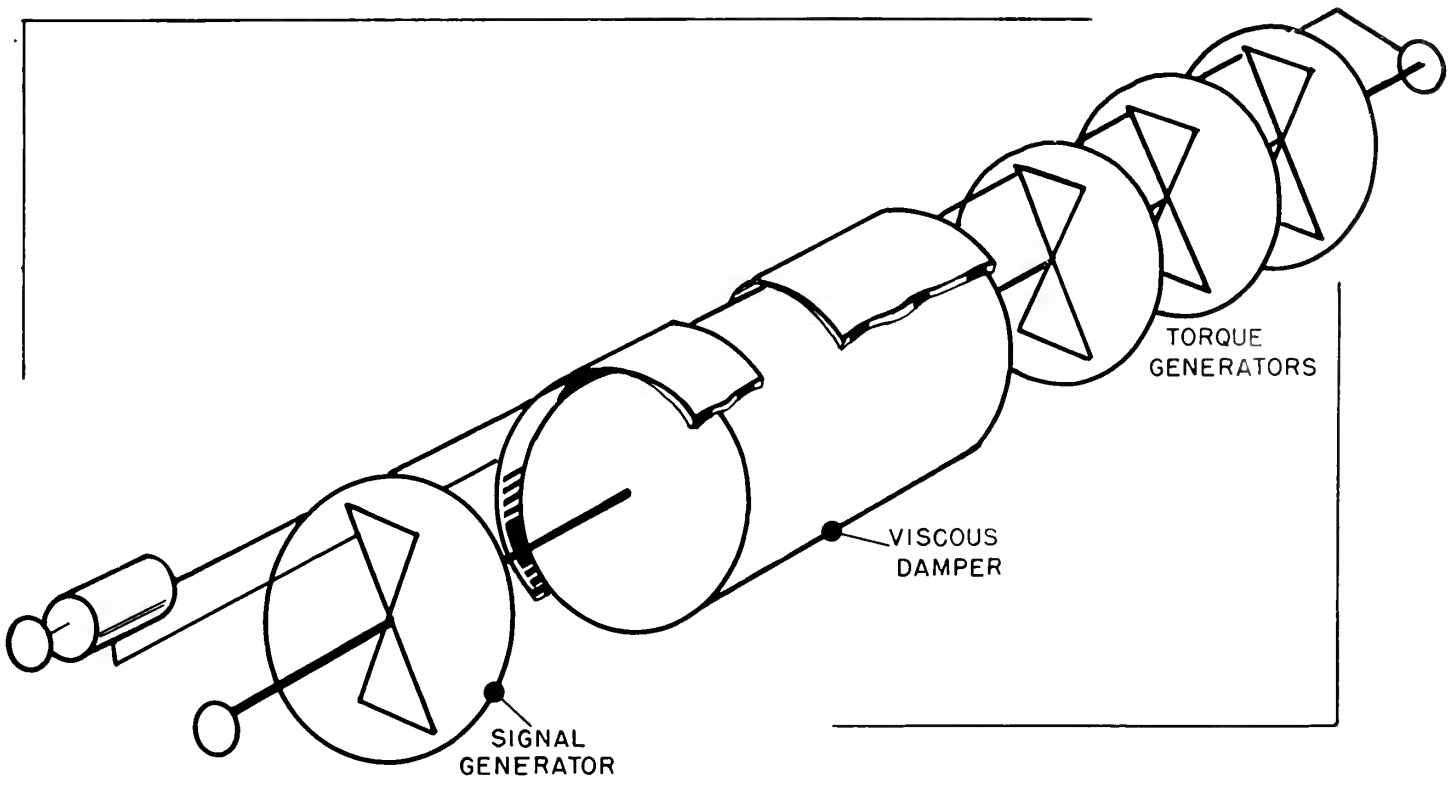

FIGURE 2-1

LINE SCHEMATIC DIAGRAM OF THE ORTHOGONAL VECTOR SUMMING SYSTEM

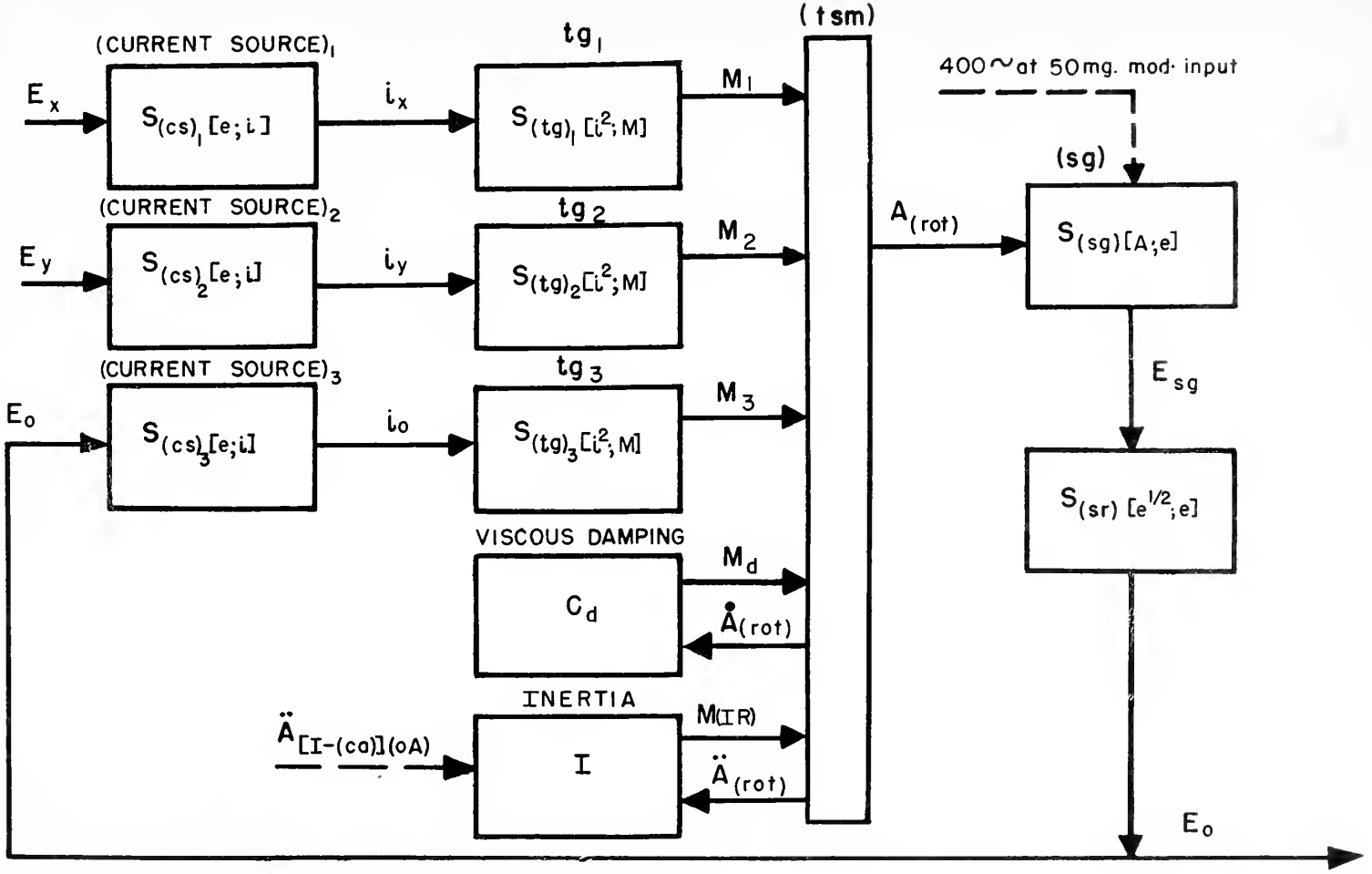

FIGURE 2-2

FUNCTIONAL DIAGRAM OF IDEAL ORTHOGONAL VECTOR SUMMING SYSTEM

clamped to the shaft to provide the necessary amount of lift. The damper consists of two concentric cylindrical surfaces one of which rotates with the shaft while the other surface is fixed to the case. A damper adjustment is provided which changes the amount of surface between the concentric cylinders. Because the viscosity of the damping fluid is critically dependent upon temperature, the unit is maintained at a constant temperature plus or minus a certain tolerance by means of electrically heated coils. A thermostat is provided which sets up a cycling process in the application of electric power to the heating coils. A portion of Chapter V will be devoted to an analysis of how changes in damping effects the dynamics of the system, and thus determine criteria for specifying how well the temperature must be regulated.

We shall now develop in detail the performance equations for the ideal system referring to Fig. 2-2. Because of the fact that we shall regard the input signals as voltages, a current source has been provided to drive each of the torque generators.

By Newton's second law, the product of the moment of inertia of the shaft plus rotors times the angular acceleration of the shaft equals the sum of the torques applied to the shaft.

$$I(\tilde{A}\left[I-(ca)\right]\ (OA) + \ddot{A}_{(rot)}) = C_{d(vis)}\ \dot{A}_{(rot)} + M_{(tg)_1} + M_{(tg)_2} + M_{(tg)_3} \qquad 2\text{-}1$$

Where I = moment of inertia of shaft including rotors of the damper and microsyn units.

$A_{(rot)}$ = angle through which a rotor has turned from its null position. We shall assume all rotors are lined up to

have the same null angle with respect to case coördinates. A positive rotation of $A_{(rot)}$ has been defined as that direction tending to increase the overlap area between the rotor and stator poles 2 and 4.

$\ddot{A}\left[I-(ca)\right]$ (OA) = the component of angular acceleration of the case with respect to inertial space about the output axis, that is, about the direction indicated by a line parallel to the shaft.

C_d = The damping coefficient of the system consisting of the following two parts: $C_{d(fixed)}$, the damping coefficient of the fixed section of the viscous damper and $C_{d(var)}$ the variable section of the viscous damper.

Torque generator 1 and torque generator 2 will be actuated by the input signals and will be defined as producing positive torques, i.e. torques tending to produce a positive rotation of shaft angle. On the other hand, torque generator 3 will be actuated by the output of the system and will be designed to produce a negative torque.

Rearranging 2-1,

$$I\,\ddot{A}_{(rot)} + C_d\,\dot{A}_{(rot)} - M(tg)_3 = M(tg)_1 + M(tg)_2 - I\,\ddot{A}\left[I-(ca)\right]\ (OA) \qquad 2\text{-}2$$

From chapter I, we have defined

$$M(tg) = S(tg)\left[i^2;M\right] i^2 \qquad 2\text{-}3$$

Define $S(cs)\left[e;i\right] = \frac{i}{e}$, sensitivity of the current source for voltage input current output. Hence

$$M(tg) = S(tg)\left[i^2;M\right] S^2(cs)\left[e;i\right] E^2 \qquad 2\text{-}4$$

Define $S_{(sr)}\left[e^{\frac{1}{2}};e\right] = \frac{E_o}{E(sg)^{\frac{1}{2}}}$, sensitivity of square root generator for $(\text{voltage})^{\frac{1}{2}}$ in, voltage out.

From Chapter I, we have defined the signal generator sensitivity as $S_{(sg)}\left[A;e\right] = \frac{E_{sg}}{A}$ where

$$S_{(sg)}\left[A;e\right] = S_{(sg)}\left[A;i,n,e\right] \; i_{(ex)} \; n_{(ex)}$$

where $i_{(ex)}$ is the excitation current of the signal generator primary winding and $n_{(ex)}$ is the frequency of the excitation current.

Using the above definitions for the parameters of the system, 2-2 becomes

$$I\,\ddot{A}_{(rot)} + C_d\,\dot{A}_{(rot)} + S_{(tg)_3}\left[i^2;M\right] S^2_{(cs)_3}\left[e;i\right] \; E_o^2 =$$

$$S_{(tg)_1}\left[i^2;M\right] S^2_{(cs)_1}\left[e;i\right] \; E_x^2 + S_{(tg)_2}\left[i^2;M\right] S^2_{(cs)_2}\left[e;i\right] E^2 y$$

$$- I\,\ddot{A}\left[I\text{-}(ca)\right] \; (OA) \qquad 2\text{-}5$$

Since

$$S_{(tg)_1} = S_{(tg)_2} = S_{(tg)_3} = S_{(tg)}$$

and

$$S_{(cs)_1} = S_{(cs)_2} = S_{(cs)_3} = S_{(cs)},$$ 2-3 becomes

$$I\,A_{(rot)} + C_d\,\dot{A}_{(rot)} + S_{(tg)}\left[i^2;M\right] S^2_{(cs)}\left[e;i\right] \; E_o^2 =$$

$$S_{(tg)}\left[i^2;M\right] S^2_{(cs)}\left[e;i\right] \left(E_x^2 + E_y^2\right)$$

$$- I\,\ddot{A}\left[I\text{-}(ca)\right] \; (OA) \qquad 2\text{-}6$$

Also,

$$E_o^2 = S^2_{(sr)}\left[e^{\frac{1}{2}};e\right] \; S_{(sg)}\left[A;e\right] \; A_{(rot)} \qquad 2\text{-}7$$

Using 2-7 and defining

$$S_{(ovss)}[A;M] = S_{(tg)}[i^2,M]\, S^2_{(cs)}[e;i]\, S^2_{(sr)}[e^{\frac{1}{2}};e] \cdot S_{(sg)}[A;e] \qquad 2\text{-}8$$

the sensitivity of the orthogonal vector summing system for shaft angle input torque output,

2-6 becomes finally

$$I\,\ddot{A}_{(rot)} + C_d\,\dot{A}_{(rot)} + S_{(ovss)}[A;M]\,A_{(rot)} = S_{(tg)}[i^2;M]\, S^2_{(cs)}[e;i] \left(E_x^2+E_y^2\right) - I\,\ddot{A}\,[I-(ca)]^{(OA)} \qquad 2\text{-}9$$

In the discussion of the ideal system to follow, we shall assume that the acceleration of the case with respect to inertial space is zero. This acceleration produces an uncertainty torque which will alter the desired result. Thus, equation 2-9 simplifies to

$$I\,\ddot{A}_{(rot)} + C_d\,\dot{A}_{(rot)} + S_{(ovss)}[A;M]\,A_{(rot)} = S_{(tg)}[i^2;M]\, S^2_{(cs)}[e;i] \left(E_x^2 + E_y^2\right) \qquad 2\text{-}10$$

Relating $A_{(rot)}$ and E_o^2 and the derivatives, we obtain

$$A_{(rot)} = \frac{E_o^2}{S^2_{(sr)}[e^{\frac{1}{2}};e]\; S_{(sg)}[A;e]}$$

$$\dot{A}_{(rot)} = \frac{\dot{E}_o^2}{S^2_{(sr)}[e^{\frac{1}{2}};e]\; S_{(sg)}[A;e]}$$

$$\ddot{A}_{(rot)} = \frac{\ddot{E}_o^2}{S^2_{(sr)}[e^{\frac{1}{2}};e]\; S_{(sg)}[A;e]} \qquad 2\text{-}11$$

where the independence of the sensitivities of the signal generator and square root generator with time are assume for the range of frequencies to be considered in this thesis. This statement will be

clarified later.

Using the above expressions for $A_{(rot)}$ and its derivatives,

$$I \frac{d^2}{dt^2} E_o^2 + C_d \frac{d}{dt} E_o^2 + S_{(ovss)}[A;M] E_o^2 = S_{(ovss)}[A;M] (E_x^2 + E_y^2) \qquad 2\text{-}12$$

or

$$\frac{I}{S_{(ovss)}[A;M]} \frac{d^2}{dt^2} E_o^2 + \frac{C_d}{S_{(ovss)}[A;M]} \frac{d}{dt} E_o^2 + E_o^2 = E_x^2 + E_y^2 \qquad 2\text{-}13$$

Equation 2-13 is a linear differential equation of the second order with constant coefficients in the ideal case. Using the standard form of the second order linear equation, we have

$$\frac{1}{W_n^2} \frac{d^2}{dt^2} E_o^2 + \frac{2(DR)_{(ovss)}}{W_n} \frac{d}{dt} E_o^2 + E_o^2 = E_x^2 + E_y^2 \qquad 2\text{-}14$$

where W_n = the natural radian frequency of the system.

$(DR)_{(ovss)}$ = the ratio of the amount of damping present in the system to that amount required for critical damping.

(DR) and W_n, when known for a second order system, completely determine its dynamic behavior. Comparing 2-13 and 2-14, we obtain,

$$\frac{1}{W_n^2} = \frac{I}{S_{(ovss)}[A;M]}$$

or

$$W_n = \sqrt{\frac{S_{(ovss)}[A;M]}{I}} \qquad 2\text{-}15$$

$$\frac{2(DR)_{(ovss)}}{W_n} = \frac{C_d}{S_{(ovss)}[A;M]}$$

or

$$(DR)_{(ovss)} = \frac{C_d}{2} \sqrt{\frac{1}{I\, S_{(ovss)}[A;M]}} \qquad 2\text{-}16$$

Since the two input quantities E_x and E_y react upon the shaft through identical operating components, we can let $E_x^2 + E_y^2 = E_{in}^2$ in further discussion of the dynamics of the system without any loss in generality. Thus, 2-13 becomes

$$\frac{I}{S_{(ovss)}\left[A;M\right]} \frac{d^2}{dt^2} E_o^2 + \frac{C_d}{S_{(ovss)}\left[A;M\right]} \frac{d}{dt} E_o^2 + E_o^2 = E_{in}^2 \qquad 2\text{-}17$$

or its equivalent form

$$\frac{1}{W_n^2} \frac{d^2}{dt^2} E_o^2 + \frac{2(DR)}{W_n} \frac{d}{dt} E_o^2 + E_o^2 = E_{in}^2 \qquad 2\text{-}18$$

Where E_{in} is understood to be a function of time.

In the steady state, 2-10 becomes,

$$S_{(ovss)}\left[A;M\right] A_{(rot)} = S_{(tg)}\left[i^2;M\right] S^2_{(cs)}\left[e;i\right]\left(E_x^2 + E_y^2\right) \qquad 2\text{-}19$$

or

$$S^2_{(sr)}\left[e^{\frac{1}{2}};e\right] S_{(sg)}\left[A;e\right] A_{(rot)} = E_x^2 + E_y^2 \qquad 2\text{-}20$$

From the steady state value of 2-13 we obtain

$$E_o^2 = E_x^2 + E_y^2 = S^2_{(sr)}\left[e^{\frac{1}{2}};e\right] S_{(sg)}\left[A;e\right] A_{(rot)} \qquad 2\text{-}21$$

Thus, it can be seen that E_o^2 and hence E_o, is not critically dependent upon the value of $A_{(rot)}$. If the product, $S^2_{(sr)}\left[e^{\frac{1}{2}};e\right] S_{(sg)}\left[A;e\right]$ is changed, $A_{(rot)}$ merely readjusts itself, within its constraints of 10^o, to a new steady state value corresponding to the required steady state value of E_o^2. However, it is very important to note at this point that a change in the product, $S^2_{(sr)}\left[e^{\frac{1}{2}};e\right] S_{(sg)}\left[A;e\right]$, does not alter the steady state conditions, the dynamics of the system are definitely altered as can be seen from 2-13, 2-15 and 2-16. The fact that a perfect square root function cannot be generated means that the sensitivity product will be continually varying over the operating range and the next chapter will go into the

details of the relationship between the dynamics of the system and the nonlinear device. It is to be noted here that the torque generator can be regarded as an almost perfect squaring device for the range of actuating currents used here. That is, the B-H curve is linear for the range of currents used, (0 to 40 ma) but there are small uncertainty torques due mainly to hysterises and to reaction torques. Reaction torques are present when the torque produced is not completely independent of rotor angle. For the present, uncertainty torques will be neglected.

When the sensitivity product $S^2_{(sr)}\left[e^{\frac{1}{2}};e\right]\ S_{(sg)}\left[A;e\right]$ is made very high, $A_{(rot)}$ decreases to a point where it becomes essentially an error signal analogous to that of a conventional servomechanism, similar to that shown in Chapter I. The system will be analyzed and designed, however, from the viewpoint that $A_{(rot)}$ can be made to cover the full 10^o. This condition is what makes this system unique from the conventional servo systems.

A very important point on the stability of the system must now be brought up. At the null position, a condition of instability exists such that if $A_{(rot)}$ goes the least bit negative, the system drives itself into the stops provided just above the 10^o mark of rotation.

Fig. 2-4 shows a stable condition where the rotor has rotated through a positive angle. The rotor has rotated to a position so that the signal which it produces causes a current i_o to be equivalent to i_{in} and thus the positive torque produced by i_{in} equals the negative torque produced by i_o. If $A_{(rot)}$ by some disturbance goes to $A_{(rot)} + d\ A_{(rot)}$ with i_{in} the same, then i_o goes to $i_o + d\ i_o$ and produces a torque tending to pull $A_{(rot)} + d\ A_{(rot)}$ back to its initial

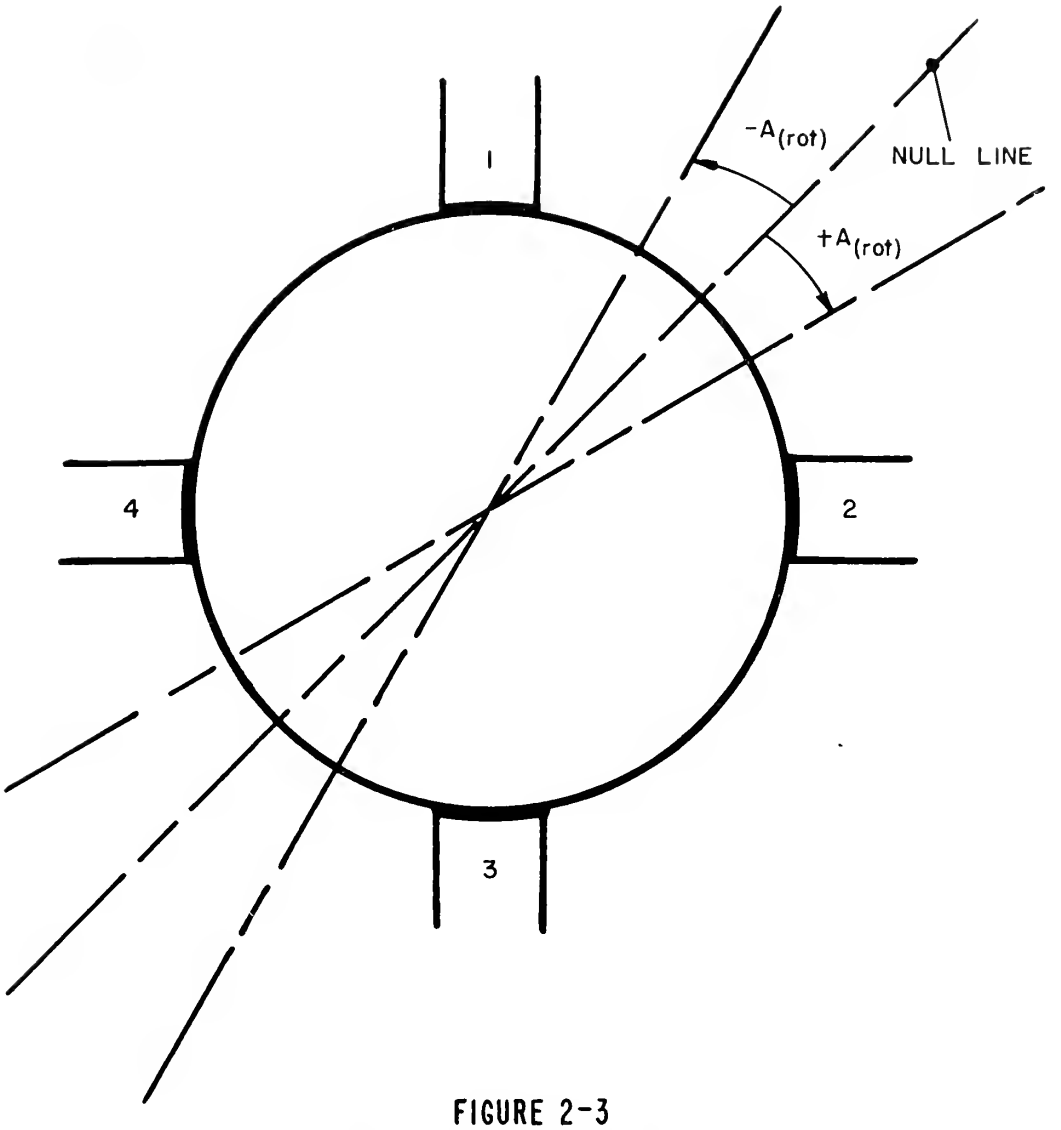

FIGURE 2-3

POSITIVE AND NEGATIVE SHAFT ANGLES

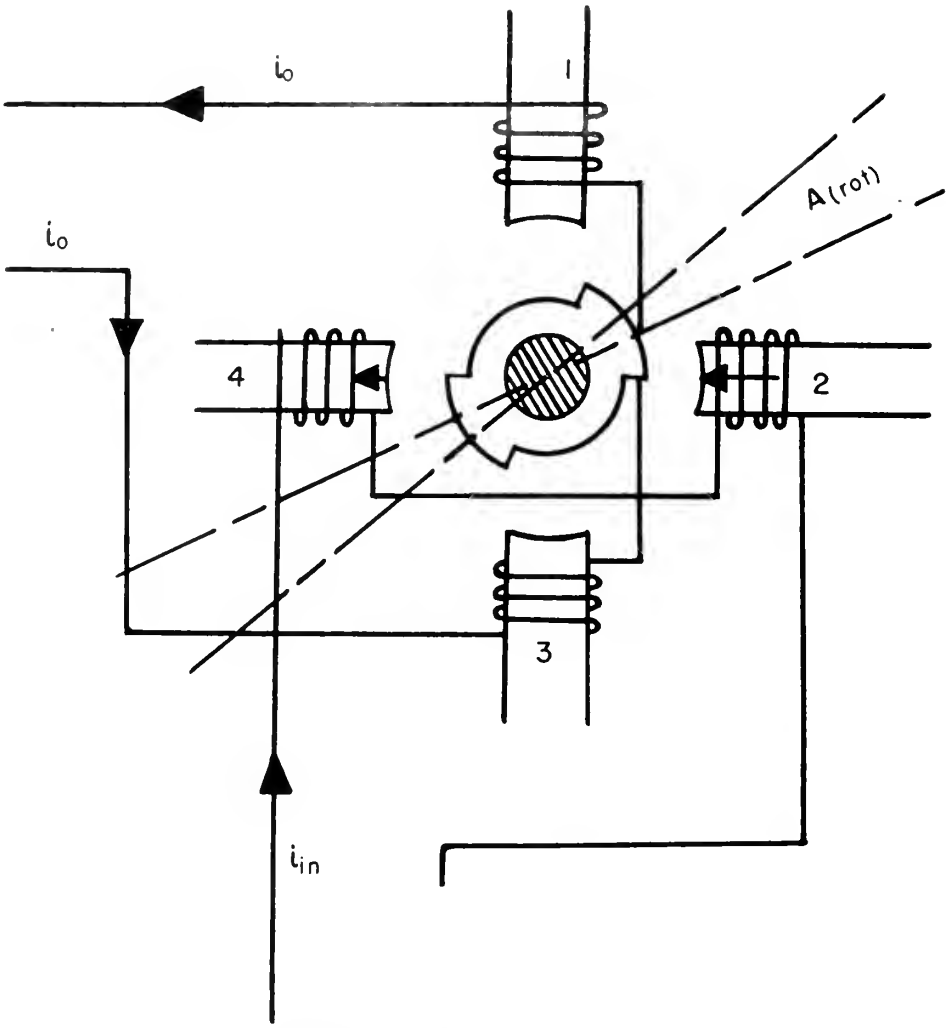

FIGURE 2-4

TORQUE GENERATOR IN STABLE REGION

value of $A_{(rot)}$. If $A_{(rot)}$ is disturbed to a position $A_{(rot)} - d\,A_{(rot)}$ i_{in} constant, then i_o becomes $i_o - d\,i_o$ and the torque produced in the 1, 3 axis is reduced thus allowing $A_{(rot)} - d\,A_{(rot)}$ to rotate back to $A_{(rot)}$. This again clearly shows the stable condition of Fig. 2-4. The configuration shown by Fig. 2-4 corresponds to a potential minimum which, of course, will thus yield a stable system.

Fig. 2-5 shows the condition of instability. Assume, initially the conditions of Fig. 2-5. $-A_{(rot)}$ produces a signal which will produce the same current, i_o, as $+ A_{(rot)}$. The condition as shown can exist just like a pendulum at the top of its arc. However, if $- A_{(rot)}$ is disturbed to a position, $-(A_{(rot)} + d\,A_{(rot)}) = - A_{(rot)} - d\,A_{(rot)}$, i_o goes to $i_o + d\,i_o$ thus increasing the negative torque which in turn increases $- A_{(rot)}$ and the system will rotate negatively until finally hitting the stops. On the other hand, if $- A_{(rot)}$ is disturbed to $- (A_{(rot)} - d\,A_{(rot)})$ or $- A_{(rot)} + d\,A_{(rot)}$, i_o goes to $i_o - d\,i_o$ and the negative torque produced by i_o is decreased thus tending to further reduce $- A_{(rot)}$ until the null is reached. A positive angle is built up on the stable side until finally the condition of Fig. 2-4 is reached. Here, we have represented a potential maximum condition, it being similar to a physical pendulum at the top of its arc. The slightest disturbance in either direction results in drastic changes in the motion of both the given computing system and the pendulum.

As a third case, assume initially there is no input excitation and $A_{(rot)} = 0$. Next assume i_{in} builds up linearly from zero. As i_{in} builds up from 0 to $d\,i_{in}$, there is a positive torque produced by the current flowing in coils 2 and 4 (see Fig. 2-4). At the same time, there is no current i_o in coils 1 and 3 and hence no negative torque

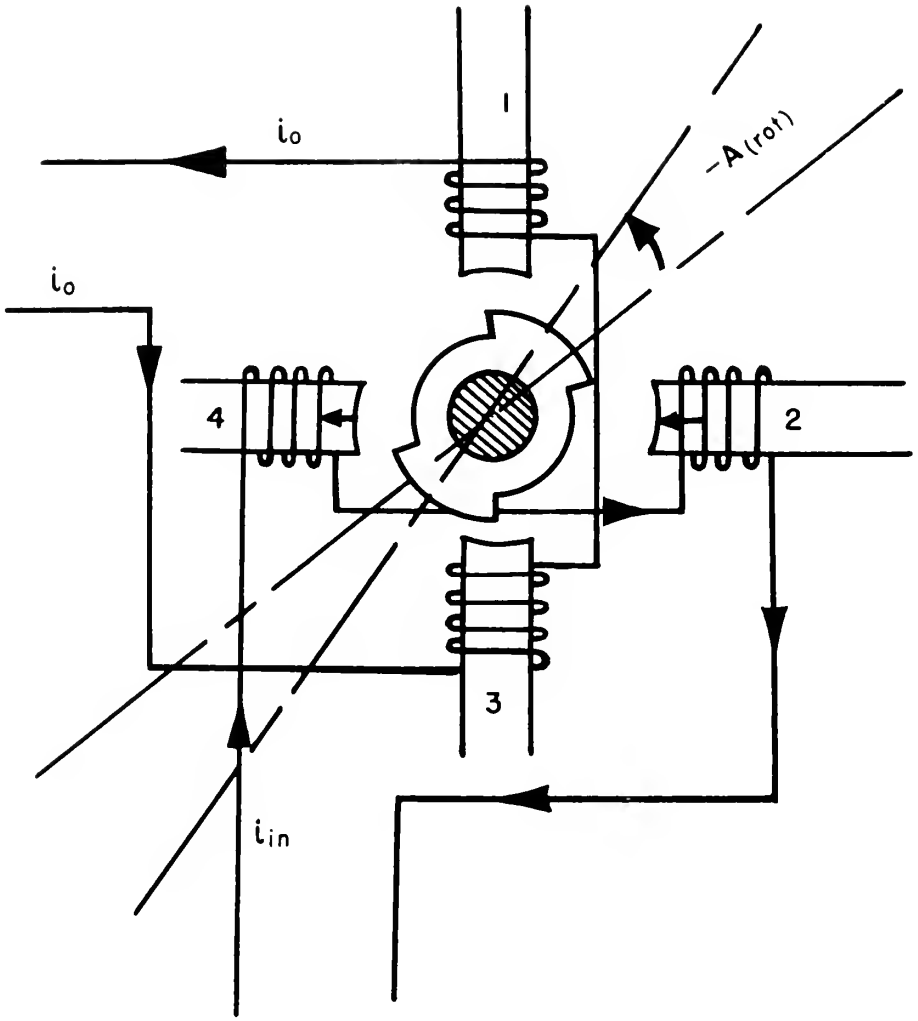

FIGURE 2-5

THE UNSTABLE REGION OF SHAFT ROTATION

is produced. This assures a positive rotation and a stable condition.

Finally, consider the case where $A_{(rot)} = 0$ and $i_{in} = 0$. If $A_{(rot)}$ is disturbed to a position $- d A_{(rot)}$, there results a signal producing an output current $d i_o$ and a negative torque which will increase the negative angle. Thus, we have the unstable case where $A_{(rot)}$ progressively increases until the stops are reached.

We conclude from the above analysis that a constraint has to be applied to the shaft so that negative angles as shown in Fig. 2-4 cannot be built up. If the constraint in the form of a mechanical stop is placed exactly at the null, then the system will produce an E_o for E_x and E_y even in the limit as E_x and E_y both approach zero. If the stop, however, is placed at a point allowing a small negative angle $- d A_{(rot)}$, then the chances are that initially the rotor will have passed into this negative region in the absence of input signals as was pointed out in the last case of instability. Thus, it will take a positive torque produced by the input signals just barely greater than the negative torque produced by $- d A_{(rot)}$ in the feedback loop to rotate the shaft into the stable region. It is difficult physically to put a stop exactly at the null, and in the last chapter it will be shown why a stop can be put on the positive side of the shaft rotation and still be able to solve the orthogonal vector addition even as the input signals approach zero. This method will be feasible, however, only if the swing of $A_{(rot)}$ is fairly large in comparison to the angular position of the constraint, and also a certain amount of tolerance is allowed on the dynamical characteristics of the system.

Equation 2-18, while linear when expressed in terms of the squares of the input and output signals, is nonlinear when expressed in terms of the input and output signals themselves.

An insight into the complexity of the nonlinear form of 2-18 can be gained if it is rewritten as follows.

$$\frac{d}{dt} E_o^2 = 2E_o \frac{dE_o}{dt}$$

$$\frac{d^2}{dt^2} E_o^2 = 2E_o \frac{d^2E_o}{dt^2} + 2\left(\frac{dE_o}{dt}\right)^2$$

Hence 2-18 becomes, upon rearranging,

$$E_o \frac{d^2E_o}{dt^2} + \left(\frac{dE_o}{dt}\right)^2 + 2(DR) W_n E_o \frac{dE_o}{dt} + \frac{W_n^2}{2} E_o^2 = \frac{W_n^2}{2} E_{in}^2(t) \quad 2\text{-}22$$

It is to be emphasized here that W_n and (DR)refer only to the linear second order system defining the square of the actual input and output quantities. Since the linear equation defining E_o^2 is convenient to use, practically all the information to be obtained from the system will be in terms of the squared functions. The last step will then be to analyze the square root of the response function associated with the linear second order equation.

CHAPTER III

The Square Root Generator Problem

The performance equations of Chapter II were developed assuming an ideal square root generator in the feedback loop. As we have already mentioned, it is very difficult to find in nature a physical device that will generate such a curve as shown in Fig. 3-1, although of course, there do exist many non-linear devices or means of synthesizing such devices.

Equation 2-8 defines the overall sensitivity of the system as

$$S_{(ovss)}\left[A;M\right] = S_{(tg)}\left[i^2;M\right]\ S^2_{(cs)}\left[e;i\right]\ S^2_{(sr)}\left[e^{\frac{1}{2}};e\right]\ S_{(sg)}\left[A;e\right]$$

Since the torque generator follows a rather precise square curve for the range of currents used, only a perfect square root function will maintain $S_{(ovss)}\left[A;M\right]$ constant over the entire range. Physically, $S_{(ovss)}\left[A;M\right]$ is analogous to the spring constant $K_{(sp)}$ of a mechanical harmonic oscillator. This is shown clearly in the equations for the natural frequency and damping ratio where

$$W_n \quad \sqrt{\frac{S_{(ovss)}\left[A;M\right]}{I}}$$

$$(DR)_{(ovss)} = \frac{C_d}{2}\sqrt{\frac{1}{I\ S_{(ovss)}\left[A;M\right]}}$$

where W_n and $(DR)_{(ovss)}$ refer to the performance equation relating the squares of the input and output functions. It is to be noted again here that the static output of the system is not dependent upon $S_{(ovss)}\left[A;M\right]$. If instead of a square root function we had a linear function, $S_{(ovss)}\left[A;M\right]$

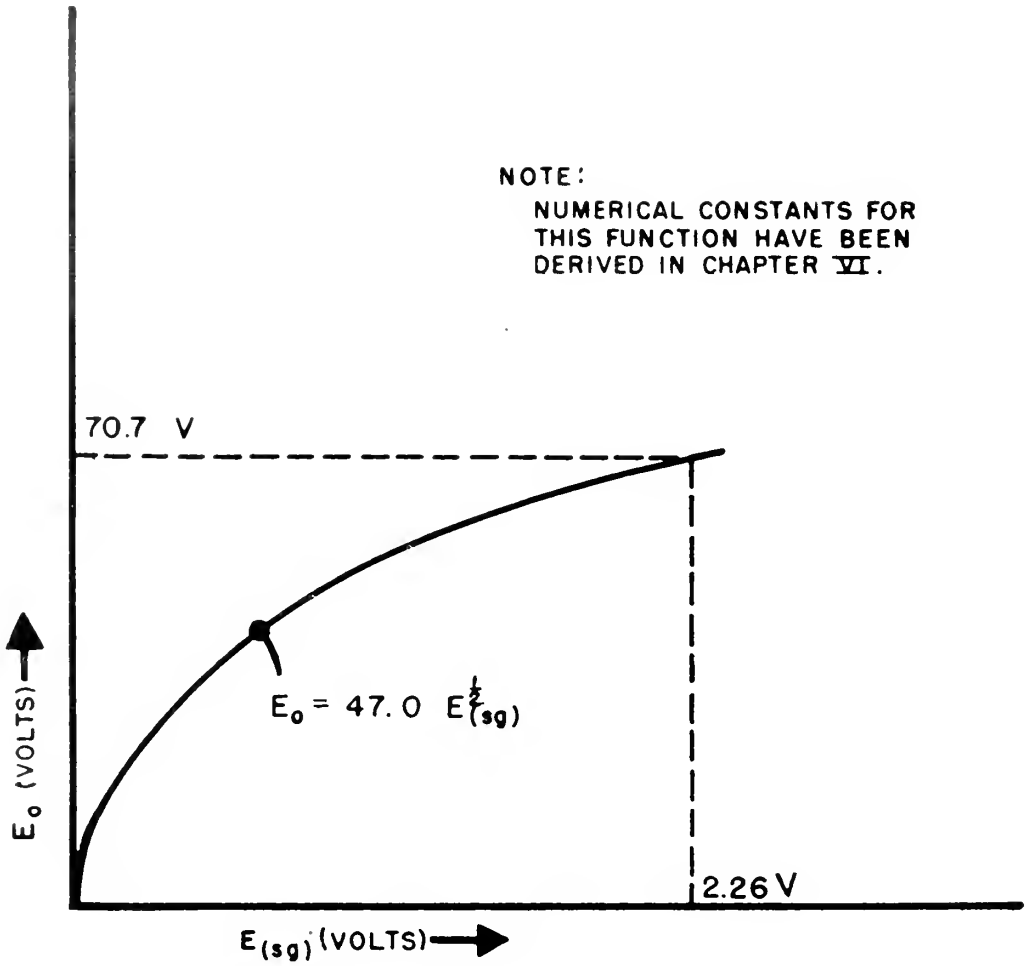

FIGURE 3-1

IDEAL NON-LINEAR CHARACTERISTICS IN FEEDBACK LOOP

would correspond to a very stiff spring for large rotor angles, and hence the W_n of the system would be high, and the $(DR)_{(ovss)}$ would be low. For low rotor angles, the reverse conditions would be true.

We thus have to resign ourselves to the fact that in an actual physical system W_n and $(DR)_{(ovss)}$ are not going to remain constant. W_n and $(DR)_{(ovss)}$ corresponding to the ideal system will now be defined as a reference natural frequency and a reference damping ratio, abbreviated,

$$W_{n(ref)} \text{ and } (DR)_{(ovss)(ref)}$$

In attempting to solve the square root generator problem, we shall apply a method of perturbations to a simplified system and then critically examine the conclusions obtained from such a system.

The simplified form of the perturbation theory will be a means of linearizing the non-linear equation relating E_o and E_{in}. The procedure will be as follows. We shall assume an arbitrary static operating point. The input signal will then be varied by a small amount and the corresponding small change in the output determined. Expansions by Taylor's series will be used when necessary and because the variations will be very small, Δ 's of higher order than one will be neglected. When the so-called perturbed equation is subtracted from the original equation, a linear equation results.

Fig. 3-2 shows the orthogonal vector summing system in somewhat simplified form where instead of square root and signal generators we have merely specified a device whose output, E_o is a function of the rotor angle, A.

From Fig. 3-2, and using Newton's second law of motion

$$I \ddot{A} = - C_d \dot{A} + M_1 + M_2 \qquad 3\text{-}1$$

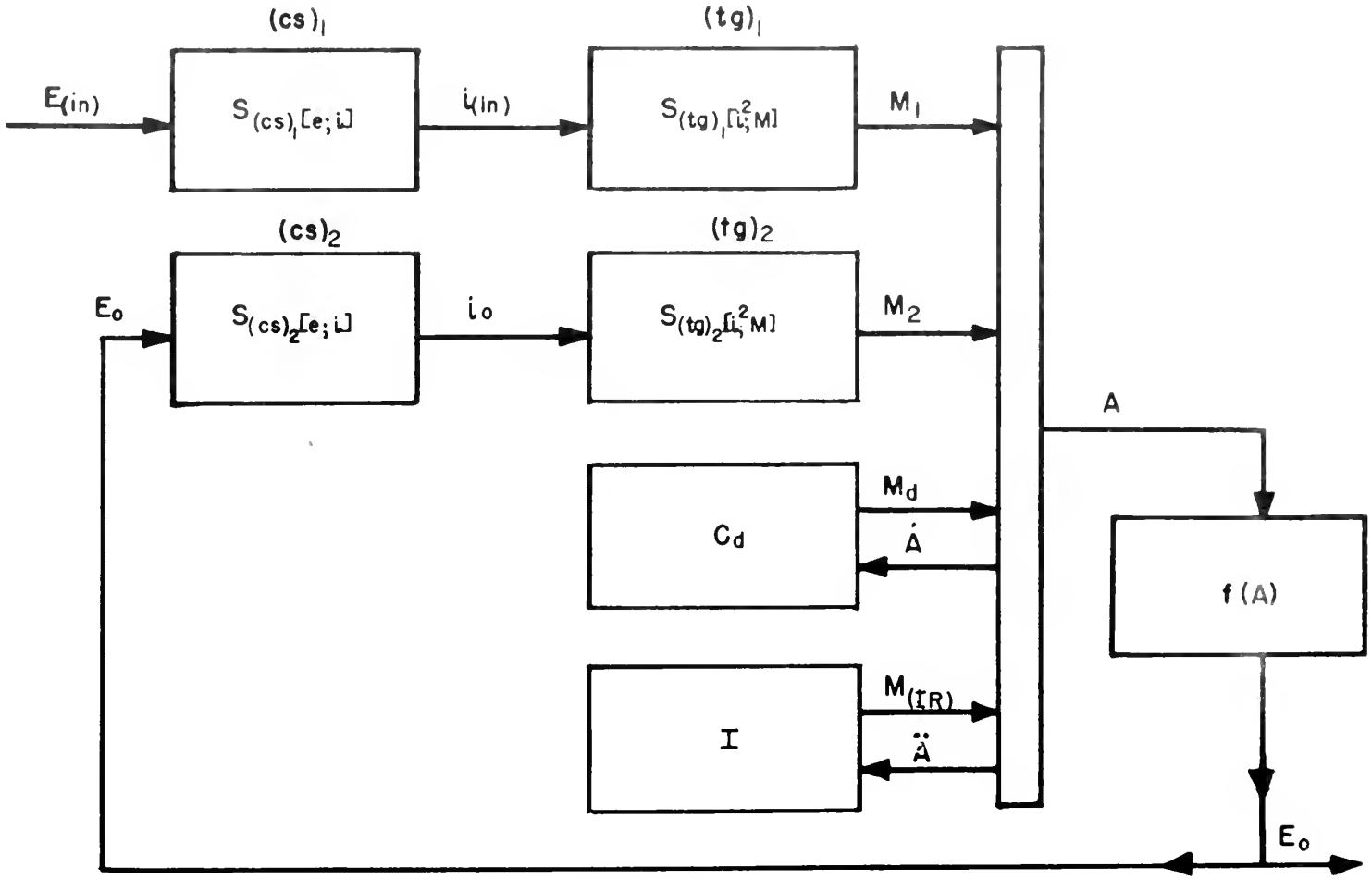

FIGURE 3-2

THE NON-IDEAL SYSTEM

or

$$I\ddot{A} + C_d\dot{A} - M_2 = M_1 \qquad 3\text{-}2$$

$$M_2 = -S(tg)\left[i^2;M\right] S^2(cs)\ e;i\left] E_o{}^2\right.$$

$$M_1 = S(tg)\left[i^2;M\right] S^2(cs)\left[e;i\right] E_{in}{}^2$$

We shall abbreviate the shaft angle $A(rot)$ to A in this chapter because of the large number of times that it will be used.

Using the fact that

$$E_o = f(A), \quad 3\text{-}2 \text{ becomes}$$

$$I\ddot{A} + C_d\dot{A} + S(tg)\ S^2(cs)\ \left[f(A)\right]^2 = S(tg)\ S^2(cs)\ E^2(in) \qquad 3\text{-}3$$

where we have assumed that the torque generator sensitivities and current source sensitivities are equal. Using the method of perturbations, we let E_{in} assume a new value $E_{in} + \Delta E_{in}$ where ΔE_{in} is a small change in the static value of the input signal. Then, corresponding to this change the output rotor changes to $A + \Delta A$ and the new output can be written $f(A + \Delta A)$.

Equation 3-3 for this change in input then becomes

$$\overline{I(A + \Delta A)}^{\cdot\cdot} + C_d\overline{(A + \Delta A)}^{\cdot} + S(tg)\ S^2(cs)\ \left[f(A+\Delta A)\right]^2 = S(tg)\ S^2(cs)\left[E_{in}+\Delta E_{in}\right]^2 \qquad 3\text{-}4$$

Expanding $f(A + \Delta A)$ in terms of $f(A)$ by means of Taylor's series we obtain,

$$f(A + \Delta A) = f(A) + \frac{d\ f(A)}{d\ A}\ \Delta A + \ldots . \qquad 3\text{-}5$$

We have neglected Δ's of higher order than one.

Thus,

$$\left[f(A + \Delta A)\right]^2 = \left[f(A)\right]^2 + 2f(A)\ f'(A)\Delta A + \ldots \qquad 3\text{-}6$$

where

$$f'(A) = \frac{df(A)}{d\ A}$$

and

$$(E_{in} + \Delta E_{in})^2 = E_{in}^2 + 2 E_{in} \Delta E_{in} \qquad 3\text{-}7$$

Substituting 3-6 and 3-7 into 3-4 gives

$$I \ddot{A} + I \Delta\ddot{A} + C_d \dot{A} + C_d \Delta\dot{A} + S_{(tg)} S^2_{(cs)} \left[f(A)\right]^2 + 2S_{(tg)} S^2_{(cs)} f(A) f'(A) \Delta A =$$

$$S_{(tg)} S^2_{(cs)} E^2_{in} + 2 S_{(tg)} S^2_{(cs)} E_{in} \Delta E_{in} \qquad 3\text{-}8$$

Subtracting the perturbed equation, 3-8 from 3-3, the following linear equation with constant coefficients is obtained for every E_{in} and its corresponding rotor angle A.

$$I \Delta\ddot{A} + C_d \Delta\dot{A} + 2 S_{(tg)} S^2_{(cs)} f(A) f'(A) \Delta A = 2 S_{(tg)} S^2_{(cs)} E_{in} \Delta E_{in} \qquad 3\text{-}9$$

Rearranging 3-9 into its conventional form and comparing the coefficients with those of the standard second order liner differential equation as was done in Chapter II, give the following two equations.

$$\frac{I}{2S_{(tg)} S^2_{(cs)} f(A) f'(A)} \Delta\ddot{A} + \frac{C_d}{2S_{(tg)} S^2_{(cs)} f(A) f'(A)} \Delta\dot{A} + \Delta A = \frac{E_{in} \Delta E_{in}}{f(A) f'(A)} \qquad 3\text{-}10$$

$$\frac{1}{W_n^2} \Delta\ddot{A} + \frac{2(DR)}{W_n} \Delta\dot{A} + \Delta A = \frac{E_{in} \Delta E_{in}}{f(A) f'(A)} \qquad 3\text{-}11$$

Thus

$$W_n = \sqrt{\frac{2 S_{(tg)} S^2_{(cs)} f(A) f'(A)}{I}} \qquad 3\text{-}12$$

and

$$(DR)_{(ovss)} = \frac{C_d}{2} \sqrt{\frac{1}{2\, S(tg)\, S^2(cs)\, f(A)\, f'(A)\, I}} \qquad 3\text{-}13$$

The fact that f(A) and f'(A) occur as products will be very important in determining tolerances on the dynamic constants of the system.

We shall now check the above analysis for the ideal system described in Chapter II.

We have shown in Chapter II that

$$E_o^2 = S^2(sr)\left[e^{\frac{1}{2}};e\right]\, S(sg)\left[A;e\right]\, A \qquad 3\text{-}14$$

Hence

$$E_o = S(sr)\left[e^{\frac{1}{2}};e\right]\, S^{\frac{1}{2}}(sg)\left[A;e\right]\, A^{\frac{1}{2}} \qquad 3\text{-}15$$

Thus, in the ideal case, we see that

$$f(A) = S(sr)\left[e^{\frac{1}{2}};e\right]\, S^{\frac{1}{2}}(sg)\left[A;e\right]\, A^{\frac{1}{2}} \qquad 3\text{-}16$$

and

$$f'(A) = \frac{d\, f(A)}{d\, A} = \tfrac{1}{2}\, S(sr)\left[e^{\frac{1}{2}};e\right]\, S^{\frac{1}{2}}(sg)\left[A;e\right]\, A^{-\frac{1}{2}} \qquad 3\text{-}17$$

and finally, we have

$$f(A)\, f'(A) = \tfrac{1}{2}\, S^2(sr)\left[e^{\frac{1}{2}};e\right]\, S(sg)\left[A;e\right] \qquad 3\text{-}18$$

which, when substituted into 3-12 and 3-13 gives

$$W_n = \sqrt{\frac{S(tg)\, S^2(cs)\, S^2(sr)\, S(sg)}{I}} = \sqrt{\frac{S(ovss)\left[A;M\right]}{I}} \qquad 3\text{-}19$$

and

$$(DR)_{(ovss)} = \frac{C_d}{2} \sqrt{\frac{1}{I\,(S(tg)\, S^2(cs)\, S^2(sr)\, S(sg))}}$$

$$= \frac{C_d}{2} \sqrt{\frac{1}{I\,(S(ovss)\left[A;M\right])}} \qquad 3\text{-}20$$

Equation 3-19 and 3-20 are identical with those developed in Chapter II for the ideal system using the conventional approach. As mentioned before, the W_n and $(DR)_{(ovss)}$ corresponding to the ideal system will be referred to as $W_{n(ref)}$ and $(DR)_{(ovss)(ref)}$.

Returning again to 3-12 and 3-13 and solving for the product $f(A)\ f'(A)$, we have for the two equations

$$f(A)\ f'(A) = \frac{W^2_n\ I}{2\ S_{(tg)}\ S^2_{(cs)}} = K_1\ W_n^2 \qquad 3\text{-}21$$

where

$$K_1 = \frac{I}{2\ S_{(tg)}\ S^2_{(cs)}}$$

$$f(A)\ f'(A) = \frac{C_d^2}{8\ S_{(tg)}\ S^2_{(cs)}\ I\ (DR)^2_{(ovss)}} = K_2\ \frac{1}{(DR)^2_{(ovss)}} \qquad 3\text{-}22$$

where

$$K_2 = \frac{C_d^2}{8\ S_{(tg)}\ S^2_{(cs)}\ I}$$

We shall now have to assume arbitrary tolerances on the undamped angular frequency and on the damping ratio of the system. Having made these assumptions, it will now be shown that certain definite limits can be set on the non-linear device used in the feedback loop with respect to its departure from an ideal square root generator. We shall first discuss the W_n parameter and attempt to determine the characteristics of the non-linear device from tolerances on W_n.

Let W_n of the non-ideal system vary from $W_{n(ref)}$ by some fraction of $W_{n(ref)}$ such as $\pm f\ W_{n(ref)}$. Thus we are allowed two limiting angular frequencies defined as

$$W_{n(L)} = W_{n(ref)} - f\ W_{n(ref)} \qquad 3\text{-}23$$

the lower limiting natural angular frequency and

$$W_{n(U)} = W_{n(ref)} + f\, W_{n(ref)} \qquad 3\text{-}24$$

the upper limiting natural angular frequency where f is to be defined as the tolerance to be set upon the system expressed as a fraction of $W_{n(ref)}$.

Thus, we see that for a given tolerance, the right side of 3-21 is uniquely determined for the two boundary values defined in 3-23 and 3-24. Solving 3-21 for the slope of the (A, E_o) curve, we

$$f'(A) = \frac{K_1 W_n^2}{f(A)} = \frac{I W_n^2}{2 S_{(tg)} S^2_{(cs)} f(A)} \qquad 3\text{-}25$$

and hence two limiting slopes are determined at every point in a plane in which A is the abscissa and $f(A) = E_o$ is the ordinate. We define the lower slope at any point $(A_1, f(A_1))$ as

$$f'(A_1)_L = \frac{I (W_{n(ref)} - f\, W_{n(ref)})^2}{2 S_{(tg)} \left[i^2;M\right] S^2_{(cs)} \left[e;i\right]} \quad \frac{1}{f(A_1)} \qquad 3\text{-}26$$

and the upper slope at any point $(A_1, f(A_1))$ as

$$f'(A_1)_U = \frac{I (W_{n(ref)} + f\, W_{n(ref)})^2}{2 S_{(tg)} \left[i^2;M\right] S^2_{(cs)} \left[e;i\right]} \quad \frac{1}{f(A_1)} \qquad 3\text{-}27$$

Fig. 3-3 shows the mapping of the A, f(A) plane for a given tolerance of W_n. Many significant points of interest can be gained from a close study of Fig. 3-3. It is first to be noted that the upper and lower limiting slopes along a line f(A) = const. are constant. If the tolerances on W_n are increased, that is we are allowed to deviate by a greater percentage from $W_{n(ref)}$ throughout the operating range, the differences in slopes at any point are increased and hence the openings between the lineal elements are increased. Such a diagram as

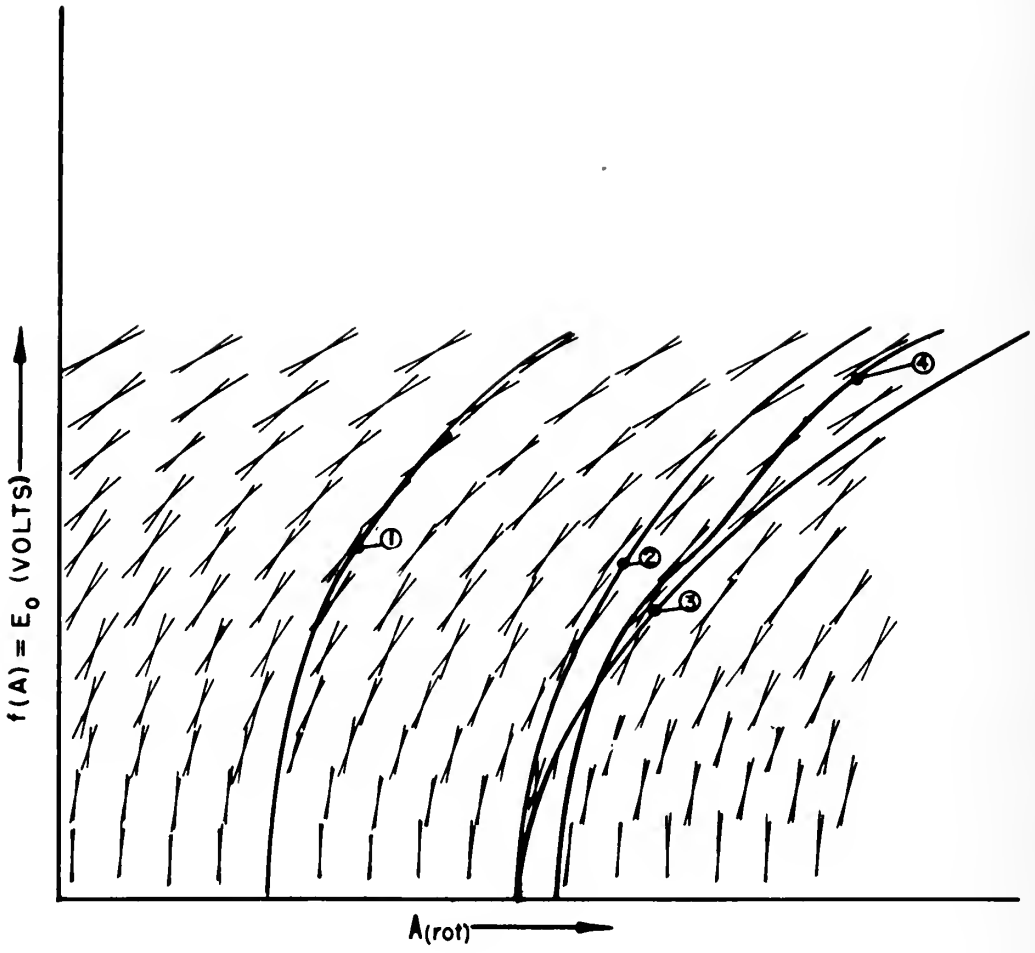

FIGURE 3-3

POSSIBLE CHARACTERISTICS OF NON-LINEAR DEVICE
IN ORDER TO STAY WITHIN ASSIGNED DYNAMIC TOLERANCES

shown in Fig. 3-3 is called a lineal element diagram.[5] Paths (1) and (2) of Fig. 3-3 follow the steepest slope at any point and hence are solutions to the differential equation 3-27. Path (3) on the other hand follows the lowest slope at every point in the A, f(A) plane starting from the same point as (2). Path (3) is a solution of 3-26. There are an infinite number of solutions to each equation, each solution differing by a constant. Path (4) shows how a path may vary and still give an W_n within the given tolerances of the system. Thus, it can be seen that a non-linear device which has an input-output characteristic whose slope at any point stays within the specified tolerances of W_n will be a satisfactory device as far as the dynamics on W_n are concerned. The $(DR)_{(ovss)}$ tolerances will be discussed in the next section.

As $f(A) \longrightarrow o$, $f'(A) \infty$ and of course it will be impossible to obtain a device that will start off with an infinite slope. Thus, for low input signals, the dynamic qualities of the system will have to be relaxed since the product $f(A)\ f'(A)$ cannot be maintained within the required limits. That is W_n will be decreased and the $(DR)_{(ovss)}$ will, of necessity, increase. The best we can do is try to obtain as steep a slope as possible for low inputs and specify the input below which the dynamic tolerances are exceeded.

We have shown that for the ideal system

$$f(A) = E_o = S_{(sr)}\left[e^{\frac{1}{2}};e\right]\ S^{\frac{1}{2}}_{(sg)}\left[A;e\right]\ A^{\frac{1}{2}} \qquad 3\text{-}28$$

which is the equation of a parabola. Let us re-define the equation of the parabola as

$$f(A) = E_o = \dot{P}A^{\frac{1}{2}} \qquad 3\text{-}29$$

and denote $P_{(ref)}$ as the constant associated with the ideal system. The limits on P are to be determined from the given tolerances on W_n

or $(DR)_{(ovss)}$

$$f'(A) = \tfrac{1}{2}PA^{-\frac{1}{2}} \qquad 3\text{-}30$$

and

$$f(A)\ f'(A) = \frac{P^2}{2} \qquad 3\text{-}31$$

Since we have shown that

$$W_n = \sqrt{\frac{2\ S_{(tg)}\ S^2_{(cs)}\ f(A)\ f'(A)}{I}}$$

In this case

$$W_n = \sqrt{\frac{S_{(tg)}\ S^2_{(cs)}}{I}}\ P \qquad 3\text{-}32$$

$$(DR)_{(ovss)} = \frac{C_d}{2}\sqrt{\frac{1}{2\ S_{(tg)}\ S^2_{(cs)}\ I\ f(A)\ f'(A)}}$$

$$(DR)_{(ovss)} = \frac{C_d}{2}\sqrt{\frac{1}{S_{(tg)}\ S^2_{(cs)}\ I}}\ \frac{1}{P} \qquad 3\text{-}33$$

Taking differentials in each case,

$$d\ W_n = \sqrt{\frac{S_{(tg)}\ S^2_{(cs)}}{I}}\ d\ P \qquad 3\text{-}34$$

and, dividing 3-34 by 3-32 gives

$$\frac{d\ W_n}{W_n} = \frac{d\ P}{P} \qquad 3\text{-}35$$

also

$$d\ (DR)_{(ovss)} = -\frac{C_d}{2}\sqrt{\frac{1}{S_{(tg)}\ S^2_{(cs)}\ I}}\ \frac{d\ P}{P^2} \qquad 3\text{-}36$$

and finally,

$$\frac{d\ (DR)_{(ovss)}}{(DR)_{(ovss}} = -\frac{d\ P}{P} \qquad 3\text{-}37$$

From the preceding equations, we have deduced the important fact that a fractional change $\pm f\ W_{n(ref)}$ equals the same fractional change in the constant associated with the ideal square root curve while the same fractional change in $(DR)_{(ovss)}$, abbreviated $\pm f(DR)$, produces an equal and opposite fractional change in the constant associated with the ideal square root curve.

Fig. 3-4 summarizes the results of the previous paragraph. Let f_1 be the specified tolerance on $W_{n(ref)}$, i.e. W_n can have any value between $W_{n(ref)} + f_1 W_{n(ref)}$ and $W_n - f_1 W_{n(ref)}$. Correspondingly, the constant P will have any value between $P_{(ref)} + f_1 P_{(ref)}$ and $P_{(ref)} - f_1 P_{(ref)}$. In addition, the $(DR)_{(ovss)}$ can assume any value between $(DR)_{(ovss)(ref)} - f_1\ (DR)_{(ovss)(ref)}$ and $(DR)_{(ovss)(ref)} + f_1\ (DR)_{(ovss)(ref)}$. It is important to note here that for a certain given tolerance on the natural angular frequency, there automatically corresponds the same tolerance on the damping ratio parameter through the upper and lower bounds of the square root curves.

In Fig. 3-4, we have shown how tolerances on the dynamic parameters allow an upper and lower bound of square root curves about the ideal curve, $E_o = P_{(ref)}\ A^{\frac{1}{2}}$. It remains to connect the development in connection with Fig. 3-4 with that of the lineal element diagram of Fig. 3-3. We have already shown that

$$E_o = f(A) = P\ A^{\frac{1}{2}} \qquad 3\text{-}38$$

$$f'(A) = \frac{P}{2}\ A^{-\frac{1}{2}}$$

$$= \frac{P^2}{2\ P\ A^{\frac{1}{2}}}$$

$$= \frac{P^2}{2\ f(A)} \qquad 3\text{-}39$$

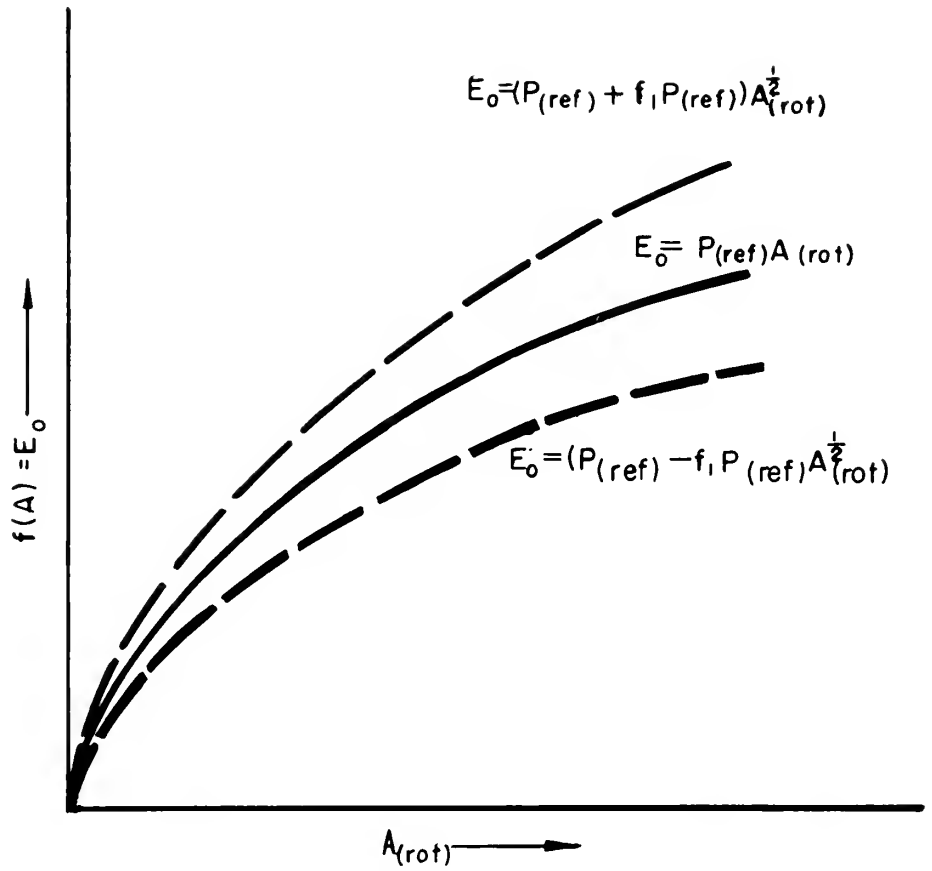

FIGURE 3-4

LIMITING SQUARE ROOT CURVES FOR A GIVEN TOLERANCE ON THE DYNAMICS OF THE SYSTEM

Where we have defined P as the upper and lower bounds of the square root curves corresponding to the tolerances imposed upon the dynamics of the system. That is, P will assume the two limiting values,

$$P_1 = P_{(ref)} + f_1 P_{(ref)} \qquad 3\text{-}40$$

$$P_2 = P_{(ref)} - f_1 P_{(ref)} \qquad 3\text{-}41$$

Thus, since

$$P_{(ref)} = S_{(sr)} S_{(sg)}^{\frac{1}{2}} \qquad 3\text{-}42$$

$$P = S_{(sr)} S_{(sg)}^{\frac{1}{2}} \pm f_1 S_{(sr)} S_{(sg)}^{\frac{1}{2}} \qquad 3\text{-}43$$

$$P^2 = \left[S_{(sr)} S_{(sg)}^{\frac{1}{2}} \pm f_1 S_{(sr)} S_{(sg)}^{\frac{1}{2}} \right]^2 \qquad 3\text{-}44$$

Using 3-19

$$P^2 = W_{n(ref)} \pm f_1 W_{n(ref)}^{\ 2} \frac{I}{S_{(tg)} S^2_{(cs)}} \qquad 3\text{-}45$$

Hence, going back to 3-39, we obtain

$$f'(A) = \frac{I}{2 S_{(tg)} S^2_{(cs)}} W_{n(ref)} \pm f_1 W_{n(ref)}^{\ 2} \frac{1}{f(A)} \qquad 3\text{-}46$$

But, by equation 3-27, we have already shown that

$$f'(A) = \frac{I}{2 S_{(tg)} S_{(cs)}^2} W_{n(ref)} \pm f_1 W_{n(ref)}^{\ 2} \qquad 3\text{-}47$$

From the fact that 3-46 and 3-27 are identical, we conclude that the tolerance limiting square root curves shown in Fig. 3-3 provide the limiting slopes not only within the band of square root curves but automatically give the slopes necessary to map the entire plane as shown in Fig. 3-3. Another important consequence in the development of 3-46 is that an assigned tolerance on the natural

undamped frequency, simultaneously fixes the same tolerance on the damping ratio.

CHAPTER IV

Transient Analysis of the Orthogonal Vector Summing System

In this chapter, we shall show in detail the response of the system to input step and ramp functions. We shall take as our starting point equation 2-18, and let E_{in} be unit step function

Thus,

$$\frac{1}{W_n^2}\ \frac{d^2}{dt^2}\ E_o^2 + \frac{2(DR)(ovss)}{W_n}\ \frac{d}{dt}\ E_o^2 + E_o^2 = 1 \qquad 4\text{-}1$$

where we have let E^2_{in} be the square of a unit step function applied at $t = 0$. Assume the system at rest at $t = 0$.

The response equations to be analyzed in this chapter will be solved by the Laplace transformation method. The Laplace transform of a function $f(t)$ will be expressed as

$$\mathcal{L}\{f(t)\} = F(p) = \int_o^\infty f(t)e^{-pt}dt \qquad 4\text{-}2$$

Taking the Laplace transform of both sides of 4-1, and assuming zero initial conditions we obtain

$$\left[\frac{1}{W_n^2}\ p^2 + \frac{2(DR)(ovss)}{W_n}\ p + 1\right]\ E_o^2(p) = \frac{1}{p} \qquad 4\text{-}3$$

Here, we have designated $E^2_o(p)$ as the Laplace transform of $E^2_o(t)$.

Rearranging 4-3,

$$E^2_o(p) = W_n^2\ \frac{1}{p(p^2 + 2(DR)_{(ovss)}\ W_n p + W_n^2)} \qquad 4\text{-}4$$

There are three cases of equation 4-4 to be considered. The three cases to be considered are for $(DR)_{(ovss)} < 1$, $(DR)_{(ovss)} = 1$, and

and $(DR)_{(ovss)} > 1$.

Before proceding further it will be important to note that because we are dealing with a second order system with a finite moment of inertia, it is impossible by any finite forcing function applied at t = 0 to produce a displacement of the shaft which will in turn produce an $E_o(t)$. This is of course true even though we have made the simplifying assumption that there are no dynamics involved between the shaft and E_o. Not only will there be no displacement at t = 0 to a forcing step function, but the rate of change of response is also zero. Thus, the square root of the time response to be derived from 4-4 will have to satisfy these conditions.

Equation 4-4 when solved by the usual method of partial fractions gives as the time response to a unit step function of E_{in},

$$E^2{}_o(t) = 1 - \frac{1}{\sqrt{1 - (DR)^2_{(ovss)}}} e^{-(DR)_{(ovss)}\omega_n t} \sin\left(\omega_n\sqrt{1-(DR)^2_{(ovss)}}\right)t$$

$$-(DRA)_{(ovss)}) \quad (DR)_{(ovss)} < 1 \qquad 4\text{-}5$$

where the dynamic response angle, abbreviated

$$(DRA)_{(ovss)} = \tan^{-1}\sqrt{\frac{1 - (DR)^2_{(ovss)}}{(DR)_{(ovss)}}}$$

To find the initial values of $E_o{}^2(t)$ and its first three derivatives, we note the following from "Transients in Linear Systems", by Gardner and Barnes.[4]

Given $\qquad \alpha \left\{f(t)\right\} = F(p)$

Then

$$f(0+) = \lim_{p \to \infty} p\, F(p)$$

$$\frac{d}{dt} f(0+) = \lim_{p \to \infty} \left[p^2 F(p) - f(0+)p \right]$$

$$\frac{d^2}{dt^2} f(0+) = \lim_{p \to \infty} \left[p^3 F(p) - f(0+) p^2 - \frac{d}{dt} f(0+)p \right]$$

$$\frac{d^3}{dt^3} f(0+) = \lim_{p \to \infty} \left[p^4 F(p) - f(0+)p^3 - \frac{d}{dt} f(0+)p^2 - \frac{d^2}{dt^2} f(0+)p \right]$$

Hence, applying the above criteria to $E^2_o(p)$ developed in 4-4, we obtain

$$E_o^2(0) = 0$$

$$\frac{d}{dt} E_o^2(0) = 0$$

$$\frac{d^2}{dt^2} E_o^2(0) = W_n^2 \qquad 4\text{-}6$$

$$\frac{d^3}{dt^3} E_o^2(0) = -2(DR)_{(ovss)} W_n^2$$

We shall abbreviate $(DR)_{(ovss)}$ to (DR) for the remainder of this chapter to shorten the notation.

From 4-5, we see that

$$E_o(t) = \left[1 - \frac{1}{\sqrt{1 - (DR)^2}} e^{-(DR)W_n t} \sin\left(W_n \sqrt{1 - (DR)^2}\, t - (DRA)_{(ovss)}\right) \right]^{\frac{1}{2}} \qquad 4\text{-}7$$

Equation 4-7 represents the response of a passive system. Thus, even with no damping in the system, the maximum value of the second term on the right would be unity. Since a fairly large amount of damping will be used for the system, the second term of 4-5 will

rapidly become small with respect to unity, and thus enable us to approximate $E_o(t)$ closely by two or three terms of a binomial expansion of 4-7.

It is shown in "Differential and Integral Calculus", by Granville, Smith, and Longley that the expression

$$(1 + x)^m = 1 + mx + \frac{m(m - 1)}{1.2} x^2 + \ldots . \qquad 4\text{-}8$$

and is valid when m is not an integer providing $|x| < 1$.

Applying 4-8 to 4-7 we obtain as a good approximation of $E_o(t)$,

$$E_o(t) = 1 - \frac{1}{2\sqrt{1 - (DR)^2}} e^{-(DR)W_n t} \sin\left(W_n\sqrt{1 - (DR)^2}\, t - (DRA)_{(ovss)}\right)$$

$$- \frac{1}{8} \frac{1}{(1 - (DR)^2)} e^{-2(DR)W_n t} \sin^2\left(W_n\sqrt{1 - (DR)^2}\, t - (DRA)_{(ovss)}\right) \qquad 4\text{-}9$$

Taking next the case where (DR) = 1, 4-5 becomes

$$E_o^2(p) = W_n^2 \frac{1}{p(p + W_n)^2} \qquad 4\text{-}10$$

Taking inverse transforms of 4-10, we obtain

$$E_o^2(t) = 1 - e^{-W_n t} (W_n t + 1)$$

Or, finally,

$$E_o(t) = \left[1 - e^{-W_n t} (W_n t + 1)\right]^{\frac{1}{2}} \qquad 4\text{-}11$$

Expanding as before, in a binomial series,

$$E_o(t) = 1 - \tfrac{1}{2}e^{-W_n t} (W_n t + 1) - \tfrac{1}{4}e^{-2W_n t} (W_n t + 1)^2 - \ldots \qquad 4\text{-}12$$

Taking finally, the case where critical damping is exceeded, we have (DR) $>$ 1 and hence the characteristic equation associated with

4-5 factors into

$$(p + (DR)W_n - W_n\sqrt{(DR)^2 - 1})(p + (DR)W_n + W_n\sqrt{(DR)^2 - 1})$$

Thus,

$$E_o^2(p) = \frac{W_n^2}{p(p + (DR)W_n - W_n\sqrt{(DR)^2 - 1})(p + (DR)W_n + W_n\sqrt{(DR)^2 - 1})} \quad 4\text{-}13$$

The time expression of 4-13 becomes

$$E_o^2(t) = 1 + \tfrac{1}{2}\frac{1}{(DR)^2 - (DR)\sqrt{(DR)^2 - 1} - 1} e^{\left[-(DR)W_n + W_n\sqrt{(DR)^2 - 1}\right]t} + \tfrac{1}{2}\frac{1}{(DR)^2 + (DR)\sqrt{(DR)^2 - 1} - 1} e^{\left[-(DR)W_n - W_n\sqrt{(DR)^2 - 1}\right]t} \quad 4\text{-}14$$

Thus we have finally, for $(DR) > 1$

$$E_o(t) = \left[1 + \tfrac{1}{2}\frac{1}{(DR)^2 - (DR)\sqrt{(DR)^2 - 1} - 1} e^{\left[-(DR)W_n + W_n\sqrt{(DR)^2 - 1}\right]t} + \tfrac{1}{2}\frac{1}{(DR)^2 + (DR)\sqrt{(DR)^2 - 1} - 1} e^{\left[-(DR)W_n - W_n\sqrt{(DR)^2 - 1}\right]t}\right]^{\frac{1}{2}}$$

$$(DR) > 1 \qquad 4\text{-}15$$

It is not feasible to expand this expression by the binomial approximation.

Curve I of Fig. 4-1 shows the solution of 4-5 for (DR) = .1. If the square root of the values representing curve I are taken at every point, we have the exact solution shown as curve II, and which represents 4-7. Since this latter result is difficult to obtain analytically, we have expanded 4-7 through the binomial series approximation to three terms in 4-9. Plot III shows the approximate value of $E_o(t)$ to a unit step input function using only the first two terms of

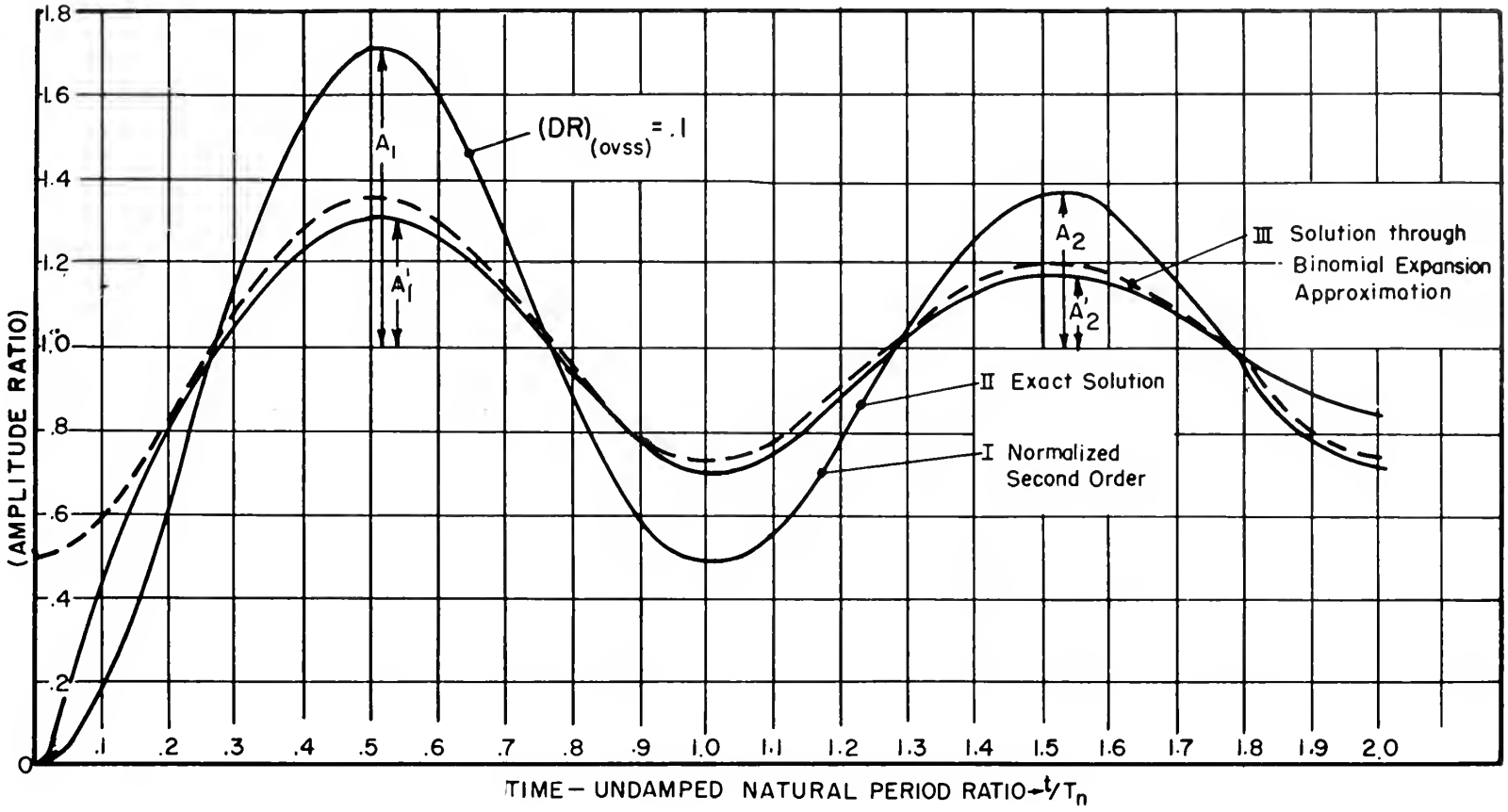

FIGURE 4 – 1

NORMALIZED TRANSIENT RESPONSE CURVES FOR $(DR)_{(ovss)}=.1$

4-9. It is to be noted that the approximation is very good except for the initial period of $\frac{t}{T_n} = .1$. Since damping ratios higher than .1 are actually to be used, the approximation will be even closer to the actual solution except that as the damping ratio increases the time for the initial overshoot will correspondingly lengthen and hence the initial large deviation will last for a longer value of $\frac{t}{T_n}$.

Throughout this thesis, it has been emphasized that the terminology used such as damping ratio, and natural frequency refers only to the linear second order system relating the squares of the output and input functions. However, one must be careful and not apply this terminology to the specific response associated with the input and output functions themselves.

In this presentation, we shall use the logarithmic decrement as our basic description parameter for the system for $(DR) < 1$. Logarithmic decrement will be defined as the natural logarithm of the ratio of the amplitudes of two values of the response to a step function differing by a period as for example two successive maxima of oscillation as shown in Fig. 4-1.

Referring to Fig. 4-1, we let A_1 and A_2 be the amplitudes of two successive peaks of the linear second order response of the squared functions while A_1' and A_2' are two successive peaks of the response for signal input as a function of signal output.

Hence, the logarithmic decrement for the linear second order response, abbreviated $(LD)_{(lin)} = \log \frac{A_1}{A_2}$, 4-16

From Equation 4-5, we see that the instantaneous height of the overshoots shown of Fig. 4-1 is

$$\frac{1}{\sqrt{1 - (DR)^2}} e^{-(DR)W_n t} \sin(W_n \sqrt{1 - (DR)^2}\, t - (DRA)_{(ovss)})$$

and hence using 4-16,

$$(LD)_{(lin)} = \log \frac{e^{-(DR)W_n t_1}}{e^{-(DR)W_n t_2}} = + (DR)W_n T \qquad 4\text{-}17$$

since A_1 and A_2 were taken at the peaks and $T = t_2 - t_1$, the period of the damped oscillation.

From 4-17, we obtain

$(LD)_{(lin)} = (DR)W_n T$ where T is the time for two positive successive peaks. But $T = \frac{2\pi}{W} = \frac{2\pi}{W_n\sqrt{1 - (DR)^2}}$, thus

$$(LD)_{(lin)} = \frac{+ 2\pi(DR)}{\sqrt{1 - (DR)^2}} \qquad 4\text{-}18$$

We shall next define the logarithmic decrement for the actual response of the system to a step input as,

$$(LD)_{(ovss)} = \log\sqrt{\frac{A1}{A_2}} = \tfrac{1}{2} \log \frac{A_1}{A_2} \qquad 4\text{-}19$$

From 4-19, we have immediately that

$$(LD)_{(lin)} = 2(LD)_{(ovss)} \qquad 4\text{-}20$$

Using 4-20 in 4-17, we obtain the important result that

$$(LD)_{(ovss)} = \frac{\pi (DR)}{\sqrt{1 - (DR)^2}} \quad (DR) < 1 \qquad 4\text{-}21$$

This last result, gives a means of describing the non-linear response in terms of a parameter describing the linear squared system.

Up to now, the development of this chapter has been with the ideal system which assumes a perfect square root function in the closed loop. The last chapter showed how close a square root function had to be generated in the closed loop in order to stay within certain pre-

assigned tolerances in the damping ratio and the undamped natural frequency. Returning to this line of argument, if we have a change in the damping ratio, $d(DR)_{(ovss)}$ then from 4-20 we obtain

$$d(LD)_{(ovss)} = \frac{\pi(1 + (DR)^2)}{(1 - (DR)^2)^{3/2}} d(DR) \quad (DR) < 1 \qquad 4\text{-}22$$

Applications of the response of the system to a forcing step function will be made in connection with the laboratory test system. The constancy of the dynamics for various magnitudes of the input signal will be tested by applying small step function increments upon the different static operating levels and recording the output response. If we have a perfect square root generator in the feedback loop, the response to a step function increment will not depend upon the magnitude of the forcing function, and hence a non-dimensional response curve can be shown by plotting $\frac{E_o}{E_{in}}$ for any point of the operating region. However, we shall use an imperfect square root generator in the feedback loop and hence small increment forcing step functions will be used and the operating points specified. Chapter VI will show in non-dimensional form, such responses as obtained from a Sanborn recorder.

The previous analysis with logarithmic decrements was made on the basis that the $(DR)_{(ovss)} < 1$. We have not developed an easy parameter to describe the non-linear system in terms of the linear squared system for $(DR)_{(ovss)} \geq 1$. However, the response can be obtained fairly easily from 4-12 or 4-15.

It was felt that to make this chapter on transient analysis complete, an analysis of the system response to a ramp forcing function should be included. Much study was devoted to the comparison of the response of a regular second order system to the one presented here, but

the results were disappointing because no simple relation or design parameter could be found relating the two. However, a brief development of ramp responses follows for (DR) < 1.

Taking the Laplace transformation of 2-18, and assuming zero initial conditions, we obtain

$$\left[\frac{1}{W_n^2} p^2 + \frac{2(DR)}{W_n} p + 1 \right] E_o^2(p) = E_{in}^2(p)$$

or

$$E_o^2(p) = \frac{E_{in}^2(p)}{\frac{1}{W_n^2} p^2 + \frac{2(DR)}{W_n} p + 1} \qquad 4\text{-}23$$

In developing the response to ramp functions, it will be best to work from the point of view of errors (both steady state and transient) between the input and output functions.

Treating 4-23 first as a linear second order system in E^2_{in}, we define the error for such a system as $\alpha^{-1}\left\{E^2_{in}(p) - E^2_o(p)\right\}$ where

$$E_o^2(p) - E^2_{in}(p) = \frac{E^2_{in}(p)\left[\frac{1}{W_n^2} p^2 + \frac{2(DR)}{W_n} p\right]}{\frac{1}{W_n^2} p^2 + \frac{2(DR)}{W_n} p + 1} \qquad 4\text{-}24$$

or

$$E_o^2(p) - E^2_{in}(p) = \frac{E^2_{in}(p)\left[p^2 + 2(DR)W_n p\right]}{p^2 + 2(DR)W_n p + W_n^2} \qquad 4\text{-}25$$

If $E^2_{in}(t)$ = a unit ramp function = t,

$$E^2_{in}(p) = \frac{1}{p^2}$$

and the linear second order error equation becomes for DR < 1

$$E_o^2(p) - E_{in}^2(p) = \frac{p + 2(DR)W_n}{p(p^2 + 2(DR)W_n\, p + W_n^2)}$$

$$= \frac{p + 2(DR)W_n}{p(p + (DR)W_n - jW_n\sqrt{1 - (DR)^2})(p + (DR)W_n + jW_n\sqrt{1 - (DR)^2})} \qquad 4\text{-}26$$

$$= \frac{K_o}{p} + \frac{K_1}{p + (DR)W_n - jW_n\sqrt{1 - (DR)^2}} + \frac{\bar{K}_1}{p + (DR)W_n + jW_n\sqrt{1 - (DR)^2}}$$

where

$$K_o = \left|(p)(E_o^2 - E_{in}^2)\right|_{p\,=\,0} = \frac{2(DR)}{W_n}$$

$$K_1 = \left|(p + (DR) - jW_n\sqrt{1 - (DR)^2})(E_o^2 - E_{in}^2)\right|_{p\,=\,-(DR)W_n + jW_n\sqrt{1 - (DR)^2}}$$

$$= \frac{e^{j\tan^{-1}\frac{2\sqrt{1 - (DR)^2}}{(DR)}}}{2\,jW_n\sqrt{1 - (DR)^2}}$$

Hence, the complete time expression for the linear second order error response to a unit ramp is

$$E_o^2(t) - E_{in}^2(t) = \frac{2(DR)}{W_n} + \frac{1}{W_n\sqrt{1 - (DR)^2}}\, e^{-(DR)W_n t} \sin\left(W_n\sqrt{1 - (DR)^2}\, t + (DRA)_{(ovss)}\right) \qquad 4\text{-}27$$

where

$$(DRA)_{(ovss)} = \tan^{-1}\frac{2\sqrt{1 - (DR)^2}}{(DR)} \qquad (DR) < 1$$

If, on the other hand, we let E_{in} = a unit ramp function = t, then

$$E_{in}^2(p) = \alpha\left\{t^2\right\} = \frac{2}{p^3}$$

and 4-25 becomes

$$E_o^2(p) - E_{in}^2(p) = \frac{2\left[p + 2(DR)W_n\right]}{p^2\left[p^2 + 2(DR)W_n p + W_n^2\right]}$$

$$= \frac{2\left[p + 2(DR)W_n\right]}{p^2\left[p + (DR)W_n - jW_n\sqrt{1 - (DR)^2}\right]\left[p + (DR)W_n + jW_n\sqrt{1 - (DR)^2}\right]}$$

$$(DR) < 1 \qquad 4\text{-}28$$

Expanding by the same method of partial fractions as in the previous case gives

$$E_o^2 - E_{in}^2 = \frac{2\left[1 - 4(DR)^2\right]}{W_n^2} + \frac{4(DR)}{W_n}\,t + \frac{2}{W_n^2(2(DR)^2 - 1)\sqrt{1 - (DR)^2}}$$

$$e^{-(DR)W_n t}\,\sin\left(W_n\sqrt{1 - (DR)^2}\,t + (DRA)_{(ovss)}\right) \quad DR < 1$$

4-29

where

$$(DRA)_{(ovss)} = \tan^{-1}\frac{\sqrt{1 - (DR)^2}}{(DR)} + \tan^{-1}\,2(DR)\sqrt{1 - (DR)^2} - \frac{\pi}{2}$$

An interesting result from 4-29 is the fact that if the $(DR)_{(ovss)}$ is made equal to .5, then the first steady state term in 4-29 is eliminated. However, the second term shows that the error between the squares of the input and output builds up linearly with time.

CHAPTER V

Steady State Harmonic Analysis of the Orthogonal Vector Summing System

An important method used to determine the dynamic characteristics of a general electro-mechanical system is the method of steady state sinusoidal harmonic analysis. Amplitude and phase graphs are plotted as functions of forcing sine wave frequencies. In this method, all transient responses are considered as having died out leaving only the steady state conditions. The dynamic quality of the system is then determined by the pre-assigned limits set upon the magnitude change and the phase change in comparison with some reference magnitude and phase determined at some reference frequency, the latter usually being zero.

In the system being considered here, it is impossible to follow such a procedure because of the squaring properties of the torque generators. Thus, only the absolute value of a function acts on the system, and of course $|\cos Wt|$, which looks like the following function,

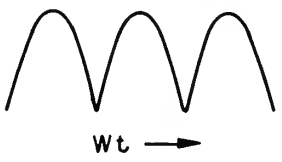

has too abrupt a change to be of any value in evaluating the speed of response of the system.

If, on the other hand, we impress upon a constant input F_o a function of Wt, $F_1 \cos Wt$, where $F_1 \leq F_o$, the discontinuity can be

prevented. Thus, let $E_{in} = F_o + F_1 \cos Wt$. Since the equation giving E_o^2 in terms of E_{in}^2 is linear, all of the solutions for inputs of E_{in} will be found through the squared functions. The equation for E_o^2 in terms of E_{in}^2 is

$$\frac{1}{W_n^2} \frac{d^2}{dt^2} E_o^2 + \frac{2(DR)}{W_n} \frac{d}{dt} E_o^2 + E_o^2 = E_{in}^2 \qquad 5\text{-}1$$

An important significance of this linearity is that if E_{in}^2 consists of a sum of terms, a solution of the equation can be obtained for each of the terms independently and the overall solution obtained by superposition of the separate solutions.

Taking an input function, $E_{in} = F_o + F_1 \cos Wt$, and squaring gives

$$E_{in}^2 = F_o^2 + 2 F_o F_1 \cos Wt + F_1^2 \cos^2 Wt \qquad 5\text{-}2$$

From trigonometry, we have the following relationship:

$$\cos^2 Wt = \tfrac{1}{2} + \tfrac{1}{2} \cos 2 Wt \qquad 5\text{-}3$$

Thus,

$$E_{in}^2 = F_o^2 + 2 F_o F_1 \cos Wt + \frac{F_1^2}{2} + \frac{F_1^2}{2} \cos 2 Wt$$

or finally,

$$E_{in}^2 = F_o^2 + \frac{F_1^2}{2} + 2 F_o F_1 \cos Wt + \frac{F_1^2}{2} \cos 2 Wt \qquad 5\text{-}4$$

Taking the $F_o^2 + \frac{F_1^2}{2}$ term and inserting it into equation 5-1 gives the response $E_o^2 = F_o + \frac{F_1^2}{2}$ in the steady state. It is to be stressed that this harmonic analysis deals only with steady state responses of the system.

The steady state solution of equation 5-1 to the fundamental sinusoidal forcing function will now be shown.

Rewriting equation 5-1 as follows:

$$\frac{1}{W_n^2}\frac{d^2}{dt^2}E_o^2 + \frac{2(DR)}{W_n}\frac{d}{dt}E_o^2 + E_o^2 = 2F_oF_1\cos Wt \quad 5\text{-}5$$

$$= \mathrm{Re}\ 2F_oF_1e^{jWt} \quad 5\text{-}6$$

Let

$$z = E_o^2$$

Assuming a particular solution of the form,

$$z_p = A\,e^{jWt}$$

$$\dot{z}_p = jWA\,e^{jWt}$$

$$\ddot{z}_p = -W^2A\,e^{jWt} \quad 5\text{-}7$$

Upon substituting the above functions into equation 5-6, we obtain

$$\left[-\frac{W^2}{W_n^2} + 1 + j\,2(DR)\frac{W}{W_n}\right]A = 2F_oF_1$$

$$A = \frac{2F_oF_1}{-\frac{W^2}{W_n^2} + 1 + j\,2(DR)\frac{W}{W_n}}$$

Thus

$$E_o^2 = \mathrm{Re}\ \frac{2F_oF_1e^{jWt}}{1 - \frac{W^2}{W_n^2} + j\,2(DR)\frac{W}{W_n}} \quad 5\text{-}8$$

$$E_o^2 = \mathrm{Re}\ \frac{2F_oF_1(\cos Wt + j\sin Wt)}{1 - (FR)^2 + j\,2(DR)(FR)} \quad 5\text{-}9$$

where

$$(FR) = \frac{W}{W_n}$$

$$= \text{Re}\ \frac{2\,F_o\,F_1(\cos Wt + j \sin Wt)(1 - (FR)^2 - j\,2(DR)(FR))}{\left[1 - (FR)^2\right]^2 + \left[2(DR)(FR)\right]^2}$$

or

$$E_o^2 = \frac{2\,F_o\,F_1}{\left[1 - (FR)^2\right]^2 + \left[2(DR)(FR)\right]^2}\left[(1 - (FR)^2)\cos Wt + 2(DR)(FR)\sin Wt\right] \qquad 5\text{-}10$$

or finally

$$E_o^2 = \frac{2\,F_o\,F_1}{\sqrt{\left[1 - (FR)^2\right]^2 + \left[2(DR)(FR)\right]^2}}\cos\left(Wt + (DRA)_1\right) \qquad 5\text{-}11$$

where

$$(DRA)_1 = \tan^{-1} - \frac{2(DR)(FR)}{1 - (FR)^2}$$

On a similar manner, the response of equation 5-1 to a function $\frac{F_1^2}{2}\cos 2Wt$ is of the form

$$\frac{F_1^2/2}{\sqrt{\left[1 - (FR)_1^2\right]^2 + \left[2(DR)(FR)_1\right]^2}}\cos\left(W_1 t + (DRA)_2\right) \qquad 5\text{-}12$$

where

$$(DRA)_2 = \tan^{-1} - \frac{2(DR)(FR)_1}{1 - (FR)_1^2}$$

Since $(FR)_1 = \frac{W_1}{W_n} = 2\frac{W}{W_n} = 2(FR)$

Thus, 5-12 becomes

$$\frac{F_1^2/2}{\sqrt{\left[1 - 4(FR)^2\right]^2 + \left[4(DR)(FR)\right]^2}}\cos\left(2Wt + (DRA)_2\right) \qquad 5\text{-}13$$

where

$$(DRA)_2 = \tan^{-1} - \frac{4(DR)(FR)}{1 - 4(FR)^2}$$

In the case of

$$4(FR)^2 << 1$$

$$(DRA)_2 \approx 2(DRA)_1 \qquad 5\text{-}14$$

This can be seen from the fact that for $(FR) << 1$ the tangent of the angle can be replaced by the angle and $(DRA)_2 \approx - 4(DR)(FR)$ as compared to $(DRA)_1^2 \approx - 2(DR)(FR)$.

This approximation is good even for $(FR) = .3$. To show this fact, we shall let $(DR)_{(ovss)} = 1$

$$(DRA)_1 = \tan^{-1} - \frac{.6}{1 - .09}$$

$$= - 33.4^\circ$$

Letting $(DRA)_2 = 2(DRA)_1$, gives $- 66.8^\circ$ for $(DRA)_2$

Actually,

$$(DRA)_2 = \tan^{-1} \frac{- 1.2}{1 - .36} = - 62^\circ$$

Thus, corresponding to

$$E_{in}^2 = F_o^2 + \frac{F_1^2}{2} + 2 F_o F_1 \cos Wt + \frac{F_1^2}{2} \cos 2Wt \qquad 5\text{-}15$$

we have in the steady state

$$E_o^2 = F_o^2 + \frac{F_1^2}{2} + \frac{2 F_o F_1}{\sqrt{\left[1 - (FR)^2\right]^2 + \left[2(DR)(FR)\right]^2}} \cos (Wt + (DRA)_1) \qquad 5\text{-}16$$

$$+ \frac{F_1^2/2}{\sqrt{\left[1 - 4(FR)^2\right]^2 + \left[4(DR)FR)\right]^2}} \cos (2Wt + (DRA)_2)$$

where $(DRA)_1$ and $(DRA)_2$ have been defined in 5-11 and 5-13.

It is now necessary to relate in some fashion, the squares of the inputs and outputs to the actual inputs and outputs themselves.

Starting with the expression $E_o^2 - E_{in}^2 = (E_o + E_{in})(E_o - E_{in})$, we can make the approximation

$$E_o^2 - E_{in}^2 = 2\,E_{in}(E_o - E_{in}) \quad \text{if } E_o \doteq E_{in}. \tag{5-17}$$

This approximation will be valid because we shall restrict ourselves to small deviations of E_o.

Dividing both sides of 5-15 by E_{in}^2 gives the result

$$\frac{E_o^2}{E_{in}^2} - 1 = 2\left[\frac{E_o}{E_{in}} - 1\right] \tag{5-18}$$

We shall define the deviation of the performance ratio of the orthogonal vector summing system as

$$D(PR)_{(ovss)} = \frac{E_o}{E_{in}} - 1 = \tfrac{1}{2}\left[\frac{E_o^2}{E_{in}^2} - 1\right] \tag{5-19}$$

where 5-15 and 5-16 are to be used to give the expression for $\frac{E_o^2}{E_{in}^2} - 1$.

Information from 5-19 will be broken into two parts, each part conforming to certain specifications. In this particular treatment we shall use the damping ratio associated with the linear second order performance equation relating the squares of the input and output functions as the necessary parameter to give us a family of performance ratio curves plotted as a function of frequency. The first of these aforementioned parts will be a comparison of the ratio of the absolute magnitudes of E_o^2 and E_{in}^2 while the second part will give the phase

lag of E_o^2 as compared to E_{in}^2 as a functional forcing frequency. It is to be noted that the amplitude deviation will be a comparison of the maximum amplitudes of input and output quantities. From the information obtained from the ratio of the absolute magnitudes of E_o^2 and E_{in}^2 we can then use 5-19 to find $D(PR)_{(ovss)}$ as a function of frequency.

In the expression for E_{in}, that is $E_{in} = F_o + F_1 \cos Wt$, F_o and F_1 have been specified as not necessarily equal. This general approach has been carried through with an eye on the future applications of this type of analysis. In considering the quality of response of the system, F_o will be made equal to F_1. However, in considering the effect of noise on the system, F_1 will usually be a small fraction of F_o. We shall apply our analysis only to measure the quality of response of the system, considering a study of noise beyond the scope of this thesis.

Thus, letting

$$E_{in} = F_o + F_o \cos Wt \qquad 5\text{-}20$$

Then

$$\frac{E_{in}}{F_o} = 1 + \cos Wt \qquad 5\text{-}21$$

Let F_o be redefined as $E_{in(ref)}$

$$\frac{E_{in}}{E_{in(ref)}} = 1 + \cos Wt \qquad 5\text{-}22$$

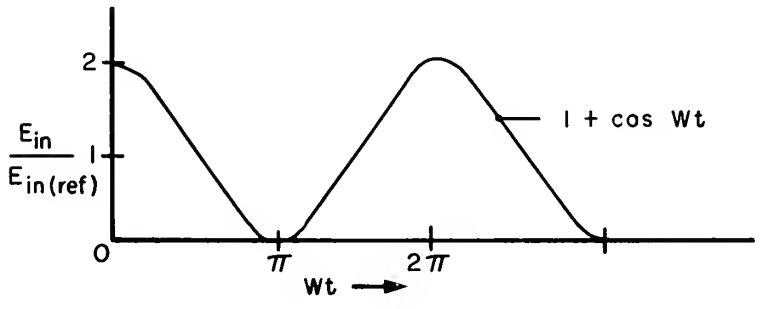

Then,

$$\frac{E_{in}^2}{E_{in^2(ref)}} = 1.5 + 2\cos Wt + .5\cos 2Wt \qquad 5\text{-}23$$

After substituting this quantity into equation 5-1,

$$\frac{E_o^2}{E^2_{in(ref)}} = 1.5 + \frac{2}{\sqrt{\left[1 - (FR)^2\right]^2 + \left[2(DR)_{(ovss)}(FR)\right]^2}}\cos(Wt + (DRA)_1)$$

$$+ \frac{.5}{\sqrt{\left[1 - 4(FR)^2\right]^2 + \left[4(DR)_{(ovss)}(FR)\right]^2}}\cos(2Wt + (DRA)_2) \qquad 5\text{-}24$$

where, for the sake of completeness

$$(DRA)_1 = \tan^{-1} - \frac{2(DR)(FR)}{1 - (FR)^2}$$

$$(DRA)_2 = \tan^{-1} - \frac{4(DR)(FR)}{1 - 4(FR)^2}$$

Fig. 5-1 shows how the input function $\frac{E^2_{in}}{E^2_{in(ref)}}$ of 5-23 is compounded. It is to be noted that $\frac{E^2_{in}}{E^2_{in(ref)}}$ has a frequency, W, but the required addition of the second harmonic causes distortion as shown in Fig. 5-1. For sufficiently high forcing frequency, $\frac{E_o^2}{E^2_{in(ref)}}$ will lag the input as shown and the absolute value of $\frac{E_o^2}{E^2_{in(ref)}}$ will drop off in general or it could very well peak for low damping ratios near the natural frequency of the system.

Fig. 5-2 shows in non-dimensional form a plot of the $D(PR)_{(ovss)}$ as a function of forcing frequency using equation 5-19. The absolute value of $\frac{E^2_{in}}{E^2_{in(ref)}}$ can be seen from equation 5-23 to be 4.

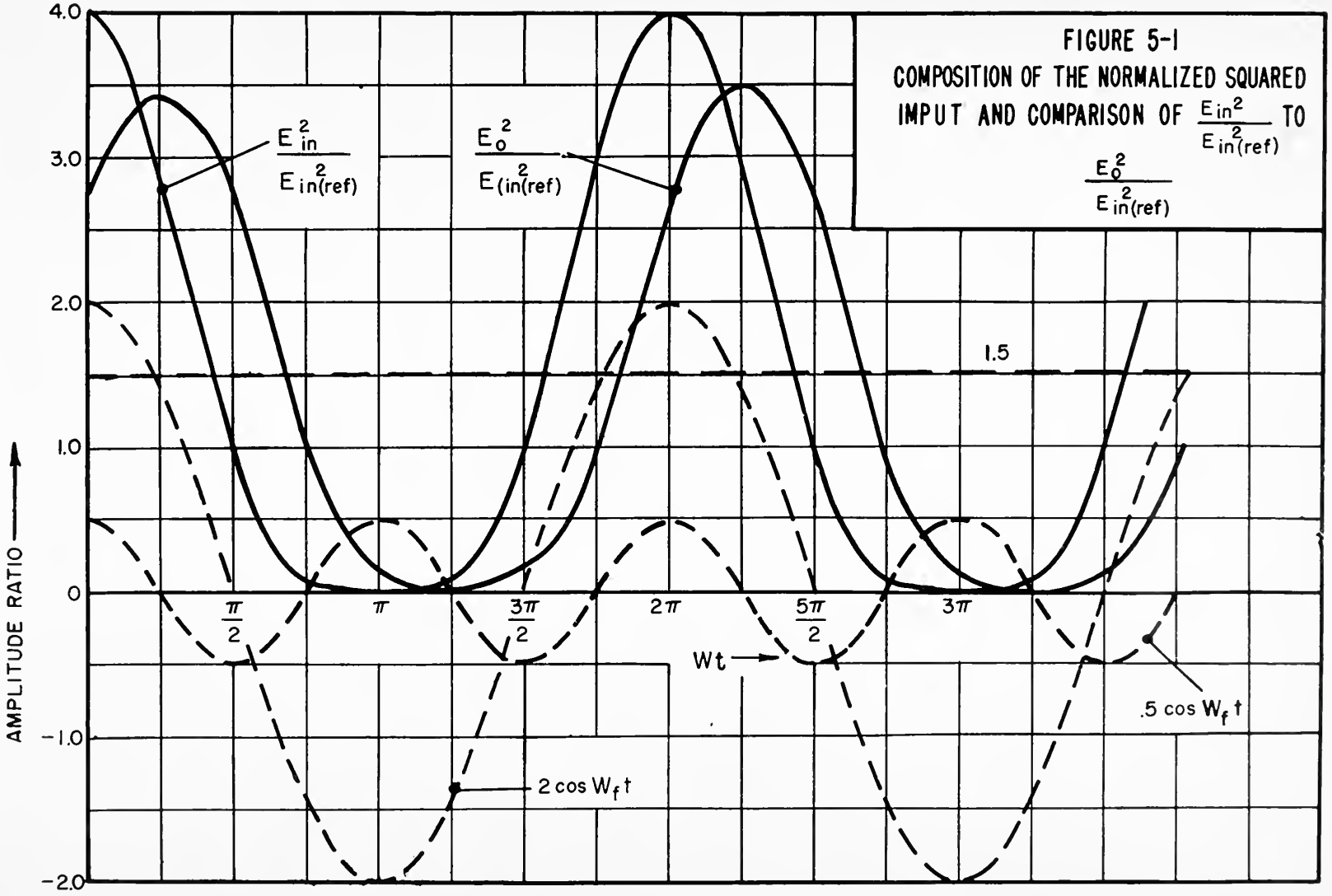

FIGURE 5-1
COMPOSITION OF THE NORMALIZED SQUARED IMPUT AND COMPARISON OF $\frac{E_{in}^2}{E_{in(ref)}^2}$ TO $\frac{E_o^2}{E_{in(ref)}^2}$

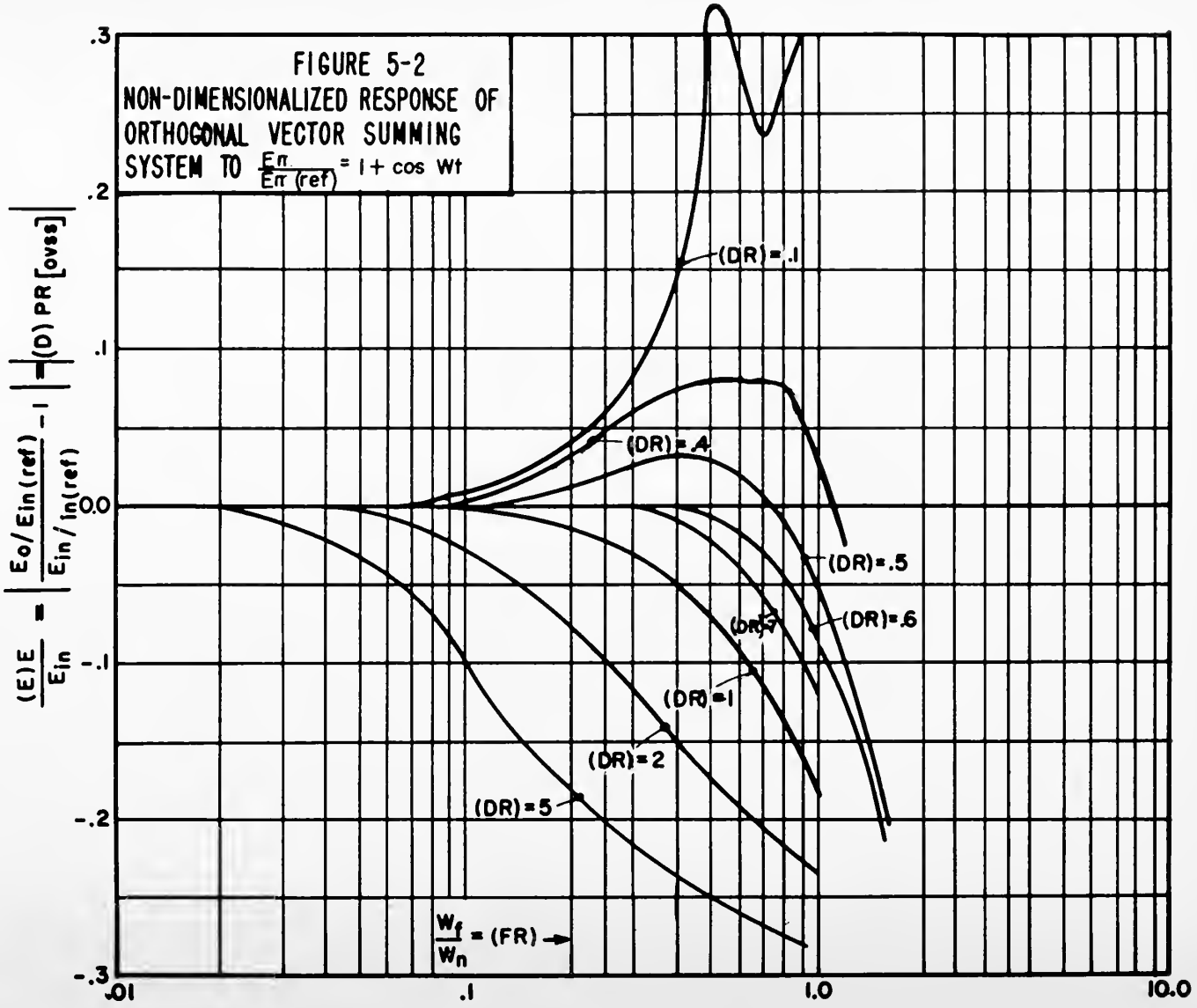
FIGURE 5-2
NON-DIMENSIONALIZED RESPONSE OF ORTHOGONAL VECTOR SUMMING SYSTEM TO $\frac{E\pi}{E\pi\,(ref)} = 1 + \cos \omega t$
$\frac{(E)E}{Ein} = \left| \frac{Eo/Ein(ref)}{Ein/In(ref)} - 1 \right| \angle (D)\,PR\,[ovss]$
.3
.2
.1
0.0
-.1
-.2
-.3
.01
.1
1.0
10.0
(DR)=.1
(DR)=.4
(DR)=.5
(DR)=.6
(DR)=1
(DR)=2
(DR)=5
$\frac{W_f}{W_n}$ = (FR)

$\frac{E_o^2}{E^2_{in(ref)}}$ can be calculated from 5-24 with $(DR)_{(ovss)}$ as the parameter. The second harmonic component will cause a resonant point at (FR) $\approx .5$ in addition to the usual resonant point, hence the broadening of this peak over the usual form in which it is seen. The fact that for low damping values the resonant peaks become narrow and high, brings out an interesting point in connection with the curve for $(DR)_{(ovss)} = .1$. Here we have two distinct peaks, the first due to the second harmonic, coming at a frequency ratio slightly less than .5.

In order to find the phase response of the system to the input function $\frac{E_{in}}{E_{in(ref)}} = 1 + \cos Wt$, it will be best to look at the squares of the outputs and inputs in rotating vector form. In setting up the relationship between the input and output rotating vectors, let us assume $(DRA)_1 = 30^o$ and $(DRA)_2 = 60^o$ as a typical case. Further, let us assume for simplicity that the amplitudes of the response vectors are the same as the corresponding input quantities.

It is obvious that the phase angle between input and output will not remain constant throughout a complete rotation of the fundamental vector due to the second harmonic vector rotating twice as fast. This changing of phase angle throughout one period becomes more pronounced as $(DRA)_2$ builds up. The best that we can do for the given system is to predict where the $(DRA)_{(ovss)}$ starts to build up to a few degrees. Inasmuch as the fundamental vector is four times the second harmonic for most cases (not near resonance for low damping ratios), we can, for small phase angles, approximate the total phase from the fundamental as can be seen from part I of Fig. 5-3. We also must define this phase angle to be determined at t = 0, 2 , etc. as shown in part I of Fig. 5-3. Fig. 5-4 gives the phase lag of the fundamental as a function

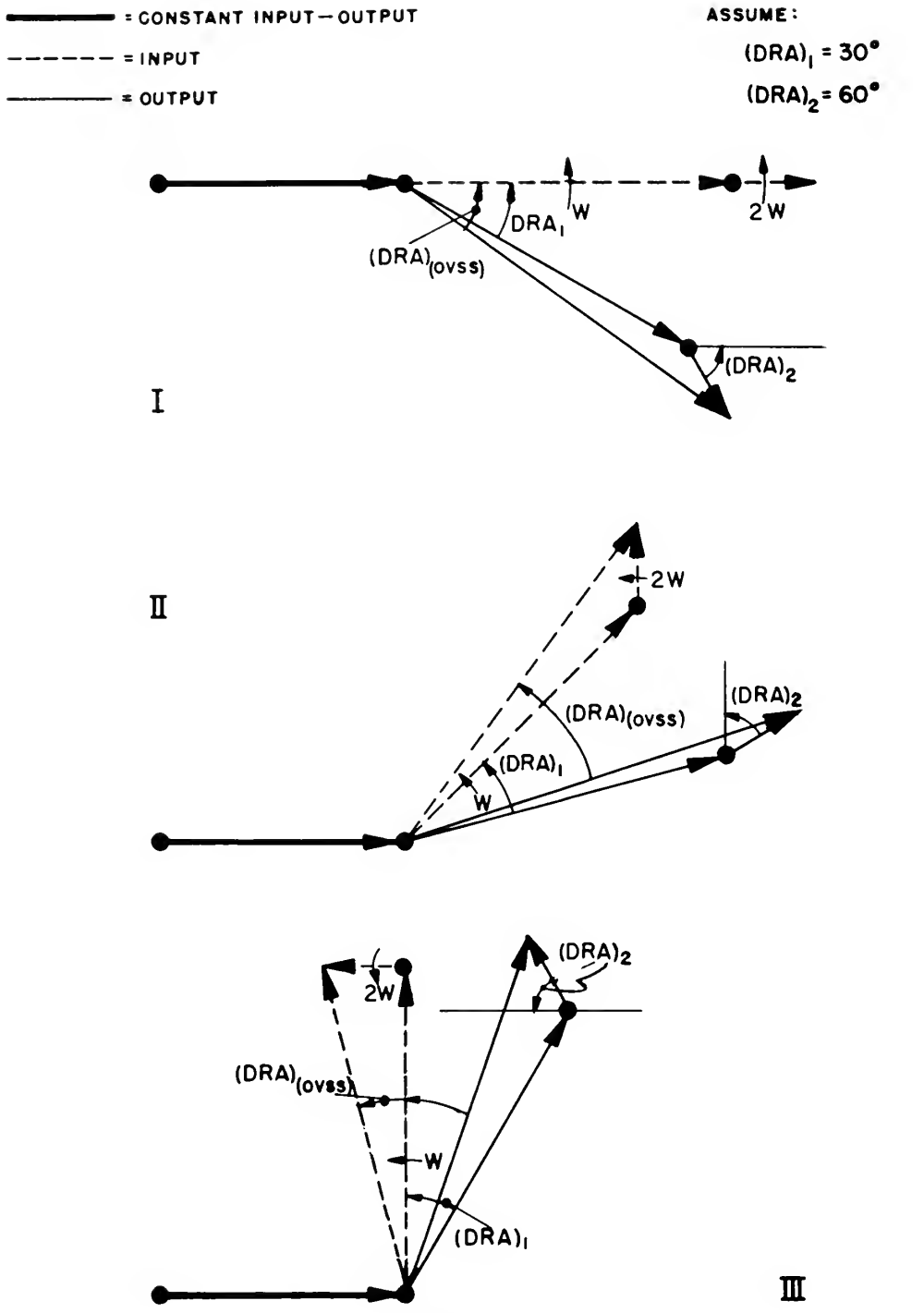

FIGURE 5-3
INSTANTANEOUS RELATIVE POSITIONS OF OUTPUT AND INPUT FUNCTIONS FOR THE FORCING FUNCTION, $\frac{E^2_{in}}{E^2_{in(ref)}} = 1.5 + 2\cos Wt + .5\cos 2Wt$

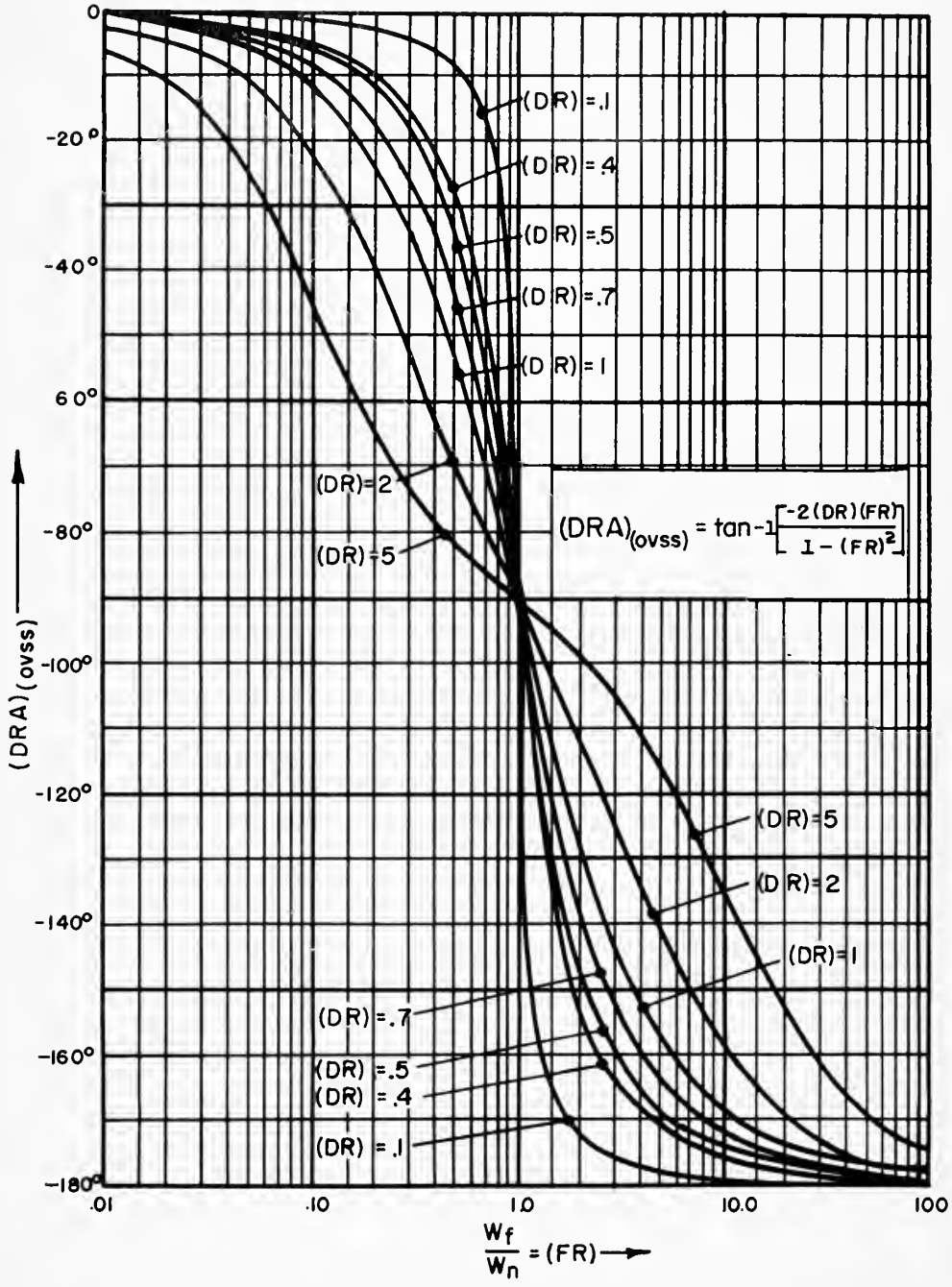

FIGURE 5-4

$(DRA)_{(ovss)}$ AS A FUNCTION OF FREQUENCY FOR $\frac{E_{in}}{E_{in(ref)}} = 1 + \cos Wt$

of frequency. Caution must be taken to use Fig. 5-4 only for small angles.

In concluding this chapter on the steady state harmonic analysis, it must be pointed out that approximations have to be made due to the non-linearities of the system. These approximations give good results at the point where the magnitude of the $(D)(PR)_{(ovss)}$ just start to build up and where the phase lags are only a few degrees. We have assumed in order to use the material presented here that a non-linear device has been inserted into the feedback loop so as to keep the dynamics essentially constant.

This chapter emphasizes the difficulties in obtaining a method of analyzing a non-linear system so as to give a clear cut picture over the entire operating range.

It is felt by the author that a step function response type of analysis is the more suitable method of ascertaining the speed of response for this type of system. The experimental results presented in the next chapter will bear out this opinion. This chapter was included mainly in keeping with the underlying spirit of this thesis, namely that it be a study of the dynamics associated with the given system.

CHAPTER VI

Design and Results of a Laboratory Test System

The general theory developed in Chapters II, III, and IV will now be applied to the design and testing of an actual system. Because of the fact that exact specifications of microsyn units are still considered restricted, we shall not use the actual values, but we have chosen the specifications so that the test results do actually give a true picture of the operation of the system.

Thus, using Fig. 2-2 as our starting point, we shall use the following design parameters for the system to be designed in this chapter.

$$S_{(tg)}\left[i^2;M\right] = 42.4 \frac{\text{dyne cm}}{\text{ma}^2} \qquad 6\text{-}1$$

$$S_{(sg)}\left[A;i,n,e\right] = 3.25 \times 10^{-4} \frac{\text{volt}}{\text{rad ma cycle/sec}}$$

$$i_{(ex)} = 100 \text{ ma}$$

$$n_{(ex)} = 400 \text{ cycles/sec}$$

$$A_{(rot)(max)} = 10^{\circ} = .174 \text{ radians}$$

$$I_{(tsm)} = 330 \text{ gm cm}^2$$

Using the above excitation values for the signal generator, we obtain

$$S_{(sg)}\left[A;e\right] = 13 \frac{\text{volts}}{\text{rad}} \qquad 6\text{-}2$$

Since 50 ma is a desirable upper limit of driving current for each torque generator, the maximum torque produced per torque generator is

$$M_{(tg)(max)} = S_{(tg)} \left[i^2;M \right] i^2_{(max)}$$

$$= 42.4 \frac{\text{dyne cm}}{\text{ma}^2} \times 2500 \text{ ma}^2$$

$$= 106{,}000 \text{ dyne cm} \qquad 6\text{-}3$$

Hence, the total maximum torque produced by the maxium input signals will be 212,000 dyne cm. Thus, the maximum torque produced by the feedback voltage E_o will have to be 212,000 dyne cm.

Fig. 6-1 shows in schematic form the torque generator winding arrangement. i_x and i_y are connected in single axis arrangement on separate microsyn units. i_o, the current due to the feedback voltage E_o, is connected in single axis arrangement but windings of poles 1 and 3 of each microsyn unit are connected in series so that the feedback current i_o produces twice the torque that it would if it were to actuate only one microsyn unit. This is necessary because we need to keep the maximum torque generator current at 50 ma.

Referring again to Fig. 2-2, it can be seen that in the steady state,

$$M_1 + M_2 = M_3$$

$$S^2_{(cs)_1}\left[e;i\right] S_{(tg)_1} E_x{}^2 + S^2_{(cs)_2}\left[e;i\right] S_{(tg)_2} E_y{}^2 = S^2_{(cs)}\left[e;i\right] S_{(tg)_3} E_o{}^2 \qquad 6\text{-}4$$

Since $S_{(cs)_1} = S_{(cs)_2}$

and $S_{(tg)_1} = S_{(tg)_2}$

$$S^2_{(cs)_{1,2}} S_{(tg)_{1,2}} \left[E_x{}^2 + E_y{}^2 \right] = S^2_{(cs)_3} S_{(tg)_3} E_o{}^2 \qquad 6\text{-}5$$

Hence

$$E_o{}^2 = E_x{}^2 + E_y{}^2 \quad \text{if}$$

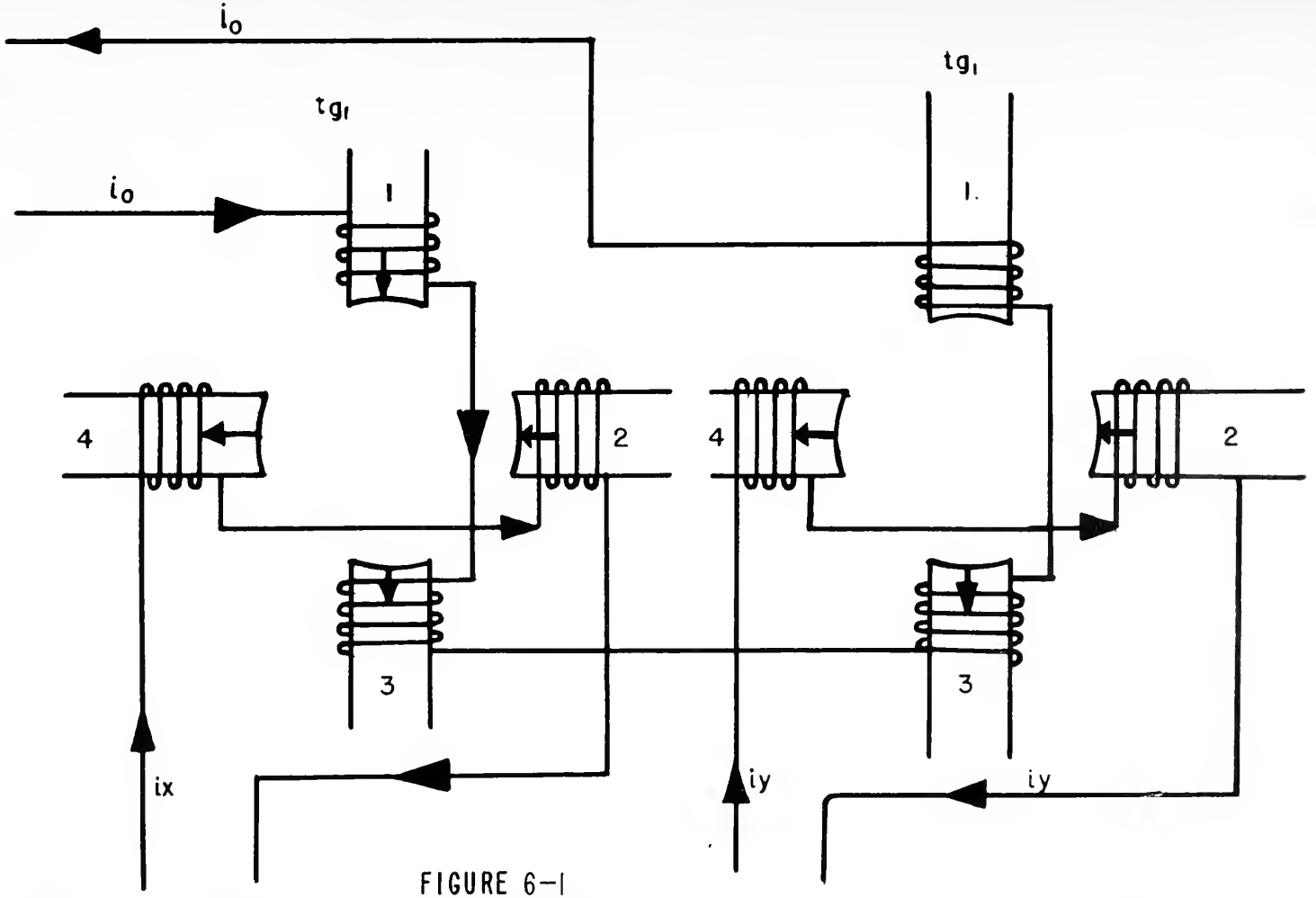

FIGURE 6-1

WIRING ARRANGEMENT OF THE TORQUE GENERATORS USED IN LABORATORY SYSTEM

$$S^2(cs)_{1,2}\left[e;i\right] S(tg)_{1,2} = S^2(cs)_3\left[e;i\right] S(tg)_3 \qquad 6\text{-}6$$

For the system described here, we can define a fictitious third torque generator as shown in Fig. 2-2 which will have twice the sensitivity of a single torque generator. The resistance of this series connection of torque generator windings will be double that of single microsyn operation. However, because of the fact that a current source actuates the torque generators, a change in resistance in the windings does not change the driving current since current sources have infinite internal resistance.

Referring to 6-6 and noting that

$$S(tg)_3 = 2\, S(tg)_{1,2}\,,$$

$$S^2(cs)_3\left[e;i\right] = \tfrac{1}{2}\, S^2(cs)_1\left[e;i\right]$$

$$S(cs)_3\left[e;i\right] = .707\, S(cs)_1\left[e;i\right] \qquad 6\text{-}7$$

From equation 2-8 we have defined

$$S(ovss)\left[A;M\right] = S(tg)\left[i^2;M\right] S^2(cs)\left[e;i\right] S^2(sr)\left[e^{\frac{1}{2}};e\right] S(sg)\left[A;e\right] \qquad 2\text{-}8$$

where it has been assumed in 2-8 that all the torque generator and current source sensitivities are respectively equal. However, in the laboratory system we have defined $S(tg)_3\left[i^2;M\right] = 2\, S(tg)_{1,2}\left[i^2;M\right]$. Nevertheless 2-8 is still valid here since we have kept the product $S(tg)\left[i^2;M\right] S^2(cs)\left[e;i\right]$ constant.

It is desired to use the full 10^o or .174 radians for rotor angle in designing the system, this angle being produced at the maximum torque level.

Hence

$$S_{(ovss)}\left[A;M\right] = \frac{212{,}000 \text{ dyne cm}}{.174 \text{ radians}}$$

$$= 1{,}220{,}000 \text{ dyne cm/rad} \qquad 6\text{-}8$$

Letting $E_{x(max)}$, and $E_{y(max)}$ be 50 volts each,

$$S_{(cs)1} = S_{(cs)2} = \frac{50 \text{ ma(max)}}{50 \text{ V(max)}} = 1 \text{ ma/volt} \qquad 6\text{-}9$$

If $E_{x(max)} = E_{y(max)} = 50V$

$$E_{o(max)} = \sqrt{2500 + 2500} = 70.7 \text{ volts} \qquad 6\text{-}10$$

Hence

$$S_{(cs)3} = \frac{50 \text{ ma(max)}}{70.7 \text{ volts}} = .707 \text{ ma/volt} \qquad 6\text{-}11$$

This latter value checks with the result of 6-7.

Using equation 2-8, we obtain

$$S^2_{(sr)}\left[e^{\frac{1}{2}};e\right] = \frac{S_{(ovss)}\left[A;M\right]}{S_{(tg)3}\left[i^2;M\right] S^2_{(cs)3}\left[e;i\right] S_{(sg)}\left[A;e\right]} \qquad 6\text{-}12$$

$$S^2_{(sr)}\left[e^{\frac{1}{2}};e\right] = \frac{1{,}220{,}000 \frac{\text{dyne-cm.}}{\text{rad.}}}{.848 \times 10^2 \frac{\text{dyne cm}}{ma^2} \times .5 \frac{ma^2}{\text{volts}} \times 1.3 \frac{\text{volts}}{\text{rad}} \times 10^1}$$

$$= 2210 \frac{\text{volts}^2}{\text{volt}}$$

or

$$S_{(sr)}\left[e^{\frac{1}{2}};e\right] = 47.0 \frac{\text{volts}}{\text{volt}^{\frac{1}{2}}} \qquad 6\text{-}13$$

Figure 3-1 shows the characteristics of the square root generator.

To actually obtain a device that will have a performance characteristic similar to Fig. 3-1 is very difficult. This is especially true near the origin where the slope of the curve becomes infinite. However, through the use of vacuum or selenium rectifier switching circuits in cascade with a linear amplifier, the curve of Fig. 3-1 can be approximated to a high degree except at the origin. The latter part of the chapter will be devoted to the design of a suitable attenuator which will stay within certain specified tolerances of the dynamics of the system.

Fig. 6-2 shows an electrical schematic of the system from which the experimental results will be obtained. High gain DC amplifiers with unity feedback, feeding into parallel connected 6SN7 triodes in each case act as current sources.

The DC amplifier arrangement as shown in Fig. 6-2 can be considered current sources because of the following conditions. The gain of the DC amplifier is very high with a phase inversion and the input impedance is also very high. Thus referring to the figure below, the input to the DC amplifier (point G below) is driven very close to ground because of the very high negative feedback.

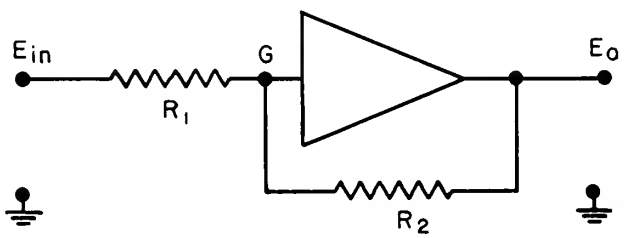

Furthermore, since the input impedance to the amplifier is very high, the current through R_1 equals the current through R_2. But since G is ideally

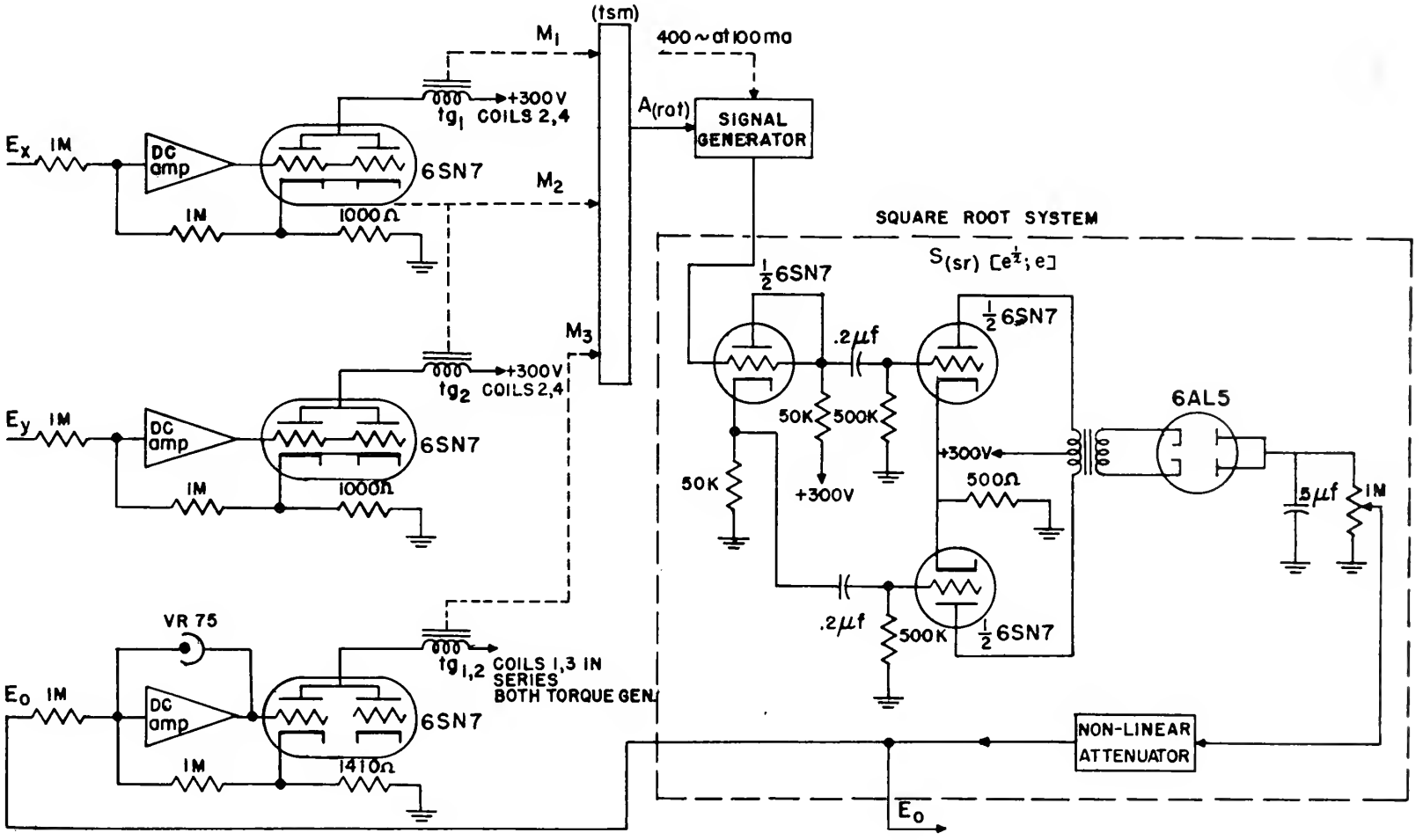

FIGURE 6-2
ELECTRICAL CIRCUIT DIAGRAM OF LABORATORY TEST SYSTEM

at ground, we can consider the current through R_1 as depending only on E_{in} and R_1 leaving R_2 to vary at will. However, through current considerations

$$\frac{E_{in}}{R_1} = \frac{E_o}{R_2}$$

or

$$\frac{E_o}{E_{in}} = \frac{R_2}{R_1} \qquad 6\text{-}14$$

Hence, E_o is determined solely by the ratio of $\frac{R_2}{R_1}$. In the actual system we have fed E_o into a cathode follower and the voltage at the feedback point of the cathode is still determined only by the ratio of the feedback resistor to the input resistor. The cathode resistor is then calculated to give a certain desired current for the given input voltage. Of course, we have to assume that the output tube operates below any non-linearities due to saturation. The cathode resistors are determined so that maximum currents of 50 ma each are delivered for each respective maximum voltage input.

Since the maximum signal from the signal generator is only about 2.25 volts rms (400 cps), an AC amplifier has been provided with a gain of around 500. This amplified signal generator voltage is then full-wave rectified and filtered before being fed through the non-linear device as DC. The output of the non-linear device gives the desired solution, E_o. The components within the dashed line box provide the $S_{(sr)}\left[e^{\frac{1}{2}};e\right]$ of the box as shown in Fig. 2-2. Because of the fact that the maximum forcing frequencies will be on the order of a few cycles, the square root section will be assumed to add no additional dynamics to the system. A VR-75 regulator tube is used around the feedback DC

amplifier in order to protect the amplifier from saturation when testing the system in the unstable region described in Chapter II.

We shall now apply the development of Chapter III to the actual system just described taking into careful consideration the need for the stop near the null in order to maintain a stable operating range.

All of the operating components of the laboratory system have been specified with the exception that the square root generator was left ideal and specified by the equation,

$$E_o = 47.0\, E_{(sg)}^{\frac{1}{2}}$$

In Chapter III, we have denoted the ideal case as

$$E_o = f(A) = P_{(ref)}\, A^{\frac{1}{2}} \qquad 6\text{-}15$$

where

$$P_{(ref)} = S_{(sr)}\left[e^{\frac{1}{2}};e\right]\, S^{\frac{1}{2}}_{(sg)}\left[A;e\right]$$

Numerically

$$P_{(ref)} = 47.0\, \frac{\text{volt}}{\text{volt}^{\frac{1}{2}}}\ \times \sqrt{13}\ \ \frac{\text{volts}^{\frac{1}{2}}}{\text{rad}^{\frac{1}{2}}}$$

or

$$P_{(ref)} = 170\, \frac{\text{volts}}{\text{rad}^{\frac{1}{2}}} \qquad 6\text{-}16$$

In setting up a workable system, let us arbitrarily set a tolerance on the dynamics so that the natural undamped frequency and the damping ratio do not vary from $W_{n(ref)}$ and $(DR)_{(ovss)(ref)}$ by more than 25%. This tolerance may seem somewhat large, but it will be seen that the principles underlying the theory developed in this chapter are more clearly and easily shown if a fairly large tolerance is assumed.

The expression for the natural angular frequency of the ideal system as given in 2-15 is

$$W_{n(ref)} = \sqrt{\frac{S_{(ovss)}[A;M]}{I}}$$

where $S_{(ovss)}[A;M] = 1{,}220{,}000$ dyne cm/rad and I = gm cm^2. Using these values

$$W_{n(ref)} = 60.8 \text{ rad/sec} \qquad 6\text{-}17$$

Thus referring to 3-23 and 3-24, we obtain

$$W_{n(L)} = 60.8 \text{ rad/sec} - (.25)(60.8) \text{ rad/sec}$$

$$W_{n(L)} = 45.6 \text{ rad/sec} \qquad 6\text{-}18$$

and

$$W_{n(U)} = 60.8 \text{ rad/sec} + (.25)(60.8) \text{ rad/sec}$$

$$W_{n(U)} = 76.0 \text{ rad/sec} \qquad 6\text{-}19$$

The two limiting slope equations are thus obtained from 3-25 and will be defined as

$$f'(A) = 3.91 \text{ volts}^2 \text{ sec}^2 \quad \frac{W_n^2}{f(A)} \qquad 6\text{-}20$$

Hence, for the case in question, the upper and lower limiting slopes become

$$f'(A)_L = \frac{8130}{f(A)} \qquad 6\text{-}21$$

$$f'(A)_U = \frac{22{,}600}{f(A)} \qquad 6\text{-}22$$

From 6-15 and 6-16, we obtained the ideal square root equation as

$$E_o = f(A) = \left(170 \frac{\text{volts}}{\text{rad}^{\frac{1}{2}}}\right) A^{\frac{1}{2}} \qquad 6\text{-}23$$

Using the arbitrary 25% tolerances, we obtain the limiting square root curves as shown in Fig. 3-3 as

$$f(A)_L = 170 - (.25)\ 170\ \frac{\text{volts}}{\text{rad}^{\frac{1}{2}}}\ A^{\frac{1}{2}}$$

or

$$f(A)_L = 127.5\ \frac{\text{volts}}{\text{rad}^{\frac{1}{2}}}\ A^{\frac{1}{2}} \qquad 6\text{-}24$$

similarly

$$f(A)_U = 212.5\ \frac{\text{volts}}{\text{rad}^{\frac{1}{2}}}\ A^{\frac{1}{2}} \qquad 6\text{-}25$$

Taking the functional derivatives of 6-24 and 6-25 and forming the respective products $f(A)\ f'(A)$ we obtain

$$f'(A)_L = \frac{8130}{f(A)} \qquad 6\text{-}26$$

$$f'(A)_U = \frac{22{,}600}{f(A)} \qquad 6\text{-}27$$

Equations 6-26 and 6-27 check with 6-21 and 6-22 and hence are valid for obtaining the limiting slopes throughout the A, f(A) plane. We shall abbreviate $A_{(rot)}$ to A to simplify the notation.

Fig. 6-3 shows in detail the limiting curves of the square root generator with the assumed tolerances of $\pm$ 25% using the full 10° of shaft angle. The limiting slopes are determined at any point A, f(A) by $f(A)_L$ and $f(A)_U$. However instead of fixing the curves at the origin, let us fix the upper end point at the ideal values corresponding to $A_{(rot)}$ = 10° or .174 radians which gives an ideal E_o = 70.7 volts. If we start at $A_{(max)}$, $E_{o(max)}$ and always follow the lowest limiting slope at every point, we notice that it is possible to stay within the dynamic tolerances and intercept the E_o axis at a value of 47 volts. This path is of course trivial because it would be impossible to form the right triangle addition for any value of the hypotenuse less than approximately 47 volts. Starting again at $A_{(max)}$, $E_{o(max)}$ and this time following the highest limiting slope at each point we find a much

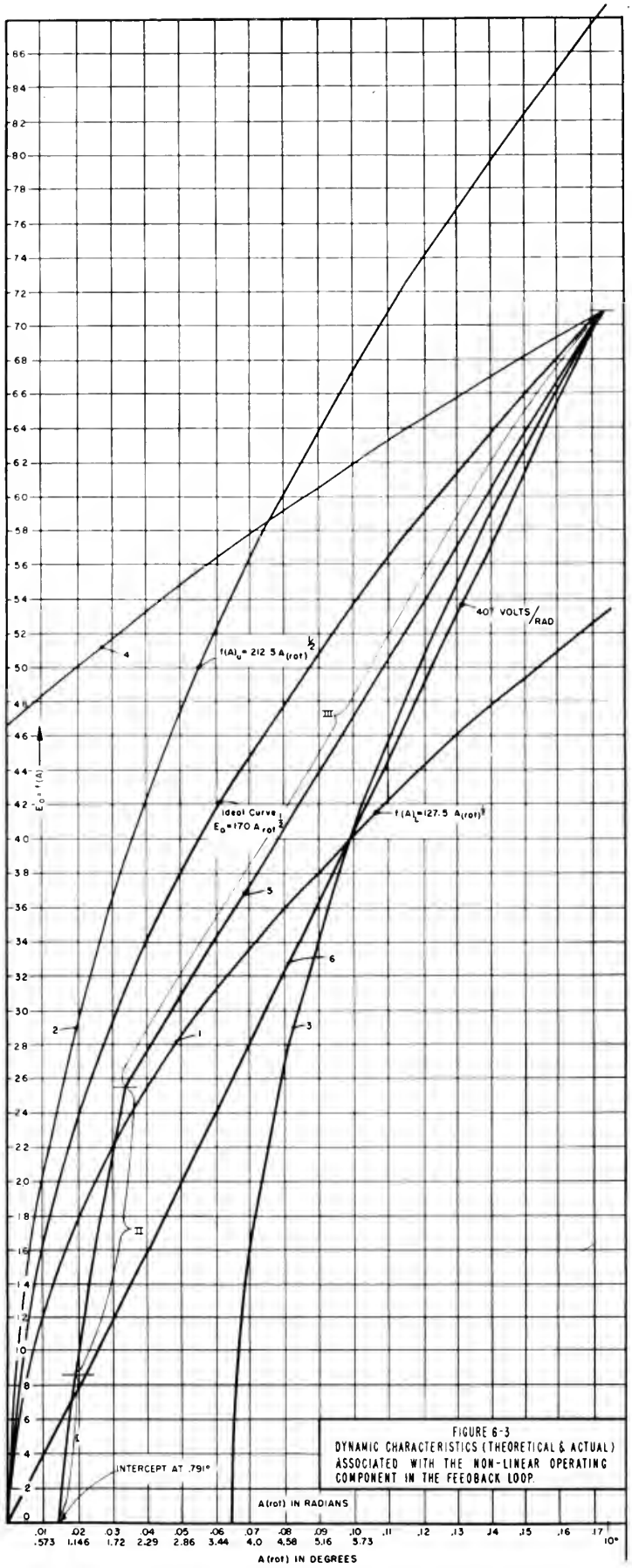

FIGURE 6-3
DYNAMIC CHARACTERISTICS (THEORETICAL & ACTUAL) ASSOCIATED WITH THE NON-LINEAR OPERATING COMPONENT IN THE FEEDBACK LOOP.

more useful situation. In this case, it is to be noted that it is possible to compute E_o down to the limiting value of zero. We observe in our case that for A = .064 rad., E_o = 0. The fact that it is possible to allow a rotation of the rotor before allowing an output suggests the feasibility of using an electrical stop at a small positive angle in order to overcome the condition of instability at the origin described in Chapter II.

It is to be emphasized again that the loop gain does not affect the steady state conditions of the system except to change the angle of the shaft, but does effect the dynamic qualities. Thus, doubling the loop gain from that amount shown in Fig. 6-3 reduces the maximum angle to 5°, increases the natural undamped frequency by $\sqrt{2}$, and decreases the damping ratio by $\sqrt{2}$.

The first condition can be seen from the following considerations. From Chapter II, we have shown that one version of the performance equation of the system is

$$I_{(rot)}\,\ddot{A} + C_d\,\dot{A} + S^2_{(cs)}\left[e;i\right] S_{(tg)}\left[i^2;M\right]\; S^2_{(sr)}\left[e^{\frac{1}{2}};e\right]\; S_{(sg)}\left[A;e\right]\; A$$

$$= S^2_{(cs)}\left[e;i\right]\; S_{(tg)}\left[i^2;M\right]\; E^2_{in} \qquad 6\text{-}28$$

Thus, in the steady state,

$$A_{(max)} = \frac{E^2_{in(max)}}{S^2_{(sr)}\left[e^{\frac{1}{2}};e\right]\; S_{(sg)}\left[A;e\right]} \qquad 6\text{-}29$$

Since the square root sensitivity will consist of a linear a-c amplifier demodulator combination in cascade with a passive attenuating network which will, in the ideal case, follow a square root function.

Hence, we may write

$$S^2_{(sr)}\left[e^{\frac{1}{2}};e\right] = S^2_{(amp)}\left[e;e\right] S^2_{(att)}\left[e^{\frac{1}{2}};e\right] \qquad 6\text{-}30$$

and

$$A_{(max)} = \frac{E^2_{in(max)}}{S^2_{(amp)}\left[e;e\right] S^2_{(att)}\left[e^{\frac{1}{2}};e\right] S_{(sg)}\left[A;e\right]} \qquad 6\text{-}31$$

But, since

$$S_{(ovss)}\left[A;M\right] = S_{(tg)}\left[i^2;M\right] S^2_{(cs)}\left[e;i\right] S^2_{(amp)}\left[e;e\right] S^2_{(att)}\left[e^{\frac{1}{2}};e\right] S_{(sg)}\left[A;e\right] \qquad 6\text{-}32$$

$$A_{(max)} = \frac{E^2_{in(max)}\, S_{(tg)}\left[i^2;M\right] S^2_{(cs)}\left[e;i\right]}{S_{(ovss)}\left[A;M\right]} \qquad 6\text{-}33$$

or finally,

$$A_{(max)} = \frac{\text{const.}}{S_{(ovss)}\left[A;M\right]} \qquad 6\text{-}34$$

Thus, we have the two results that increasing the sensitivity of the amplifier-demodulator in cascade with the non-linear attenuator by the factor $\sqrt{2}$, doubles the loop gain and cuts the shaft angle in half.

Referring again to Fig. 6-3, we have shown that at any point in the (A, E_o) plane

$$\left(\frac{dE_o}{dA}\right)_L = \frac{8130}{f(A)} \qquad 6\text{-}35$$

and

$$\left(\frac{dE_o}{dA}\right)_U = \frac{22{,}600}{f(A)} \qquad 6\text{-}36$$

in order to stay within our 25% tolerances on the natural frequency and damping ratio of the system.

Starting at the point, (10°, 70.7V), 6-35 is represented by curve 4 and 6-36 is represented by curve 3. It will be easier to design a non-linear device if we plot 6-35 and 6-36 as shown in Fig. 6-4. As long as we stay within the curves (A) and (B) as E_o is changed, then we are meeting the required tolerances on W_n and $(DR)_{(ovss)}$. In the laboratory test system, we shall use a straight line attenuator which will abruptly bend at points where the slope of the original line will cause the tolerances on the dynamics to be exceeded if carried any further.

Thus, starting at the point, (70.7V, 320V/rad), on Fig. 6-4, we proceed along the constant slope III until E_o is lowered to 25.5V where we must break in order to stay within the required boundary curves A and B. The same procedure is carried out for slopes II and I. Slope I is carried straight through to the $E_o = 0$ line and the dynamic tolerances are exceeded at $E_o = 3.2V$. Because of the infinite slope required at the origin, the best we can do is to make the slope for low signal levels as steep as possible and specify for what levels the tolerances on W_n and $(DR)_{(ovss)}$ are exceeded. Fig. 6-3 shows how curves I, II, and III look on the A, f(A) plane. An important point to be brought out here is that slope I crosses the abscissa at some small positive rotation of A. Thus, we have achieved our goal of putting a stop (electrical in this case) so as to keep A from passing into the unstable region. Our next step is to instrumentize a suitable system to give the response represented by slopes I, II, and III.

Our first step in developing an actual circuit that will represent the three different regions is to determine from Fig. 6-3 the actual gains that are required for each region. What will be done

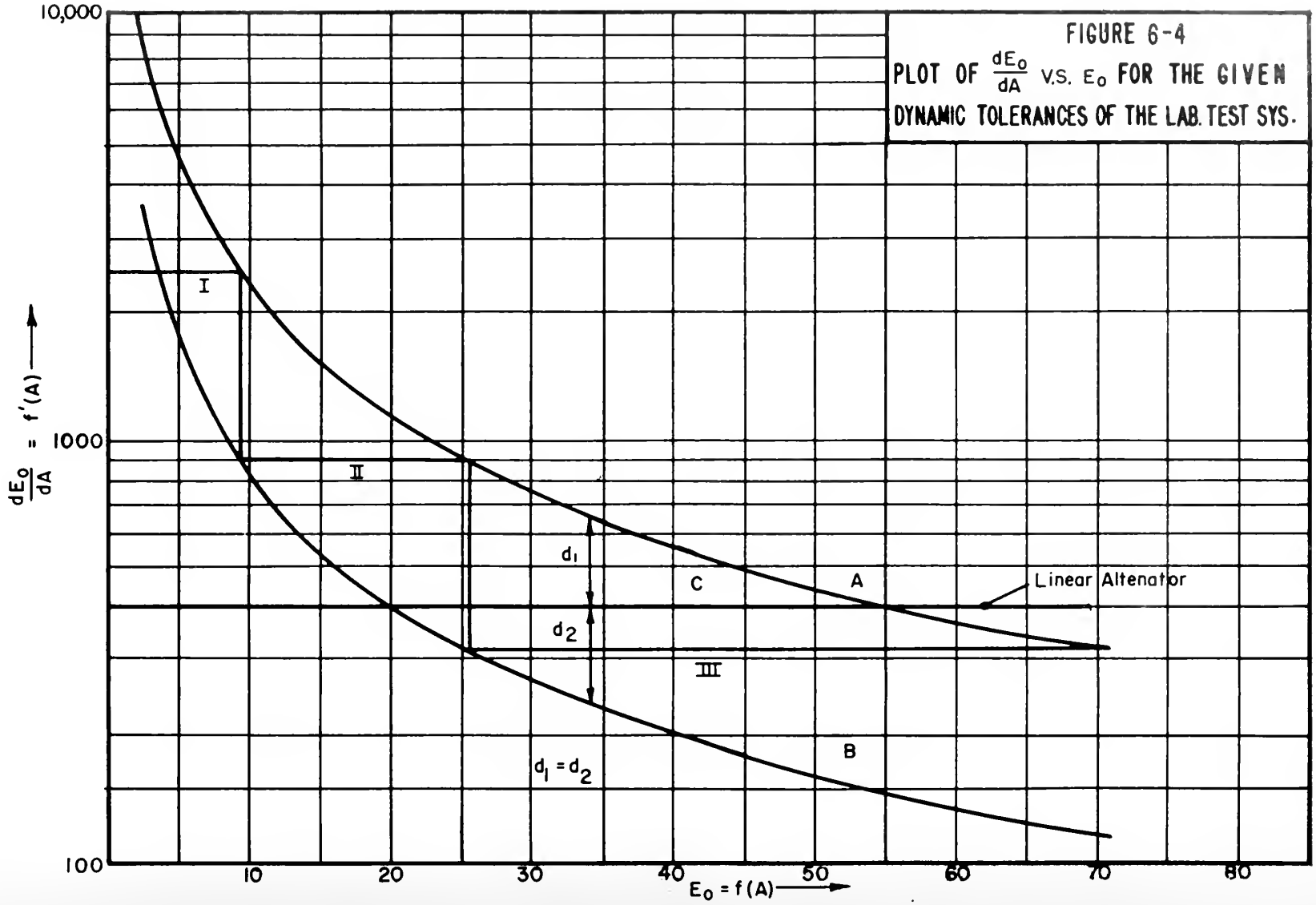

FIGURE 6-4

PLOT OF $\frac{dE_o}{dA}$ V.S. E_o FOR THE GIVEN DYNAMIC TOLERANCES OF THE LAB. TEST SYS.

will be to attenuate the amplifier gain required for step I when passing into regions II and III.

Taking the slopes from Fig. 6-3 which will give us the full ten degree of shaft rotation for maximum E_o we have

Slope	$S_{(amp)\ E;e}$
I	192.3 v/v
II	68.1 v/v
III	23.9 v/v

If we desire five degrees for maximum shaft angle, then each of the above gains are multiplied by the square root of two.

The experimental results to follow will also show how the dynamics vary quite radically when a purely linear device is used in the feedback loop. For ten degree operation this characteristic is represented by slope 6 of Fig. 6-3 and C of Fig. 6-4. From Fig. 6-4, we see that the required 25% tolerances are met for values of E_o ranging from 20V to 56V. For values of E_o greater than 56V, the slope of the linear feedback device is too high as can be seen from Fig. 6-4 and hence the natural undamped frequency is more than 25% greater than $W_{n(ref)}$ and conversely the damping ratio becomes less than $(DR)_{(ovss)(ref)} - 25\% (DR)_{(ovss)(ref)}$. Just the opposite is true for $0 \leqq E_o \leqq 20V$.

Fig. 6-5 shows the attenuator used in the laboratory test system which, in conjunction with a conventional a-c amplifier and demodulator, will follow slopes I, II, and III of Fig. 6-3.

In order to design the attenuator of Fig. 6-5, we need the equations of slopes I, II, and III, which are obtained as follows from Fig. 6-3.

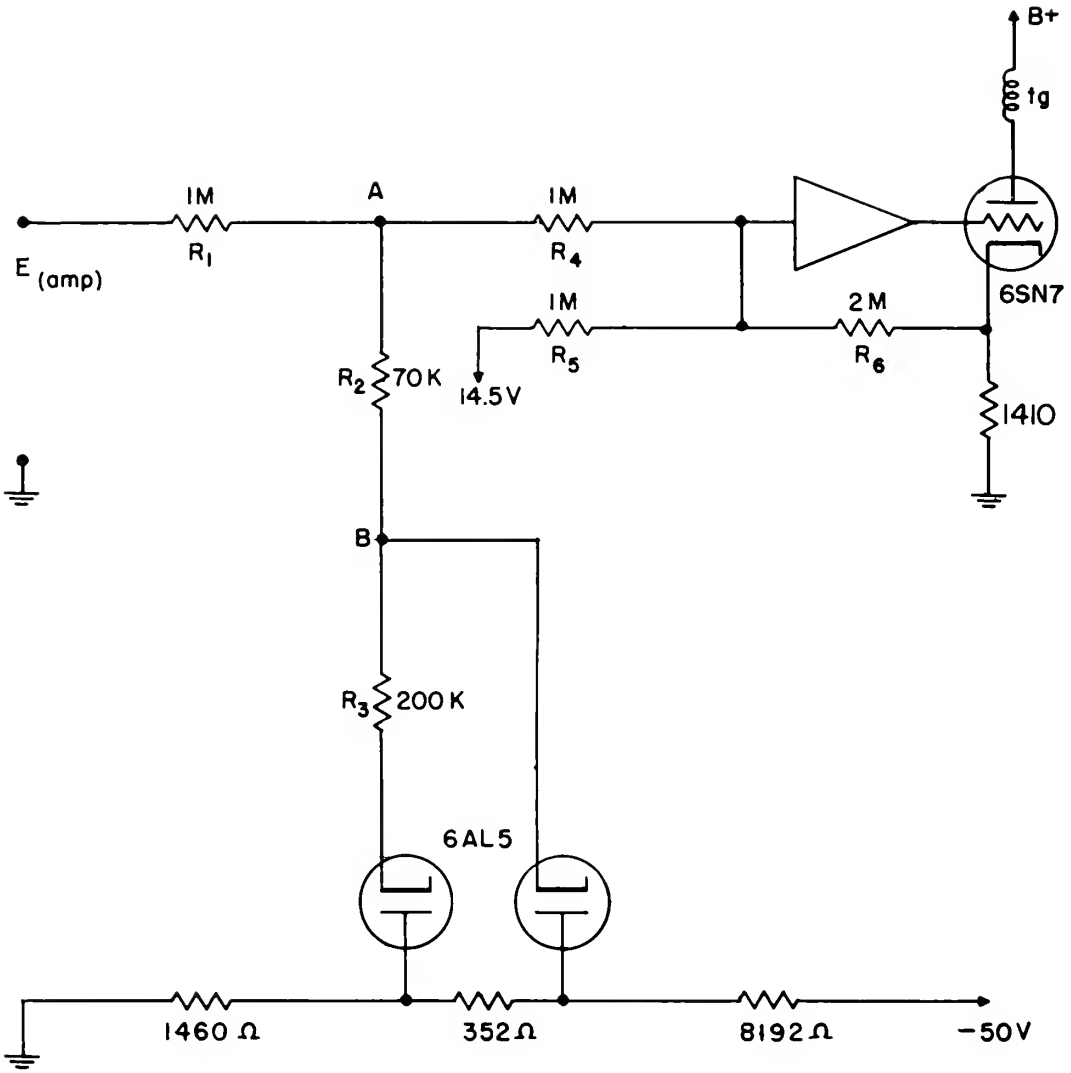

FIGURE 6-5
LABORATORY NON-LINEAR ATTENUATOR

Slope I : $E_o = E_{(amp)} - 29$

Slope II : $E_o = .354\ E_{(amp)} - 9.91$

Slope III : $E_o = .124\ E_{(amp)} + 14.7$

Since the maximum slope to be obtained from the attenuator shown in Fig. 6-5 is .5, we shall double the original value for the gain of slope I to compensate for this. Thus, the actual equations to be fitted by the attenuator are

Slope I : $E_o = .5\ E_{(amp)} - 14.5$

Slope II : $E_o = .177\ E_{(amp)} - 4.96$

Slope III : $E_o = .062\ E_{(amp)} + 7.35$

The diode switching circuit shown in Fig. 6-5 will follow the double line curve shown in Fig. 6-7. This characteristic plus the negative 14.5 volts is then summed by the feedback amplifier to give the desired characteristic. In the actual circuit, all polarities are reversed since the DC amplifier involves a 180 degree phase change and only positive outputs of the DC amplifier are possible because of the unidirectional flow of current in the current source vacuum tube.

Specifically, the operation of the diode switching circuit is explained as follows. As the input, $E_{(amp)}$, increases from zero along slope I, neither diode is conducting and the voltage at A fed into the summing amplifier is

$$E_A = \frac{R_4}{R_1 + R_4} E_{(amp)} = .5\ E_{(amp)}$$

However, when A = .0175 rad as seen from Fig. 6-7, it is necessary to change this characteristic to follow slope II. Thus, at

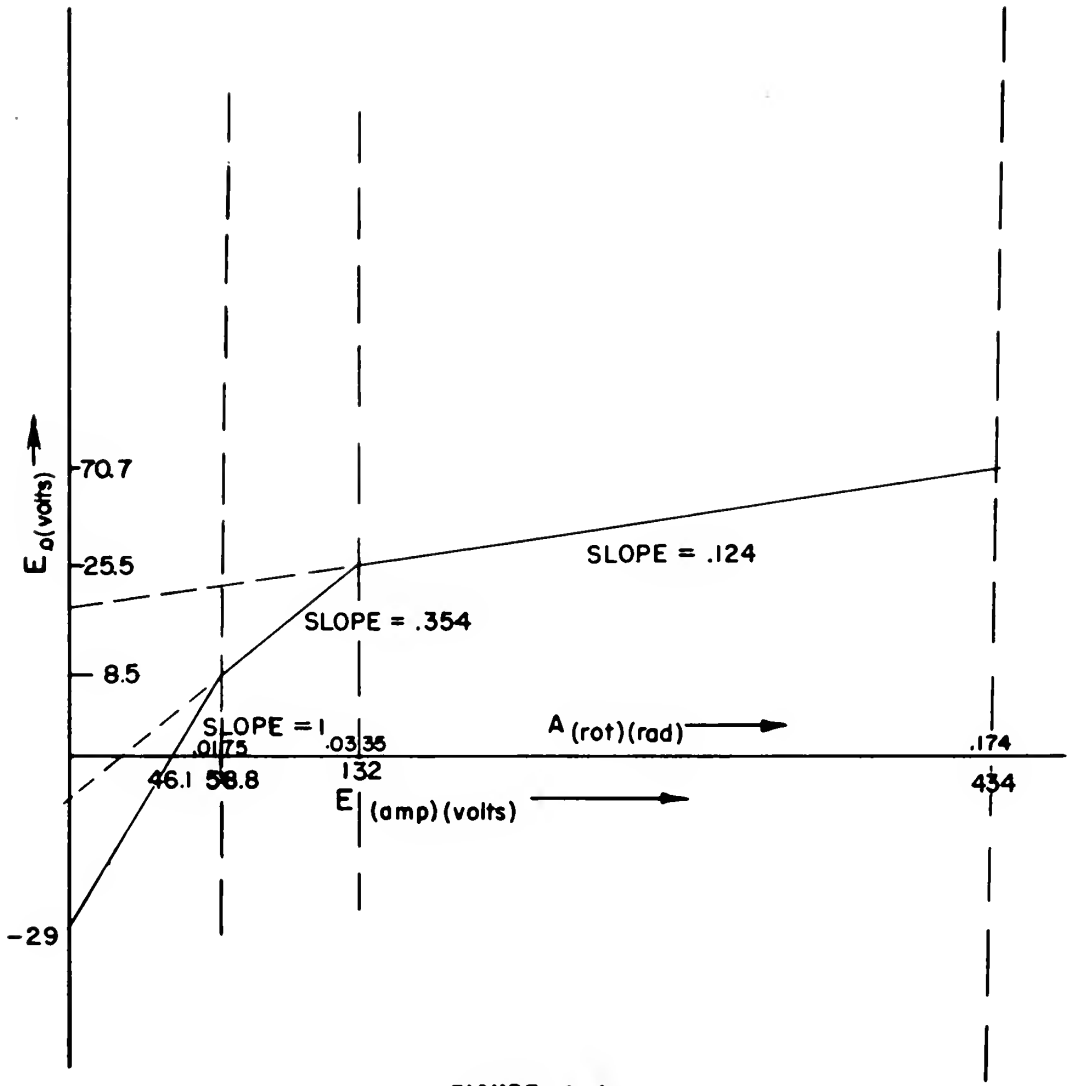

FIGURE 6-6

DESIRED CHARACTERISTIC TO BE
FOLLOWED BY NON-LINEAR ATTENUATOR

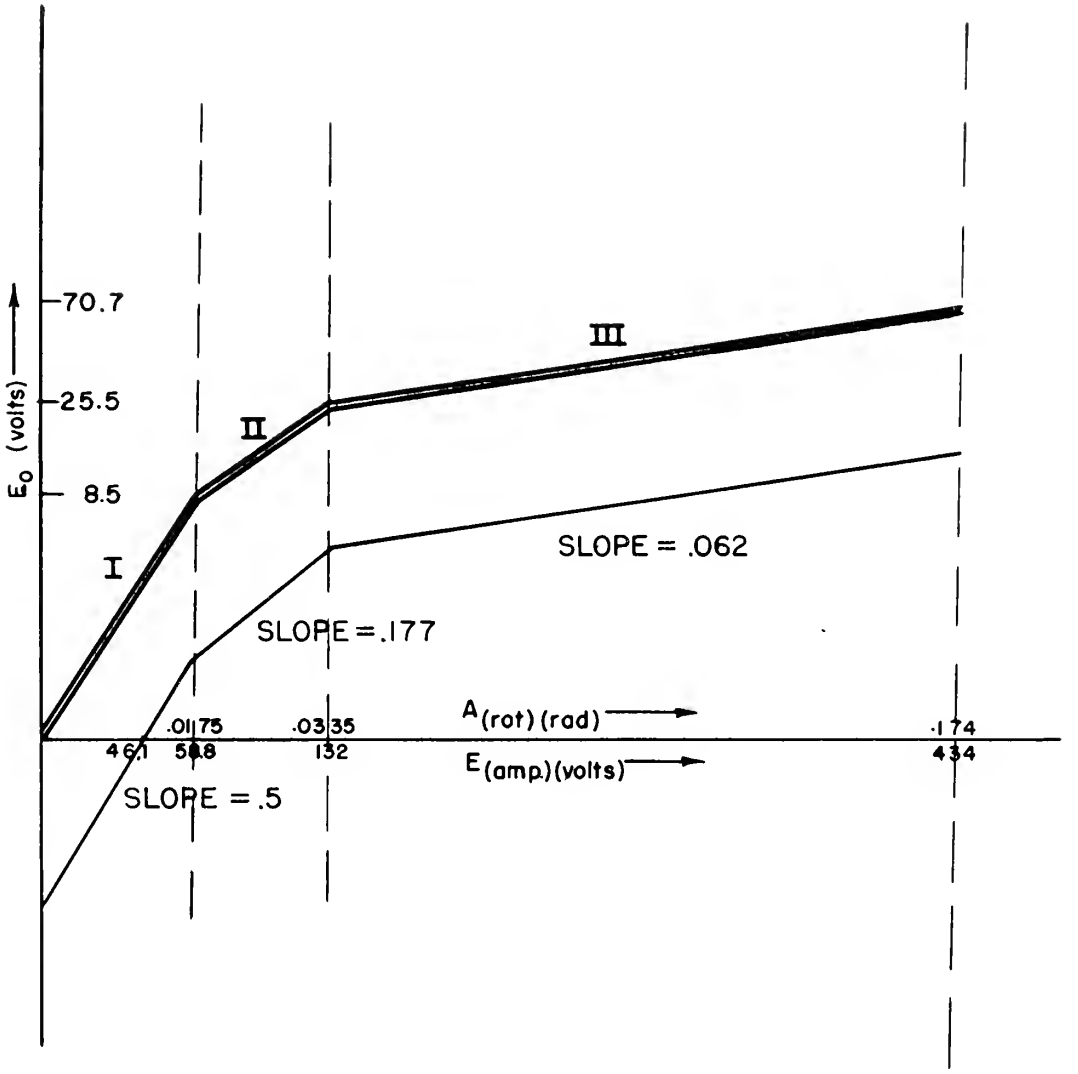

FIGURE 6-7

ACTUAL ATTENUATOR CHARACTERISTICS

this point, V-1 goes into operation and the slope is now determined to a very close approximation by

$$\frac{\dfrac{(R_2 + R_3)(R_4)}{R_2 + R_3 + R_4}}{R_1 + \dfrac{(R_2 + R_3)(R_4)}{R_2 + R_3 + R_4}} = .177$$

In the above expression, we have neglected the small resistance of the 6AL5 diode (varying from 200 to 1000 ohms) and that of the biasing network.

Going through elementary calculations it is found that when A = .0175 rad, the desired switching point, then the voltage at point A is - 7.3V. Thus, with the plate of V-1 set at - 7.3V as shown, the correct breakpoint is determined. Slope II is followed until A = .0335 rad. for the full ten degree operation. At this point, we desire V-2 to start conducting thus effectively shorting R_3. The slope for $\frac{E_A}{E(amp)}$ is then quite closely found to be

$$\frac{\dfrac{R_2 R_4}{R_2 + R_4}}{R_1 + \dfrac{R_2 R_4}{R_2 + R_4}} = .062$$

Again, elementary calculations have shown that when A = .0335, point B of Fig. 6-5 is at - 9V. Thus, setting the plate at - 9V will give the proper switching action.

Fig. 6-8 shows the response of the orthogonal vector summing system to 3 volt step functions without a non-linear attenuator in the feedback loop. A Sanborn pen recorder was used to plot the output of the system as a function of time in seconds. The gain was set so that

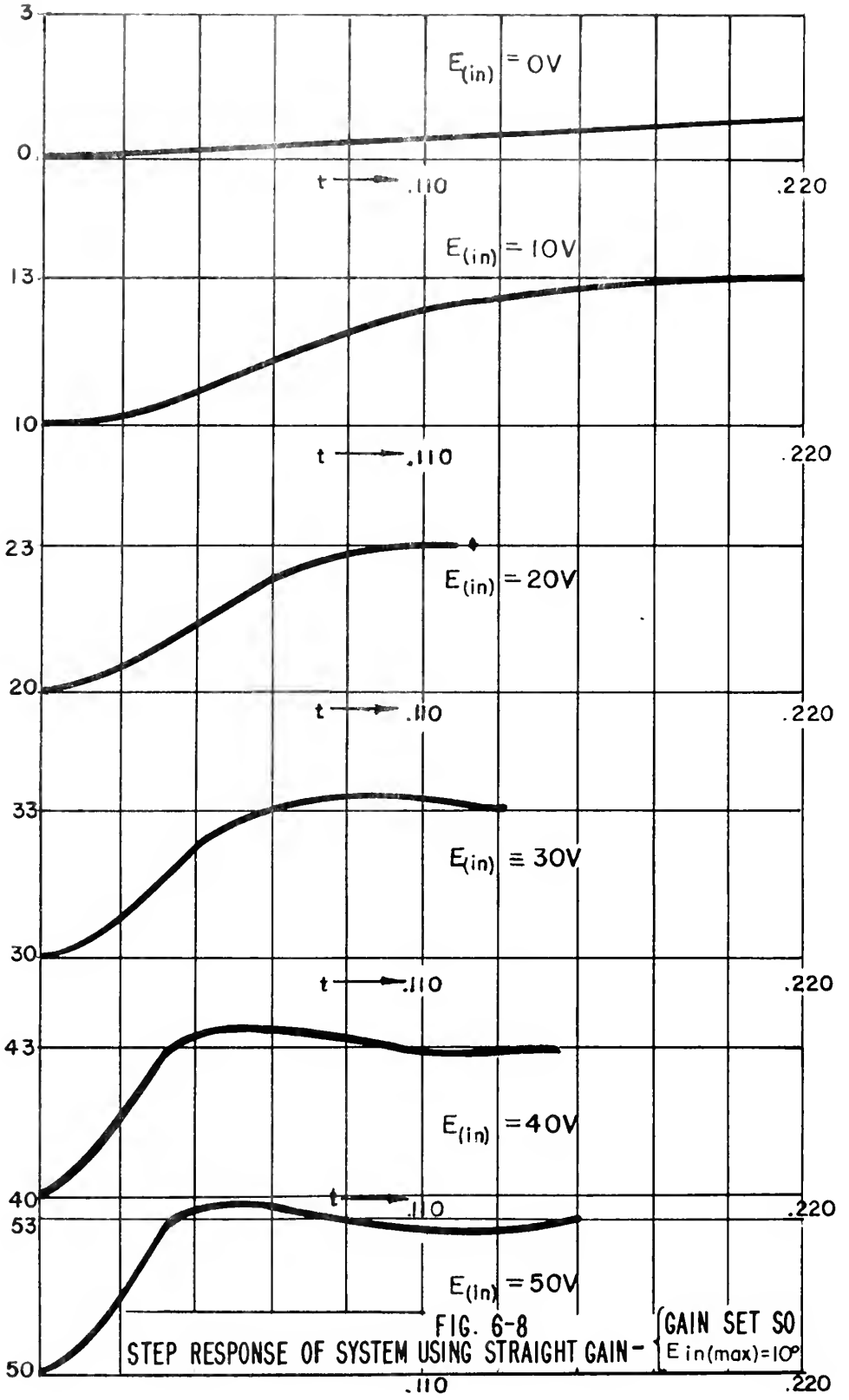

FIG. 6-8
STEP RESPONSE OF SYSTEM USING STRAIGHT GAIN - {GAIN SET SO, E in(max)=10

70.7 volts output gave the full ten degree operation. As explained previously, plot C of Fig. 6-4 shows the straight gain characteristic for full ten degree operation. Only at E_o = 34 volts is the slope of the linear characteristic the same as that of the ideal curve. This is the point on Fig. 6-4 where $d_1 = d_2$ since the ideal curve is half way between A and B.

From Fig. 6-8, it appears that the $(DR)_{(ovss)}$ referring to the linear second order system at E_o = 34V is about .6.

To check this, we make use of the theoretical expression

$$(DR)_{(ovss)} = \frac{C_d}{2} \sqrt{\frac{1}{S_{(ovss)}[A;M]\, I}} \qquad 6\text{-}37$$

C_d has been found to be $2.5 \times 10^4 \frac{\text{dyne cm}}{\text{rad/sec}}$ at 200°F. This was calculated by putting a known small current through a torque generator winding and measuring the time taken to travel through a given angle.

Substituting numerical values into 6-37 gives

$(DR)_{(ovss)}$ = .625 which is a good check on the experimental result.

W_n has already been found to be 60 rad/sec for the ideal case. Thus, a rough check on the time it takes for the output to first pass through its final asymptotic value can be found by the expression.

$$T_p = \tfrac{1}{4} \times \frac{2\pi}{W}$$

or

$$T_p = \frac{\pi}{2W_n \sqrt{1 - (DR)^2}} \qquad 6\text{-}38$$

In the case of the ideal system, T_p = .033 sec, a value that

should correspond to the 34V point. Interpolating between the 30V and 40V points on Fig. 6-8, this value is fairly well checked.

Fig. 6-9 shows the same straight gain type of system as that of Fig. 6-8 except that $E_{o(max)}$ corresponds to 5° of shaft angle instead of the full 10° in the previous case. Thus, at corresponding input levels, the damping ratio associated with the linear squared system of Fig. 6-9 is $\frac{1}{\sqrt{2}}$ times those of Fig. 6-8. On the other hand, the undamped natural frequencies of the levels of Fig. 6-9 are $\sqrt{2}$ times those of the corresponding levels of Fig. 6-8. A good checkpoint for comparing the two systems is at the 30V point. From Fig. 6-8, the damping ratio can be seen to be about .7. On Fig. 6-9, it appears that the damping ratio of the same level is between .4 and .5. But $\frac{1}{\sqrt{2}}$ times .7 is .49. Because of the small scale required of the recorder, the data is necessarily rough and thus it is quite proper to speak of any constants derived from the experimental results only in approximate terms.

We shall now use the non-linear attenuator which was described earlier in this chapter. Figs. 6-10A and 6-10B show the responses of the system to a 3V step function for various operating levels. It is to be noted that for all levels from 3V to 50V, the dynamics are essentially constant. Even at the zero volt level, the response is greatly improved due to the very high gain at the very low levels.

Maxima were limited to 50V in the experimental results since only one input was used and each input channel was designed to take a maximum of 50V.

In conclusion, it is hoped that a fairly logical approach has been made in analyzing this particular non-linear system. Admittedly

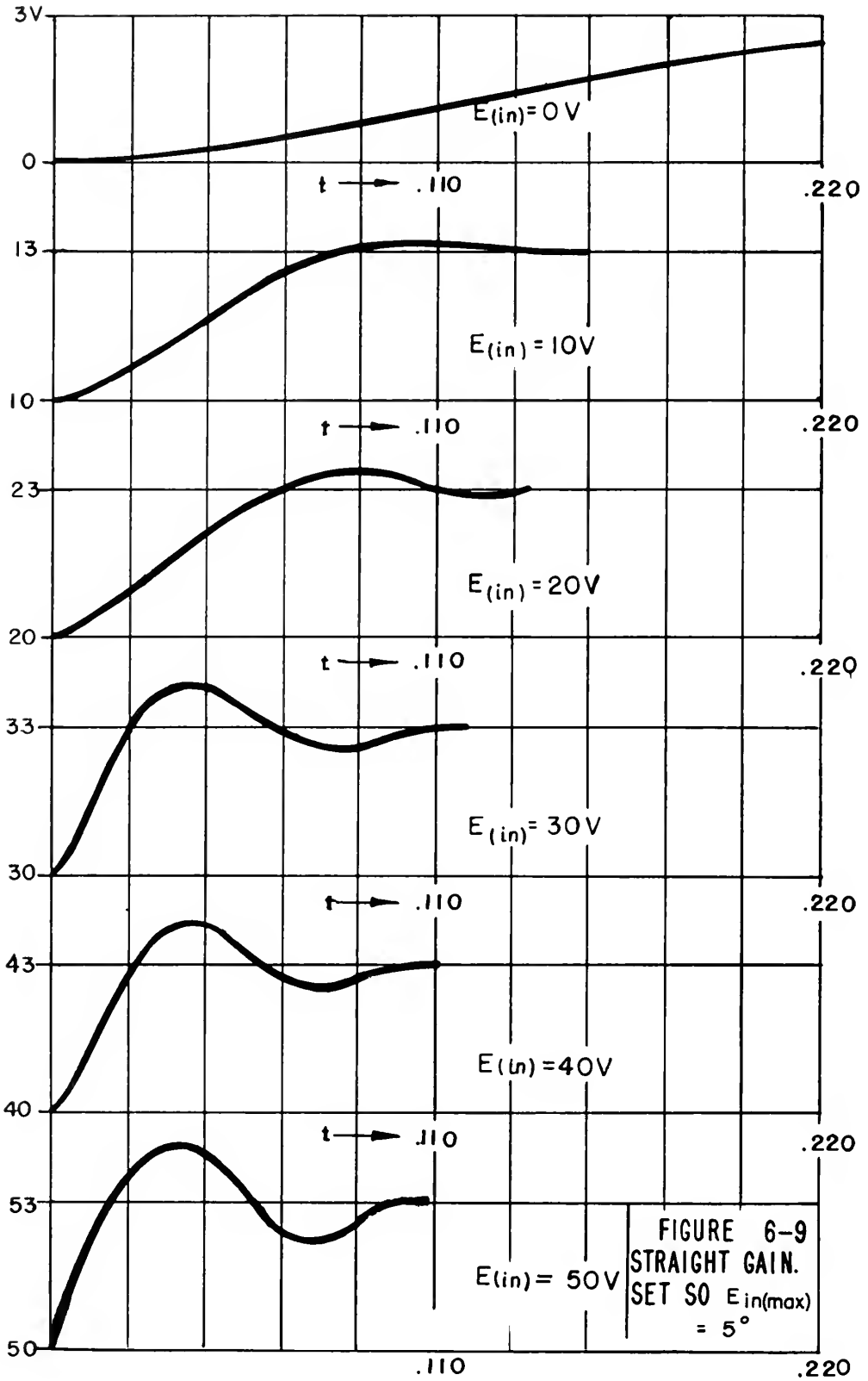

FIGURE 6-9
STRAIGHT GAIN.
SET SO $E_{in(max)}$ = 5°

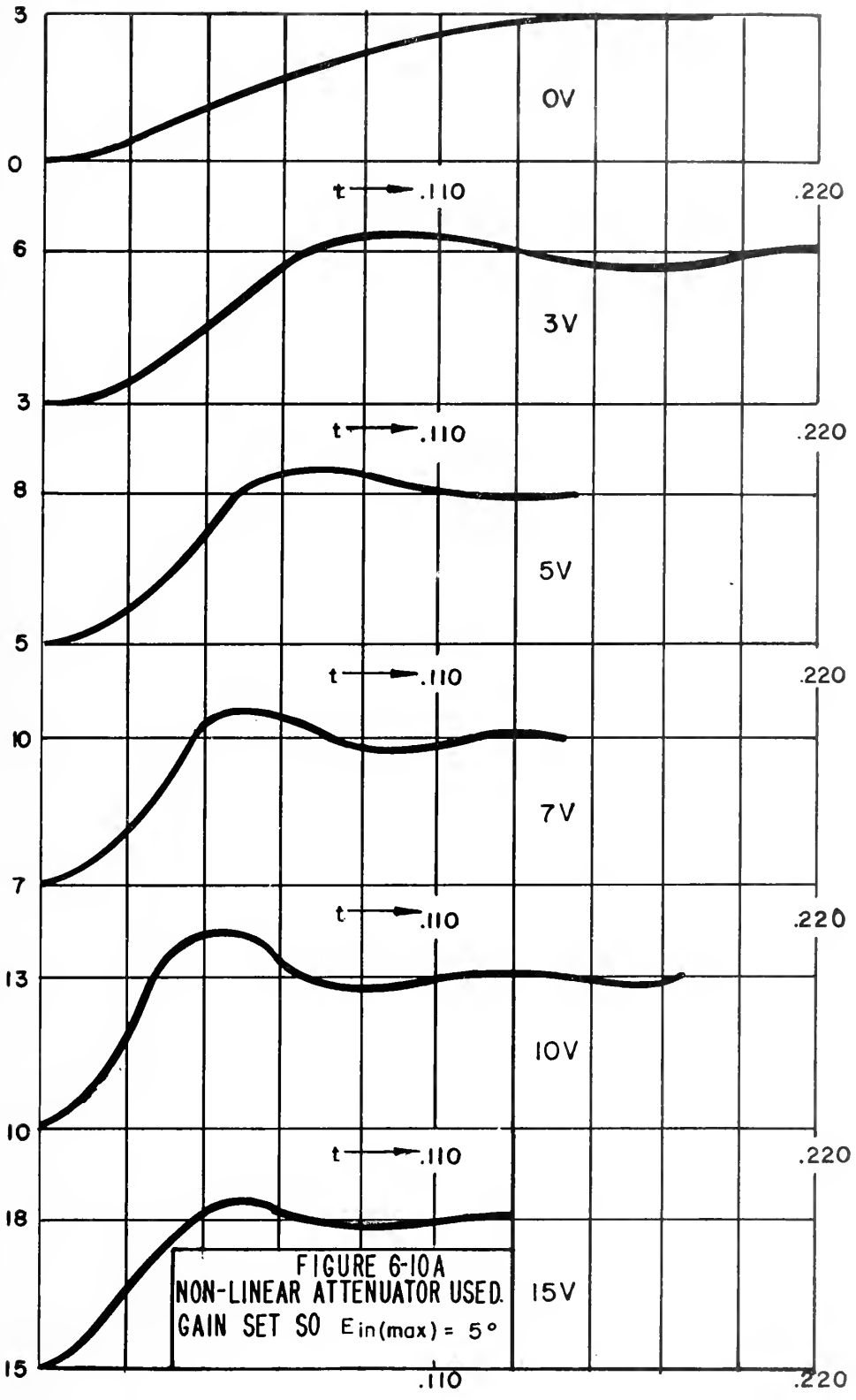

FIGURE 6-10A
NON-LINEAR ATTENUATOR USED.
GAIN SET SO $E_{in(max)} = 5°$

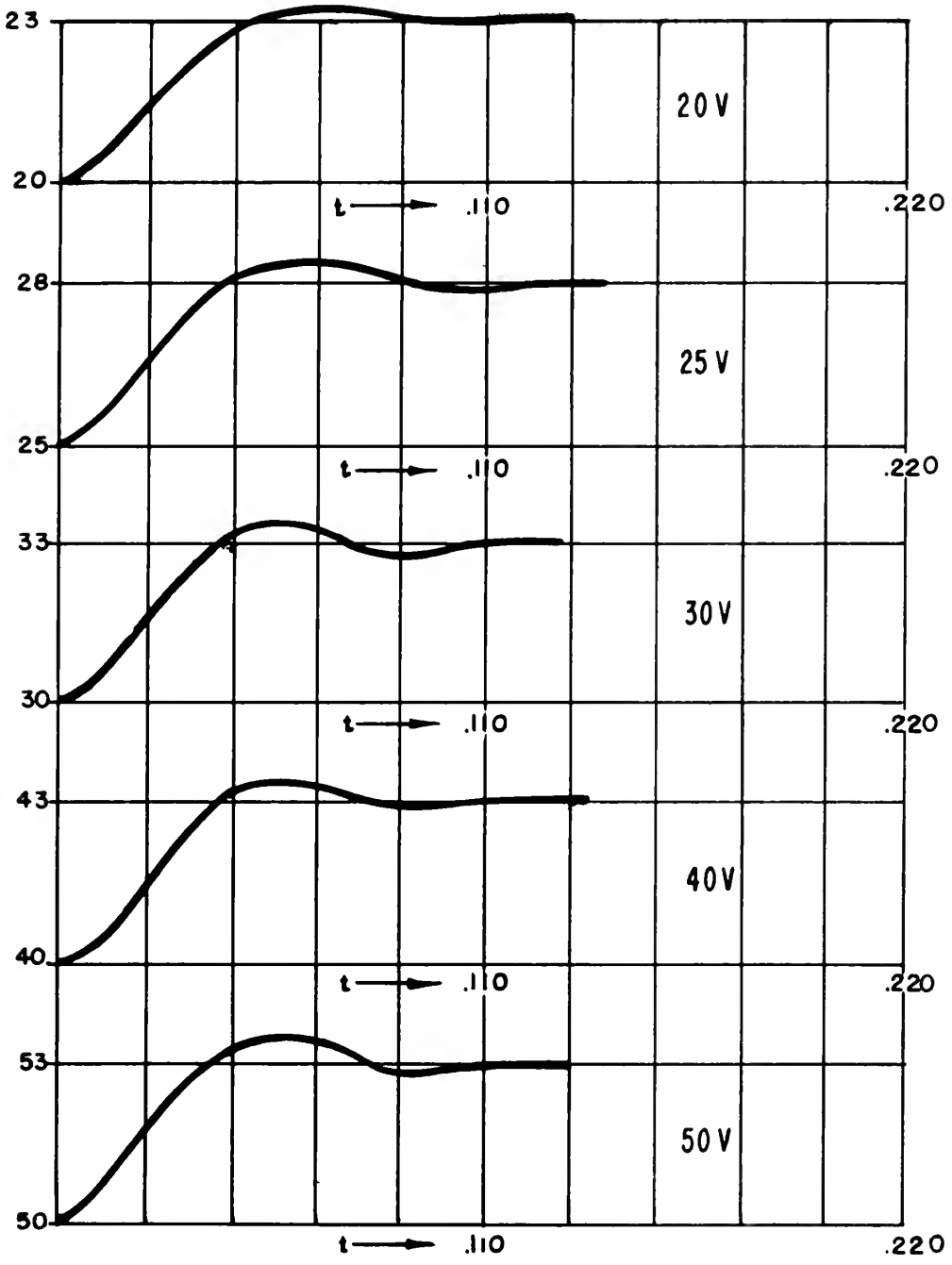
23
20
20 V
t → .110
.220
28
25
25 V
t → .110
.220
33
30
30 V
t → .110
.220
43
40
40 V
t → .110
.220
53
50
50 V
t → .110
.220

FIGURE 6 — 10 B

the title, "A Study of the Dynamics Associated With A Non-linear Closed Loop System," left a certain amount of leeway in just what was to be accomplished. However, the instrumentation of the ideal system in Chapter II in addition to the development of a method for designing a practical system shown in Chapter III should cover most of the background necessary to develop a practical system similar to that shown in Chapter VI.

The author developed a firm appreciation for the difficulties involved in analyzing non-linear systems, and why they are avoided if possible. Although the use of perturbation theory is the most general method for attacking a non-linear system, each non-linear system is a separate problem in itself and must be treated as such. Thus, the method used to attack the Orthogonal Vector Summing System using microsyns probably will apply to very few if any, other non-linear systems.

As can be seen from the data sheets, the results from the laboratory test system seemed to agree very well with the general theory developed prior to Chapter VI. Of course, there are probably better and easier methods for obtaining the required non-linear attenuator than the diode switching circuits. A light bulb could very well have the desired non-linear characteristics so that the pre-assigned tolerances on the dynamics will be maintained throughout the operating range, (except near zero). However, the diode switching circuit does not take much space and is fairly easy to design. Furthermore, by using more diode switches, the ideal square root curve can be approached as closely as desired.

BIBLIOGRAPHY

1. R. K. Mueller Microsyn Electromagnetic Components, Special Report No. 6398-S-9, Massachusetts Institute of Technology, March 1950. (Restricted)
2. Magnetic Circuits and Transformers Electrical Engineering Department, Massachusetts Institute of Technology, pages 117-121.
3. D. G. Hoag, Performance Study of Torque Summation Computer, a Master's thesis, Report No. 6581-T-1, Instrumentation Laboratory, Massachusetts Institute of Technology, 1950. (Confidential)
4. M. F. Gardner and J. L. Barnes, Transients in Linear Systems, Vol. I, John Wiley & Sons, Inc., New York, 1942.
5. R. P. Agnew, Differential Equations, McGraw-Hill, New York and London, 1942.
6. N. W. McLachlan, Ordinary Non-linear Differential Equations in Engineering and Physical Sciences, Clarendon Press, Oxford, 1950.
7. A. A. Andronow and C. E. Chaikin, Theory of Oscillations, Princeton University Press, Princeton, N. J., 1949.

APPENDIX

Brief Explanation of Terminology Used in This Thesis

Given: 1. An operating component, oc.
2. An input quantity, q_i.
3. An output quantity, q_o.

Then the operating component performance function, $(PF)_{(oc)}$, relates the input and output quantities as follows:

$$q_o = (PF)_{(oc)}\, q_i$$

$(PF)_{(oc)}$ can be separated into a static sensitivity, $S_{(oc)}\left[q_i;q_o\right]$, which is a constant of proportionality relating the input and output quantities, and a frequency function, $(FF)_{(oc)}$, which tells how q_o is effected dynamically by the operating component.

For example, if we have a torque generator acting on a shaft, referred here as a torque summing member, (tsm), then

$$M_{(tsm)} = S_{(tg)}\left[i^2;M\right] i^2(in) .$$

This equation is read, torque applied to the torque summing member is equal to the product of the sensitivity of the torque generator for input current squared and torque out multiplied by the square of the input current.

The frequency function will be of the form

$$\frac{a_m p^m \quad a_{m-1} p^{m-1} \quad \cdots \quad 1}{b_m p^m \quad b_{m-1} p^{m-1} \quad \cdots \quad 1}$$

where p, as used in this thesis, is the Laplace transform variable. For further explanation of the Laplace transform, the reader is referred to Reference 4 of the Bibliography.

19388

Thesis
05 Olson
A study of the dynamics associated with a non-linear closed loop system.